석 . 박사 학위논문 등표지

三維有限空間內熱流及溫度分佈的逆問題研究

諾曼•馬力克 二〇〇九

碩士學位論文

Application and Computer Analysis of Solar Systems for the Indoor Daylighting

濟州大學校大學院

에너지工學科

마크무도프 이스칸다르

2010 年 2 月

Application and Computer Analysis of Solar Systems for the Indoor Daylighting

指導教授 千 院 基

마크무도프 이스칸다르

이論文을 工學碩士學位論文으로 提出함

2010 年 2 月

마크무도프 이스칸다르의 工學 碩士學位 論文을 認准함

審査委員長_____印

委　　員_____印

委　　員_____印

濟州大學校大學院

2010 年 2 月

Application and Computer Analysis of Solar Systems for the Indoor Daylighting

Iskandar Makhmudov
(Supervised by Professor Wongee Chun)

A thesis submitted in partial fulfillment of the requirement
for the degree of Master of Science

2009. 12

This thesis has been examined and approved.

.....
Thesis director, Wongee Chun, Prof. of Department of
Nuclear and Energy Engineering

.....
Yoon Joon Lee, Prof. of Department of
Nuclear and Energy Engineering

.....
Nam Jin Kim, Prof. of Department of
Nuclear and Energy Engineering

2009.12
.....
Date

Department of Nuclear and Energy Engineering
GRADUATE SCHOOL
JEJU NATIONAL UNIVERSITY

ACKNOWLEDGEMENTS

First of all I would present my humble gratitude in front of Almighty Allah, the most merciful and the most beneficent, who enabled me to accomplish the dignified cause of education and learning. I pray to Him that He make me able to utilize my knowledge and edification for the betterment of humanity and its development. It is a matter of great honor for me to extend my heartiest indebtedness to all those who have provided guidance, offered a helping hand to me and have contributed directly or indirectly in this work. I feel extremely indebted to my advisor during my MS studies, Professor Wongee Chun for his continuous guidance and support throughout this period at Jeju National University. His thorough professionalism, thought-provoking lectures, seminars and discussions and never-ending teaching appetite I will admire and cherish forever. His encouragement and guidance during my high times and support and kindness during the down times have all been a source of motivation towards learning more and more and giving out my best which I have tried to during my MS studies.

I will always respect and honor Professor Yoon Joon Lee for his helpful support during my studies and research as well. His all-round personality and insightful comments on my work have made me think and have been a cause of constant motivation towards my research. I also wish to extend my deep-hearted thanks to Professor Heon Joo Lee and other professors of my department, especially Professor Nam Jin Kim and Professor Bum Jin Chung for their extremely useful and thoughtful lectures and seminars. I would always commend the devotion and hard work of Mrs. Mee Jin Kim for her Korean language teachings. I would like to take this opportunity to thank Dr. Alexey Penkov and Dr. Vadim Plaksin for their kindness and encouragement.

There have been many friends over this period who have constantly mentored me and have been a source of comfort and companionship. They never let me feel alone even in times of worries and hardships. I would first like to thank Seung Jin Oh for whom I am greatly indebted for his endless help when he acted as a counselor as well as a friend at the same time. I am especially grateful to Won Jong Oh and Young Min Kim for all their help, support and friendship.

I would like to thank Nauman Malik, Khalid Rehman, Jinlong Park, Yanin Limpanont, Wang Rong Li, Ahmar Rashid, Ahsan Rehman, Asif Ali Rehmani, Adnan

Ali, Salim Khan, Srikant Saini, Anil Kumar, Gunasekaran Venugopal, Muhammad Rakib, Abhijit Saha, Nadun Karunatilleke, Mahanama DeZoysa and all Jeju National International Students Organization members for their friendship and support.

Finally, it is an honor for me to pay reverence and salute to my parents who have taken and are still taking great care of me and have been a great source of encouragement for me. They have given me confidence, self-respect, patience and faith in the hard work. I believe all these merits will be invaluable in my further endeavors.

Contents

요약 1

SUMMARY 3

I. INTRODUCTION 5

1.1 Background 5

1.2 Objectives 7

1.3 Method 7

1.4 What is light? 7

1.5 Daylighting 8

1.6 Energy saving 9

1.7 Overview of existing daylighting systems 9

1.7.1 Himawari Solar Lighting Systems 11

1.7.2 Hybrid Solar Lighting Systems 13

1.7.3 Parans SP2 15

1.7.4 Solar Tracking Skylights 17

1.7.5 Universal Fiber Optics System 19

1.7.6 Monodraugh SunCatcher 21

1.7.7 Whilkor WDF 800 22

II. SOLAR DAYLIGHTING SYSTEM DESIGN 23

2.1 Solar concentrator 23

2.2 Solar Tracking System 28

2.2.1 Solar Position and Sunrise & Sunset 29

2.2.2 Algorithm for solar tracker 30

2.2.3 Sunrise and Sunset time 31

2.2.4 Major components 32

2.2.5 Application Software 33

2.3 The concept of total daylighting system 36

III. EXPERIMENTAL PROCESS 38

3.1 Photometric measurements 38

3.2 Measurement instruments 40

3.2.1 Photometric sensor LP 471 PHOT 40

3.2.2 Luminance meter LS-100 41

3.2.3 Thermal Imaging InfraRed camera FLIR i40 42
3.2.4 Pyranometer LP PYRA 02 43
3.2.5 UV-Vis Spectrophotometer SCINCO S-3100 44
3.3 Simulation 43
3.3.1 RADIANCE 45
3.3.2 ECOTECT 47
IV. RESULTS AND DISCUSSION 51
4.1 Classroom with north-oriented windows 55
4.2 Classroom with south-oriented windows 63
4.3 Test cells 71
4.4 Computer-based thermal and daylighting performance analysis of the standard schoolroom 77
V. CONCLUSIONS 81
REFERENCES 82

List of Figures

Fig. 1 Global temperature and CO2 change during 1961-2009 years.....5
Fig. 2 A comparison of predictions of global warming from 8 different climate models assuming the SRES A2 emissions scenario.....6
Fig. 3 Breakdown by sector of global greenhouse gas emissions.....6
Fig. 4 Electromagnetic spectrum with light highlighted.....7
Fig. 5 Typical spectral response of LI-COR photometric sensors and the CIE Standard observer curve vs. Wavelength.....8
Fig. 6 General view of the Himawari Solar Lighting System.....11
Fig. 7 Main components of the Himawari Solar Lighting System.....11
Fig. 8 Schematic view of the solar tracking principle.....12
Fig. 9 General view of the Hybrid Solar Lighting System.....13
Fig. 10 In a solar lighting and power system, the roof-mounted concentrators collect sunlight and distribute it through the optical fibers (enlargement) to hybrid lighting fixtures in the building's interior.....14
Fig. 11 General view of the Parans SP2.....15
Fig. 12 General view of the Solar Tracking Skylights.....17
Fig. 13 Components of Solar Tracking Skylights.....17
Fig. 14 General view of the Universal Fiber Optics System: (a) a solar collector, (b) internal light diffuser.....19
Fig. 15 Components of Universal Fiber Optics System.....20
Fig. 16 General view of the Monodraught SunCatcher.....21
Fig. 17 Components of Monodraught SunCatcher.....21
Fig. 18 General view of the Whilkor WDF 800.....22
Fig. 19 The structural drawing of WDF 800.....22
Fig. 20 (a) Schematic view of the dish type solar concentrator, (b) prototype.....23
Fig. 21(a) General view and, (b) cross sectional view of the homogenizer.....26
Fig. 22 Optical fiber with lens.....26
Fig. 23 Goniophotometer measurements for luminous intensity distribution: (a) a test kit with a 50W halogen lamp, (b) light emanating from diffuser, (c) test kit mounted on goniophotometer.....27
Fig. 24 (a) Base components and, (b) general view of the full system.....28

Fig. 25 The horizon coordinator and the celestial equator.....30
Fig. 26 The algorithm for solar tracking; (a) the altitude and azimuth, (b) the sunrise and sunset time 31
Fig. 27 The principle of solar tracking system 32
Fig. 28 The main components of solar tracking system 33
Fig. 29 The block diagram for system control.....34
Fig. 30 Solar altitude 35
Fig. 31 Solar azimuth 36
Fig. 32 A fiber optic mini-dish solar concentrator daylighting system installed on the roof of a building 36
Fig. 33 Control algorithm of the daylighting system 37
Fig. 34 (a) Overall dimensions and (b) sensors' location 38
Fig. 35 Hemispherical pictures of classroom with (a) north-oriented and (b) south-oriented windows.....39
Fig. 36 Photometric sensor (probe) LP 471 PHOT 40
Fig. 37 LP 471 PHOT sensor with its shadowing ring 40
Fig. 38 Luminance Meter LS-100 41
Fig. 39 Thermal Imaging InfraRed camera FLIR i40. 42
Fig. 40 Pyranometer LP PYRA 02 43
Fig. 41 UV-Vis Spectrophotometer SCINCO S-3100 44
Fig. 42 The main components of the Radiance rendering system.....45
Fig. 43 (a) Plan view, (b) general view of classroom model in ECOTECT 50
Fig. 44 Internal view of classroom model generated by RADIANCE 50
Fig. 45 Sensors' location in the schoolroom model generated by RADIANCE 51
Fig. 46 Location of measured points in the schoolroom.....52
Fig. 47 Luminance ratio (contrast) maps of sky luminance in December 22, 2009 53
Fig. 48 Luminance distribution in classrooms.....54
Fig. 49 Luminance distribution without [(a),(b)] and with [(c), (d)] at 10:00 am.....55
Fig. 50 Illuminance distribution without [(a),(b)] and with [(c), (d)] at 10:00 am.....56
Fig. 51 Luminance distribution without [(a),(b)] and with [(c), (d)] at 12:00 pm.....57
Fig. 52 Illuminance distribution without [(a),(b)] and with [(c), (d)] at 12:00 pm 58
Fig. 53 Luminance distribution without [(a),(b)] and with [(c), (d)] at 2:00 pm.....59
Fig. 54 Illuminance distribution without [(a),(b)] and with [(c), (d)] at 2:00 pm 60
Fig. 55 Luminance distribution without [(a),(b)] and with [(c), (d)] at 4:00 pm.....61

Fig. 56 Illuminance distribution without [(a),(b)] and with [(c), (d)] at 4:00 pm 62
Fig. 57 Luminance distribution without [(a),(b)] and with [(c), (d)] at 10:00 am.....63
Fig. 58 Illuminance distribution without [(a),(b)] and with [(c), (d)] at 10:00 am.....64
Fig. 59 Luminance distribution without [(a),(b)] and with [(c), (d)] at 12:00 pm.....65
Fig. 60 Illuminance distribution without [(a),(b)] and with [(c), (d)] at 12:00 pm 66
Fig. 61 Luminance distribution without [(a),(b)] and with [(c), (d)] at 2:00 pm.....67
Fig. 62 Illuminance distribution without [(a),(b)] and with [(c), (d)] at 2:00 pm 68
Fig. 63 Luminance distribution without [(a),(b)] and with [(c), (d)] at 4:00 pm.....69
Fig. 64 Illuminance distribution without [(a),(b)] and with [(c), (d)] at 4:00 pm 70
Fig. 65 (a) Overall dimensions and, (b) general view of test cells.....71
Fig. 66 Sensors' location in test cells (cell 1/cell 2 respectively) 72
Fig. 67 Luminance values in test cells without (a) and with (b) daylighting system in October 6, 2009 at 1 pm 73
Fig. 68 Global total and diffuse illuminances at different times on a clear day.....73
Fig. 69 Correlation between the global illuminance and irradiance.....74
Fig. 70 Iso-illuminance contour map for the test cell with the solar daylighting system in September 26, 2009 at 1:00 pm: (a) 2D, (b) 3D.....75
Fig. 71 Infrared pictures showing the distribution of internal temperatures in test cell with solar daylighting systems at different hours of the day: 10:03 am, 1:02 pm and 4:00 pm.....76
Fig. 72 Schematic (a) and plan (b) views of the schoolroom model.....77
Fig. 73 Schematic view of the schoolroom south-facing area.....78

List of Tables

Table 1 Specifications of the Himawari Solar Lighting System 12
Table 2 Parans SP2.1 Specifications 16
Table 3 Materials and components of Parans SP2.1 16
Table 4 Technical parameters of the parabolic dish reflector.....24
Table 5 Technical parameters of the second reflector (convex).....25
Table 6 Measurement and simulation comparison of sensor values 51
Table 7 Luminance values (cd/m2) in the north-oriented classroom in December 22, 2009 (sunny day).....52
Table 8 Luminance values (cd/m2) in the north-oriented classroom in December 23, 2009 (cloudy day) 52
Table 9 Illuminance value compared at different locations between the measured and simulation (lux) 79
Table 10 Temperature comparison between SUNCODE and ECOTECT (°C) 80

요약

지난 수년간, 환경문제에 대한 관심과 에너지 소비의 지속적인 증가는 과학자들로 하여금 에너지활용의 새로운 방법을 개발하게 만들었다. 환경문제를 해결하기 위한 최적의 방법은 인간사회에서의 폭넓은 신재생에너지의 활용이다.

이 방법 중 하나는 주거 및 상업 건물에서의 태양광을 활용한 자연채광 시스템으로써, 이는 건물의 에너지 효율을 증가 시킬 수 있고 안락하고 편안한 실내환경을 구현 할 수 있다.

건물에서의 전기에너지 소비 중 조명부분이 30%를 차지하고 있으며, 이는 자연채광을 적용하면 상당량 감소 시킬 수 있다. 게다가, 자연채광은 시각적인 환경과 인간의 웰빙 증진을 위한 중요한 요소이다.

지난 수 십 년간, 태양에너지를 활용한 자연채광시스템의 설계와 제작에 있어서 다양한 접근방법 및 시스템들이 개발 되어 왔다. 하지만, 이들 시스템들은 여전히 효율이 낮고 초기 및 유지 비용이 높아 자연채광 시스템의 보급과 개발에 큰 장애요소가 되어 왔다.

본 연구에서는 실내 자연채광을 위한 새로운 태양 집광 시스템의 성능을 조사하였다. 태양 집광 시스템은 직경이 15cm dish 형 집광기와 고정밀도 태양 추적장치, 광섬유 와 빛의 확산을 위한 디퓨저로 구성 된다. 이 시스템의 자연채광 성능 및 효율을 분석하기 위해, 몇 개의 실험을 수행 하였다.

이들 실험 중 하나는 자연 채광시스템을 제주대학교에의 두 개의 강의실에 적용하는 것이다. 한 개의 강의실은 창문이 남향이고, 나머지 한 개의 강의실은 북향 창문을 갖고 있으며 강의실의 크기는 모두 동일 하다. 두 강의실 모두 ECOTECT 에서 모델링을 하여 RADIANCE 로 불러들여져서 자연채광 시뮬레이션을 수행 하였다. 측정 실험과 시뮬레이션의 결과값을 비교 분석하였으며, 이를 통하여 신빙성을 입증하였다. 또한, 강의실내의 경제적인 조도 조건에 의하여 자연채광 시스템을 설치하였을 경우의 결과값을 시뮬레이션을 통하여 도출 하였다. 그 결과, 남향창문의 강의실인 경우 북쪽 벽의 조도 및 휘도 값의 각각 729 lux 와 127.4 cd/m^2 에서 1296.4 lux 와 228.6 cd/m^2 로 증가 하였고, 북향창문의 강의실인 경우 남쪽 벽의

조도 및 휘도 값이 각각 603.1 lux 와 111.0 cd/m^2 에서 862.7 lux 와 148.6 cd/m^2 로 증가 하였다.

추가적인 실험으로 실제 건물이 아닌 1/2 사이즈(3 m x 1.5 m x 1.5 m)의 두 개의 셀을 제작하여 자연 채광 성능 실험을 수행 하였고, 문헌에 나와있는 초등학교의 실내 조도 값을 활용하여 시뮬레이션을 구현하여 자연채광성능을 분석 하였다.

SUMMARY

A steady increase of energy costs and ever growing environmental concerns in recent years have forced scientists to look for new methods of energy utilization. To resolve these dire problems, the application of renewable energy sources has been considered in various human activities in every sector of society. One of them is the development of solar daylighting systems for residential and commercial buildings, which can improve building energy efficiency and create comfortable indoor environment. Electric lighting represents up to 30 % of building electricity consumption. Therefore, using sunlight in indoor daylighting can significantly reduce electricity consumption in residential and commercial buildings. Moreover, daylight is an important factor in visual environment and improving human well-being.

In last decades, different approaches to the design of solar daylighting systems have resulted in various innovative solutions to efficiently introduce natural light in buildings. But their efficiency and cost are still one of primary obstacles in the wider development and distribution of solar daylighting systems. In this study, we investigated the performance of a new solar concentrator system for indoor illumination. The solar concentrator system consists of 30 cm dish concentrators, high precision solar trackers, optical fibers and diffusers for a light distribution. In order to assess the daylighting system's efficiency, there were carried out several experimental measurement series. One of them was an application of our solar daylighting system to two standard classrooms with south- and north-oriented windows in Jeju city, Korea. At the same time classrooms were modeled by using ECOTECT and exported to RADIANCE for daylighting simulations. Results from the measurements and simulations were analyzed comprehensively to establish the reliability of the modeling process. Following this, we modeled both classrooms with the abovementioned daylighting systems according to ergonomic lighting conditions in classrooms. As a result, illuminance and luminance values boosted up to 862.7 lux and 148.6 cd/m^2 at the center of opposite wall in the north-oriented classroom, 1296.4 lux and 228.6 cd/m^2 at the center of opposite wall in the south-oriented classroom from their lowest original values (i.e., the cases without daylighting systems) of 603.1 lux and 111.0 cd/m^2, 729 lux and 127.4 cd/m^2 respectively.

Experimental investigations are also conducted by using two test cells with a size of 3 m x 1.5 m x 1.5 m (1:0.5) in the same geographical location.

Finally, the design, simulation and in-site measurement results are introduced for a prototype schoolroom with some passive solar features other than large south-facing windows.

I. INTRODUCTION

1.1 Background

Consequences of climate change have become obvious over past 10-15 years throughout the world. Many different researches have already proved human activity as the main reason of environmental issues. Therefore natural, economic and social perspectives of human development for next decades are still being discussed by scientists and politicians globally. As result of initial steps on preserving Earth's environment for future generations, the Kyoto Protocol treaty came into force 16 February, 2005. The major feature of the Kyoto Protocol is that it sets binding targets for 37 industrialized countries and the European community for reducing greenhouse gas (GHG) emissions (Fig. 1). The first commitment period of Kyoto protocol should be completed by 2012 and replaced by a new international framework. Although recent 2009 United Nations Climate Change Conference in Copenhagen could not bring parties to common ground, all countries recognized that climate change is one of the greatest challenges of the present and that actions should be taken to keep any temperature increases to below 2°C (Fig. 2).

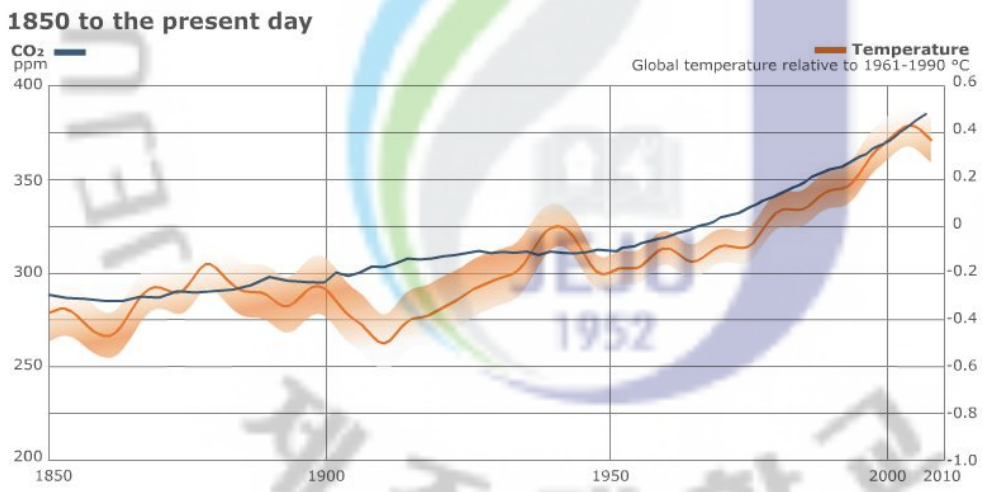

Figure 1: Global temperature and CO_2 change during 1961-2009 years [1]

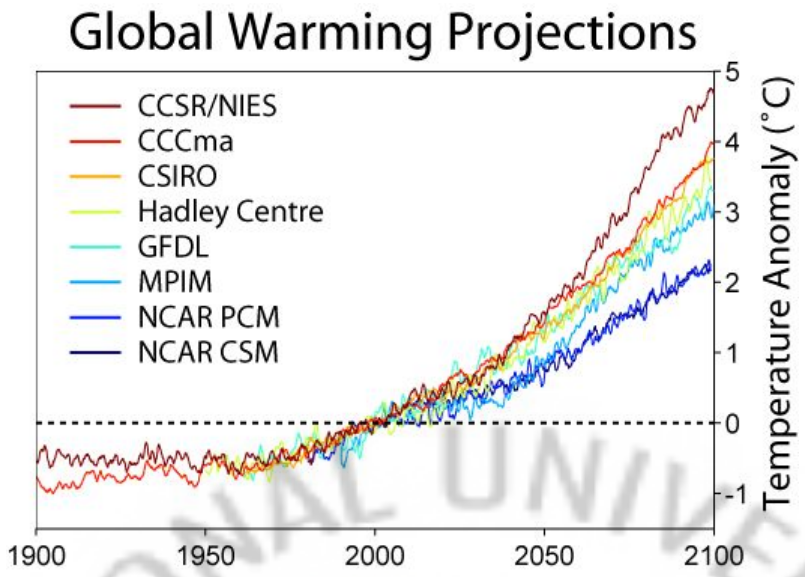

Figure 2: A comparison of predictions of global warming from 8 different climate models assuming the SRES A2 emissions scenario [2]

The research results conducted in 2004 by the Intergovernmental Panel on Climate Change (IPCC) showed that more than 25 % of greenhouse gas emissions were produced by energy sector (Fig. 3). Consequently, renewable energy systems and energy efficient systems would be one of the effective solutions in decreasing the amount of greenhouse emission that lead to climate change.

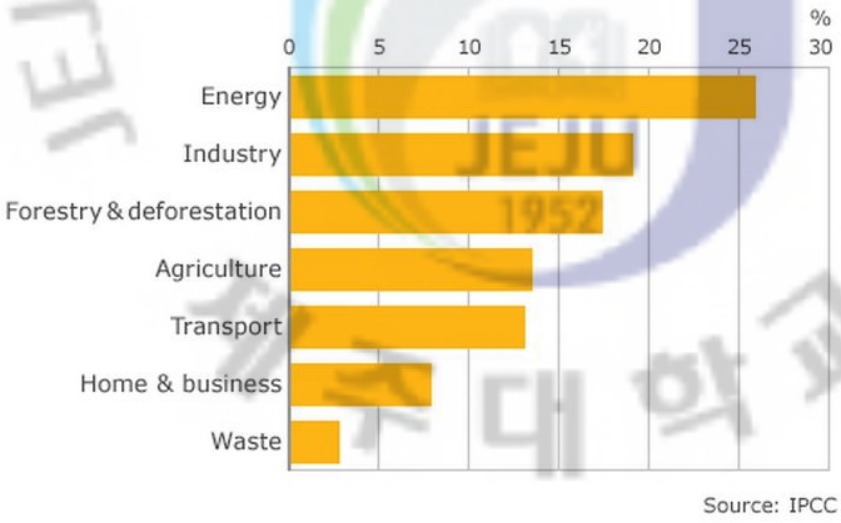

Figure 3: Breakdown by sector of global greenhouse gas emissions, 2004 [2]

1.2 Objectives

The main objectives of this master's thesis were:

1. Design a new active solar daylighting system.
2. Investigate system's indoor daylighting performance and its efficiency.
3. Model different conditions with simulation software and perform a comparison analysis of its results.

1.3 Method

In order to carry out a research, the new solar daylighting mini-dish system with solar tracker was designed and two test cells on Jeju (South Korea) built for the assessment of system's performance. ECOTECT and RADIANCE were used for the modeling different conditions on the computer.

1.4 What is light?

Light is electromagnetic radiation, particularly radiation of a wavelength that is visible to the human eye (about 400–700 nm, or perhaps 380–750 nm). In physics, the term light sometimes refers to electromagnetic radiation of any wavelength, whether visible or not (Fig. 4).

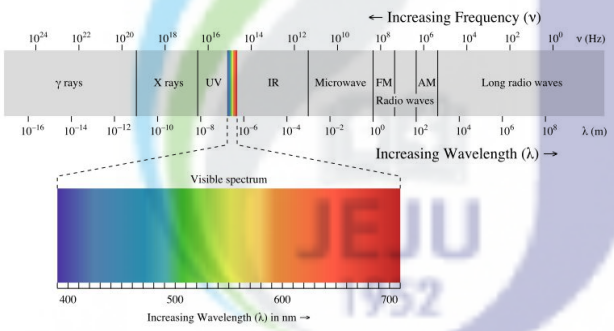

Figure 4: Electromagnetic spectrum with light highlighted

The visible part of natural light is often measured in units of lumen, which are calculated on the basis of the sensitivity of the human eye. The lumen is commonly used to classify the output of electric light fittings and daylighting devices [3]. The sensitivity of the eye is not constant with respect to the wavelength of light and peaks at 555nm. Light measuring cells are usually designed to conform to a CIE Standard Observer or Photoptic curve, as it is this sensitivity curve that defines the unit of lux,

which is a measure of visible light intensity and hence has units of lumens/m2. The Photoptic curve is shown in Fig. 5.

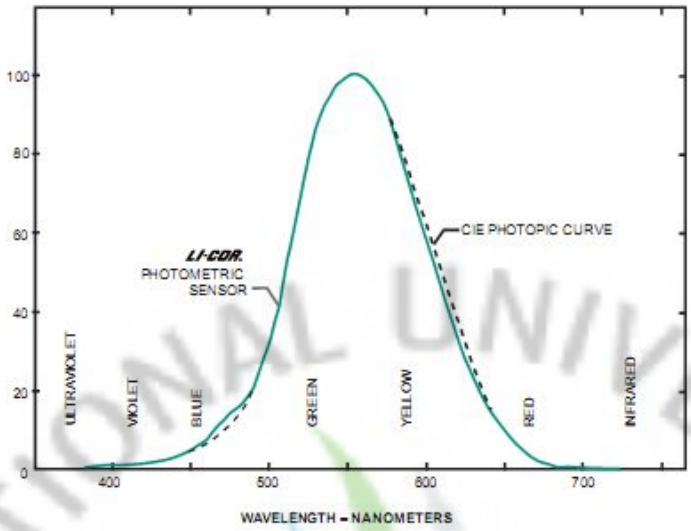

Figure 5: Typical spectral response of LI-COR photometric sensors and the CIE Standard observer curve vs. Wavelength

Such light properties as abovementioned total flow of the light from light source (lumen), its intensity in space (candela), illuminance at the point (lux) and the luminance of a surface (candela per square meter) were standardized in the SI units [4].

1.5 Daylighting

Daylighting is important in achieving a good quality of life and comfort in buildings. It was proven that an access to windows affects to mood motivation and productivity at work, through reduced fatigue and stress. Working long-term under electric lighting is believed to be deleterious to health; working under daylight is believed to result in less stress and discomfort.

Historically, the main daylighting devices are windows, which are still the dominant source of daylight globally today. For a variety of reasons, however, the vertical glazing unit is not always an ideal source of illumination. Direct sunlight is often not a good source of illumination in the built environment as its intensity and directional nature generates glare for building occupants. Diffused light, however,

does not penetrate far into rooms fitted with windows. The challenge, therefore, is to develop means of utilizing both direct and diffuse natural light in buildings while maintaining and improving occupant visual comfort, particularly at greater distances from the external walls.

1.6 Energy saving

Application of modern daylighting technologies in buildings is one of perspective ways of zero-carbon emission houses development. Savings from daylighting can cut lighting energy use by up to 75 - 80 percent according to the US Department of Energy's Federal Energy Management Program [5]. Therefore different researches on daylighting technologies became one of the key directions of science during the last years.

Daylighting falls broadly into the category of energy efficiency, as it does not generate power, but reduces the demand for it. The amount of energy demand generated by the use of electric lights is considerable and gives the possibility of significant savings by daylighting. In commercial and public buildings 40 to 50 % of the energy consumption accounts for artificial light and 10 to 20 % of energy consumption in industry. Nicklas and Bailey showed that application of daylighting technologies to public schools can decrease the energy cost from 22 % to 64 % compared to a typical school [6]. For example, a public school with daylighting systems in North Carolina saves about 40 000 USD annually comparing to a typical school [7]. In addition, with daylighting systems the density of lighting can be reduced in some public buildings from 23.7 W/m^2 to 9.5 W/m^2 [8].

1.7 Overview of some existing daylighting systems

Daylighting systems reflect sunlight through an opening in the roof or sidewall of a building into the desired room or space, thereby replacing the light required from electric sources. In rooms or areas that require the certain amount of light throughout the day, the daylighting system uses sensors to detect changing light patterns. The system controls then adjust electrical light fixtures to augment light levels if the system falls below a pre-determined threshold. The daylighting systems also contain a light baffling system to reduce or eliminate daylight should the user desire a darkened room during daylight hours. The technologies investigated have two primary

differences: (1) how they capture sunlight; and (2) how they transmit the light into the building.

- *Capturing sunlight.* Daylighting systems capture daylight on a building's roof or sidewall either passively with a stationary mirror/prism or actively via a mirrored mechanism that tracks the angle of the sun throughout the day.

- *Transmitting sunlight.* The daylight captured on the roof or sidewall must be transmitted to the desired area. Daylighting systems accomplish this either: (1) directly by redirecting sunlight into a space using architectural features, (2) indirectly through tubes using mirrors to enhance light transmission, or (3) through fiber optics.

Advantages:

- Provides an alternative to high-cost electrical energy;
- Contributes to improved well-being of a worker, which may result in improved productivity, better performance, higher-quality work, and increased employee retention.

Disadvantages:

- Some daylighting technologies have long economic payback periods;
- A conventional lighting system is still required to augment the daylight system during dark periods;
- Some of the lighting technologies are new and require some improvements to overcome issues, such as flickering;
- Many of the roof-mounted technologies are only viable for the top floor of a building, or at most, down one level from the top floor.

Further some types of solar daylighting systems will be described.

1.7.1 Himawari Solar Lighting Systems

Figure 6: General view of the Himawari Solar Lighting System [9]

The solar collector consists of two parts. The first part is a set of highly efficient lenses and a sun-tracking sensor equipped with twin-axle motors and covered by an acrylic dome. The second part is consisted of a controlling unit housed in a supporting base (Fig. 6).

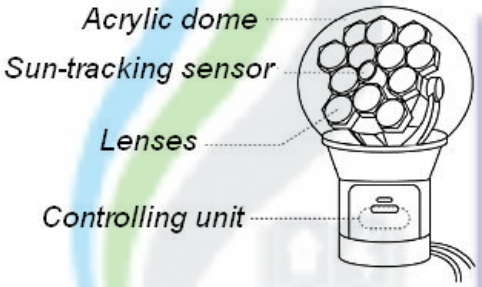

Figure 7: Main components of the Himawari Solar Lighting System

Himawari has an internal clock mechanism, a sun-sensor, and a microprocessor to determine the position of the sun and adjust its own angle (Fig. 7).

In good weather, the exact location of the sun is ascertained by the sensor. When the sun is hidden behind clouds, it switches to its internal clock mechanism. So Himawari can respond quickly to the conditions, collecting sunlight efficiently in fine weather. After sunset, it shuts off and positions itself so that it's ready for the next sunrise.

Table 1: Specifications of the Himawari Solar Lighting System


XF-160S/198AS


XF-110S/90AS


XD-100S/36AS


XD-50S/12AS

Type	Number of lenses	Lens size(mm)	Light receiving area(cm2)	Dome diameter (mm)	Height (mm)	Weight (kg)	Number of cables	Total luminous flux(lm)	Electric power supply	Power consumption
XF-160S /198AS	198	95	14,035	1,630	2,500	628	33	53,790	AC85V ~ 264V	15W
XF-110S /90AS	90	95	6,379	1,170	2,045	346	15	24,450	AC85V ~ 264V	12W
XD-100S /36AS	36	95	2,552	1,000	1,475	88	6	11,520	AC85V ~ 264V	5W
XD-50S /12AS	12	95	851	520	810	14	2	3,840	AC85V ~ 264V	2W

Features of the system:

Highly efficient and stable collection of the sunlight through a combination of Lens + Optical Fiber Cable

The outdoor collector catches the maximum quantity of sunlight throughout daytime. It is immune from limitations such as the orientation of a room, the exposure of a window, or the altitude of the sun, to which skylight and mirror-reflection systems of other makers are subject.

The automatic tracking system tracks the sun precisely.

Himawari's lenses automatically track the sun throughout the day to position themselves at a right angle to the sunlight as shown in the Fig. 8.

Figure 8: Schematic view of the solar tracking principle

Transmission of sunlight by optical fiber cables

Sunlight is condensed about 10,000 times through a highly efficient lens. The inlet-end of an optical fiber cable is positioned at the focal point of the lens. The sunlight enters the cable through the inlet and proceeds through the fiber cable, repeating its full reflection, and is emitted from the outlet of the fiber cable.

A highly pure quartz glass fiber cable transmits the visible rays with very little attenuation. A cable made of flexible optical fibers can be installed in any new or existing building to transmit sunlight to wherever it is needed.

1.7.2 Hybrid Solar Lighting Systems

Figure 9: General view of the Hybrid Solar Lighting System

The hybrid solar lighting system uses a roof-mounted solar collector (Fig. 9) to concentrate visible sunlight into a bundle of plastic optical fibers. The optical fibers penetrate the roof and distribute the sunlight to multiple "hybrid" luminaires within the building (Fig. 10). The hybrid luminaires blend the natural light with artificial light (of variable intensity) to maintain a constant level of room lighting. One collector powers about eight fluorescent hybrid light fixtures, which can illuminate about 93 square meters [10].

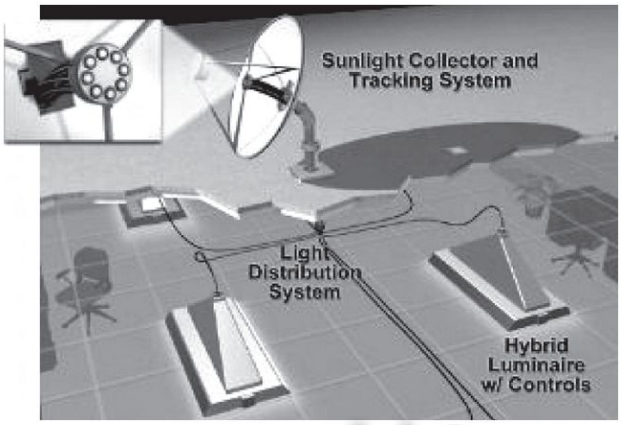

Figure 10: In a solar lighting and power system, the roof-mounted concentrators collect sunlight and distribute it through the optical fibers (enlargement) to hybrid lighting fixtures in the building's interior

When sunlight is plentiful, the fiber optics in the luminaires provides all or most of the light needed in an area. During times of little or no sunlight, a sensor controls the intensity of the artificial lamps to maintain a desired illumination level. Unlike conventional electric lamps, the natural light produces little to no waste heat, having an efficacy of 200 lumens/Watt (l/W), and is cool to the touch. This is because the system's solar collector removes the infrared (IR) light from the sunlight— the part of the spectrum that generates much of the heat in conventional bulbs. Because the optical fibers lose light as their length increases, it makes sense right now to use hybrid solar lighting in top-story or single-story spaces. The current optimal optical fiber length is 50 feet or less. The hybrid solar lighting technology can separate and use different portions of sunlight for various applications. Thus, visible light can be used directly for lighting applications while IR light can be used to produce electricity or generate heat for hot water or space heating. The optimal use of these wavelengths is the focus of continued studies and development efforts.

The payback period for hybrid solar lighting lengthens in proportion to the efficiency of the electric lamps used in combination with distributed sunlight. Because linear fluorescent lamps are very efficient (65-90 lm/W), the models indicate that a hybrid configuration used with such lamps will require more than 10 years to pay for itself in most regions of the country during the early years of commercialization. As prices fall, hybrid solar lighting has the potential to become cost-competitive in most indoor lighting scenarios.

1.7.3 Parans SP2

Figure 11: General view of the Parans SP2 [11]

Parans SP2.1 employs 62 pivot-suspended optical Fresnel lenses (Fig. 11) that follow the solar path and focus incident sunlight into optical fibers. The optical fibers are bundled into four flexible optical cables that transport the collected sunlight up to 20 meters. Parans SP2.1 can be installed on both roofs and facades which generates a wide range of installation possibilities.

The solar tracking in Parans SP2.1 represents a significant technology improvement. A new sun sensor, based on a PSD chip, has been developed and assures increased accuracy in detection and tracking of the sun in a large variety of weather conditions. The software combines input from the sensors with historical data of the solar path from each day that the panel has been installed. This allows for alignment of the lenses towards the sun even on cloudy days, so that sunlight can be harvested as soon as the sky is clear.

The sunlight output from Parans SP2.1 depends on the sunlight conditions and the length of the fiber optic cables. The light transport is immediate; it cannot be stored and is not transformed. If a cloud passes by for example, the same shadow will be cast indoors and if the sunlight is tinted red in the evening so will the light output. For light to be able to flow through an optical fiber, it must enter from an angle which lies within the fiber's acceptance angle. In practice, this means that only the parallel light rays of direct sunlight can be efficiently collected. The light output on cloudy days is therefore little or none depending on the thickness of the clouds.

At direct incident sunlight at 100 000 lux, the sunlight output, or luminosity, from Parans SP2.1 is 3000 +/- 300 lumens. The transmission in the optical cables is 95.5% per meter, which means for example that 63% luminosity remains after 10 m.

Table 2: Parans SP2.1 Specifications

Dimensions	980 x 980 x 180 mm
Weight solar panel	30 kg
Weight optical cable	273 g / m
Power Supply	AC 100 - 250 V
Power Consumption	0 - 6 W
Operating Temperature	-20°C – 40°C
Luminous Output	3 000 +/- 300 lm

Table 3: Materials and components of Parans SP2.1

Materials, Components	Weight (g)
Aluminum EN AW-5754 H22	16 220
Toughened safty glass (EN12150). Antireflective Centro Solar HiTC+	5 120
Zink (alloy ZL 0410)	3 660
Stepping motor Type 16PM-M009-02, MINABEA CO LTD, Thailand	822
Plastic (PMMA)	341
Stainless Steel	148
Electrogalvanized Steel	128
PA6	< 100g
POM - Delrin 500AL NC010	< 100g
Ertalyte TX (PET-P w/ solid lubricant)	< 100g
Silicone, Loctite 5140	< 100g
UV curing glue, Loctite 3103	< 100g
EPDM rubber	< 100g
Nickleplated brass	< 100g

1.7.4 Solar Tracking Skylights

Figure 12: General view of the Solar Tracking Skylights [12]

Solar Tracking Skylights (Fig. 12) consist of highly reflective mirror panels within a clear plastic enclosure, which move continuously to follow the sun's position in the sky. By aligning to the exact position of the sun, the mirrors reflect light down into the space that would be otherwise lost due to the low incident angle of the sun through much of the day.

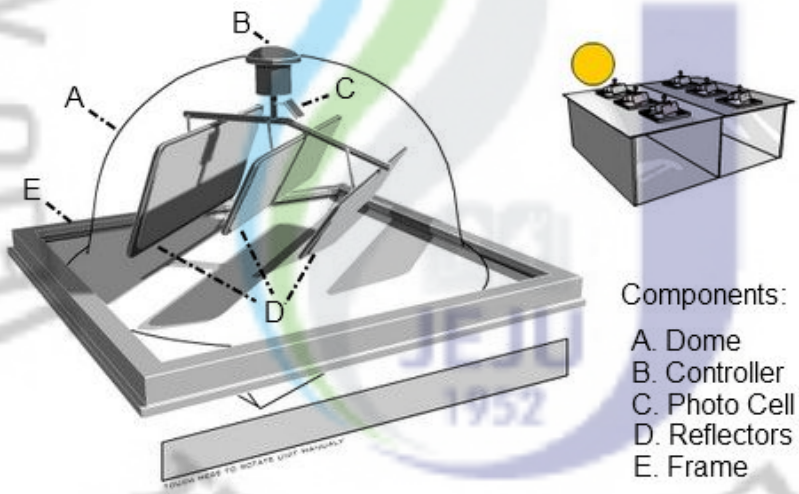

Figure 13: Components of Solar Tracking Skylights

At the location below using the same total square footage of Solar Tracking Skylights generates an addition three to five hours a day of usable daylight in the space. On an annual basis, there is a 427% gain in the useable hours where no electric lights are needed (Results vary by location).

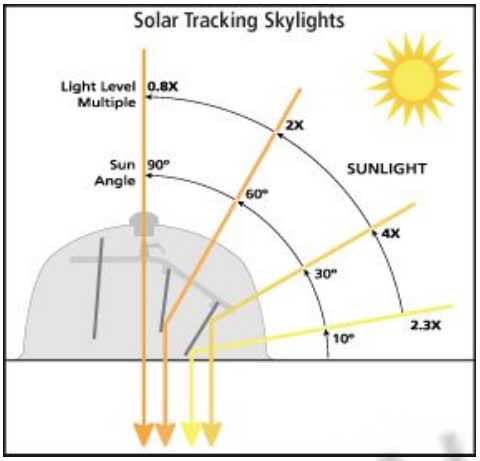

Tracking the sun's movement generates up to 4 times the light levels in the space below. In the summer when the sun is directly overhead, the reflectors actually lower light levels and solar heat gain 20%.

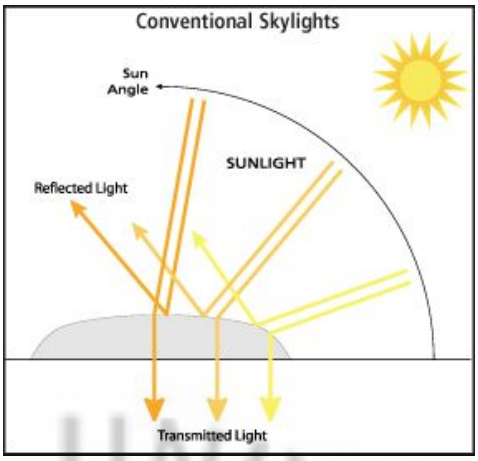

As the sun rises and sets and is lower in the sky during different seasons much of the available light is reflected off the convention skylight.

The biggest shortcoming of any skylight is heat loss and gain. Even with an optimal design, up to 45% of the electrical lighting savings produced from skylights is lost in additional HVAC expense.

Solar Tracking provides two or more times the amount of light compared to conventional skylights. So Solar Tracking Skylights can provide the same light levels and duration as conventional with a fraction of the units or square feet of coverage. The result is fewer skylights need to be installed, which translates into lower construction costs, lower HVAC requirements, and a decrease in the number of possible roof leaks.

1.7.5 Universal Fiber Optics System

(a)

(b)

Figure 14: General view of the Universal Fiber Optics System: (a) a solar collector, (b) internal light diffuser [13]

The system is based on a roof-standing heliostat with a 1.0 meter Fresnel lens as shown in the Figure 15. The unit tracks the path of the sun collecting sunlight, which, using a specially designed cool coupling, is fed into the building via a liquid light guide. This cable can be introduced into buildings through ventilation ducts, dry risers, any hollow conduit and even suitable lift shafts. Because this is a passive system, integration into most building types is easy.

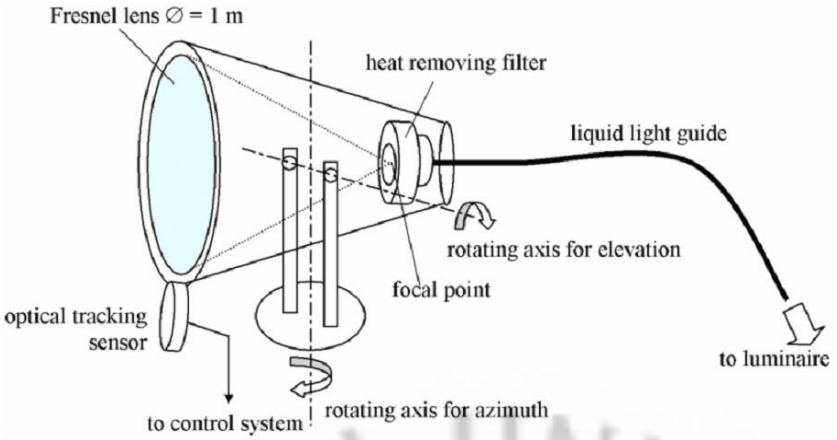

Figure 15: Components of Universal Fiber Optics System

At the end of the liquid light guide, a luminaire is attached. It is designed to act as a light and a coupling device between natural sunlight and an artificial back up source. The system is controlled by a photocell, which monitors the light levels. When the sun becomes obscured the luminaire switches automatically to the artificial light source, which is relayed into the system by a fiber optic cable with minimum apparent change to the intensity of the light.

The heart of the luminaire is Prismex™, an acrylic based product coated with a specially designed dot pattern. This spreads the light, when brought to one or more of its edges, to pass through the acrylic panel and deliver an even brightness across its whole surface.

New technology will further enhance the capability and the effectiveness of the system. For example Light Emitting Diodes (LEDs) and/or fluorescent lamps have the potential to become a more practical back-up light source. They are flexible, have a very long life and react instantaneously. Liquid light guides will improve allowing greater penetration into the buildings.

1.7.6 Monodraugh SunCatcher

Figure 16: General view of the Monodraught SunCatcher [14]

The Monodraught SunCatcher system (Fig. 16) provides controlled natural ventilation as well as providing all the benefits of natural daylight. Any prevailing wind pressure carries a continuous fresh air supply through weather protected louvers on the windward side of the system at roof level. The wind movement is encapsulated by internal quadrants which turns the wind through 90° forcing air down through internal ducts into the room below, slightly pressurizing the internal space. Warm, stale air is expelled from the room by the Passive Stack ventilation principle of differential temperatures and the natural buoyancy of air movement. Manual or motorized motors at the base of the system control the rate of ventilation. The central SunPipe is integrated into the system and conveys natural daylight to the same room or internal space (Fig. 17).

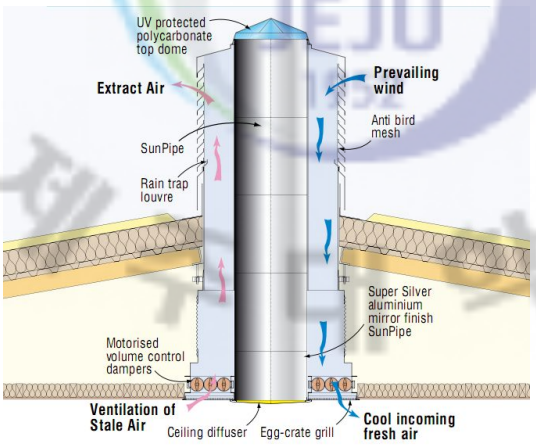

Figure 17: Components of Monodraught SunCatcher

The SunCatcher has the unique advantage that with air intakes on all four sides, it does not matter which way the wind is blowing since one side of the system will always act as the air intake, whilst the opposite side, being in the low pressure zone, related to the system, becomes a natural extract to the room. When the wind changes direction, so the intake and extract will also change their function maintaining a balanced condition but providing energy free air conditioning.

1.7.7 Whilkor WDF 800

Figure 18: General view of the Whilkor WDF 800 [15]

The Whilkor WDF 800 system (Fig. 18) is used in sunlight transportation for long distances (70m-1km).

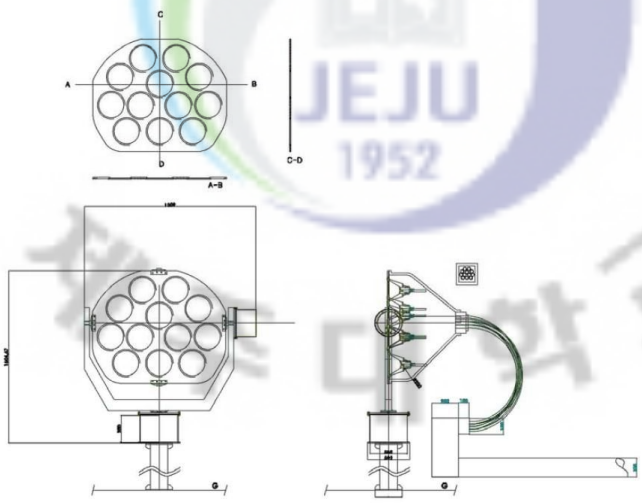

Figure 19: The structural drawing of WDF 800

II. SOLAR DAYLIGHTING SYSTEM DESIGN

2.1 Solar Concentrator

Active daylighting schemes allow flexibility in applying sunlight for indoor illumination by utilizing it more aggressively. Especially, a daylighting system with movable heliostat(s) could effectively deliver sunlight to any desired location as it constantly tracks the sun.

In the study there was designed a dish type solar concentrator which is shown in Figure 20. One of the advantages of this system is its portability.

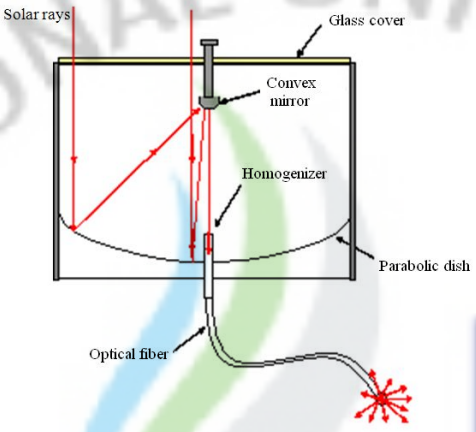

(a)

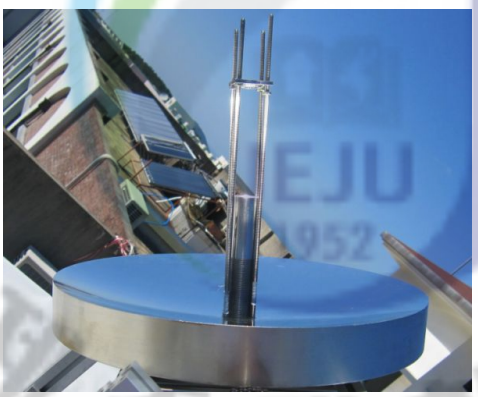

(b)

Figure 20: (a) Schematic view of the dish type solar concentrator, (b) prototype

Solar concentrator consists of a parabolic dish reflector, a secondary reflector, a homogenizer and an optical fiber. Main material for components was aluminum. Transparent cover can be used for the protection from environment impacts.

Solar concentrator works as follows: first, solar rays are concentrated by the parabolic dish reflector in the secondary one and then reflected into homogenizer which is connected to optical fiber. Finally, the concentrated rays coming through optical fiber spread out from its end. Table 4 shows the technical parameters of the mini dish.

Table 4: Technical parameters of the parabolic dish reflector

Dish diameter (cm)	30.00
Focal distance (65% of D - cm)	19.5
Dish radius (cm)	15
Rim angle (degrees)	42.07506

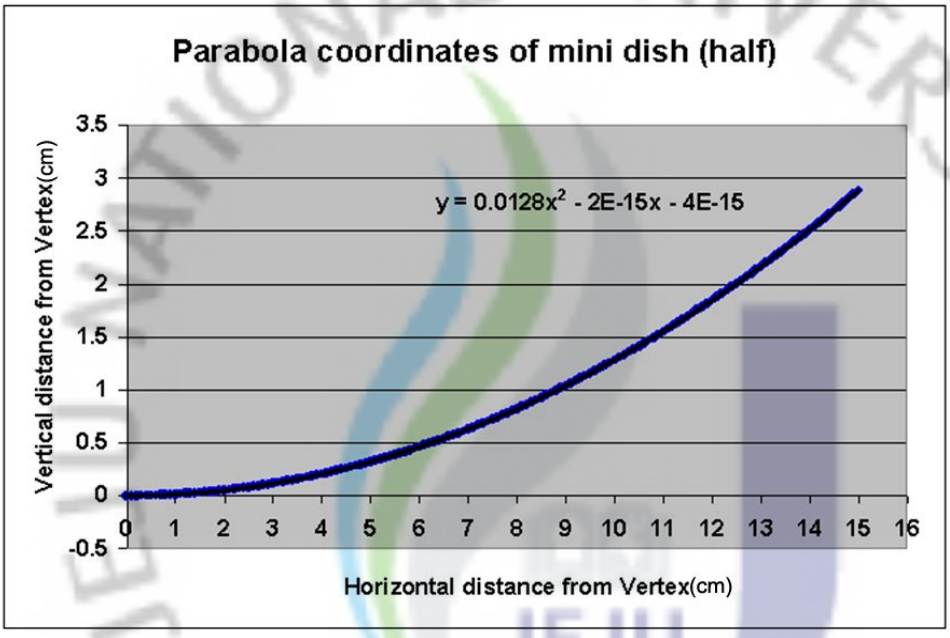

In the experiments two types of second reflector used are convex and concave. In the table 5 are given technical parameters.

Table 5: Technical parameters of the second reflector (concave)

Dish diameter (cm)	3.0
Focal distance (65% of D - cm)	1.95
Dish radius (cm)	1.5
Rim angle (degrees)	42.07506

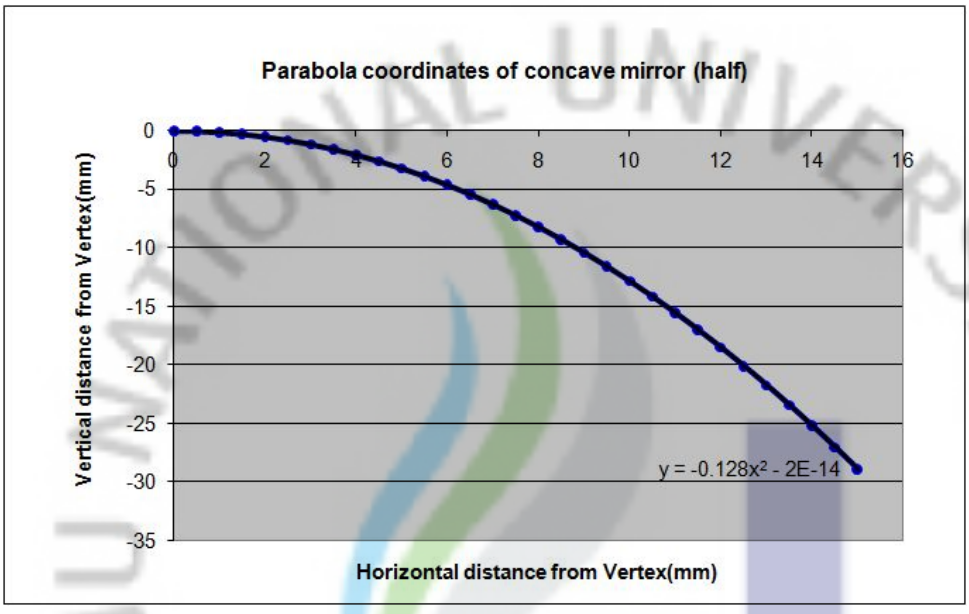

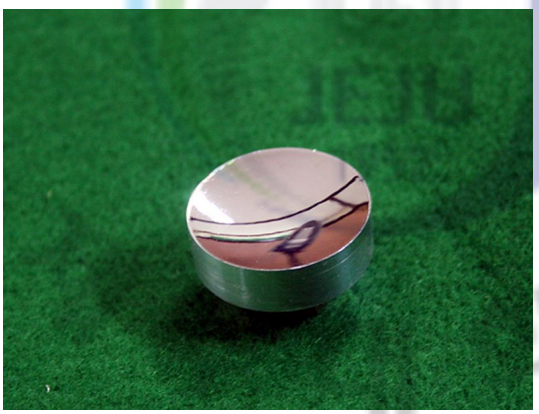

Homogenizer transfers reflected rays into the optical fiber. Its total length is 175 mm, an outer diameter of inlet and outlet is 25 mm and 15 mm respectively (Fig. 21).

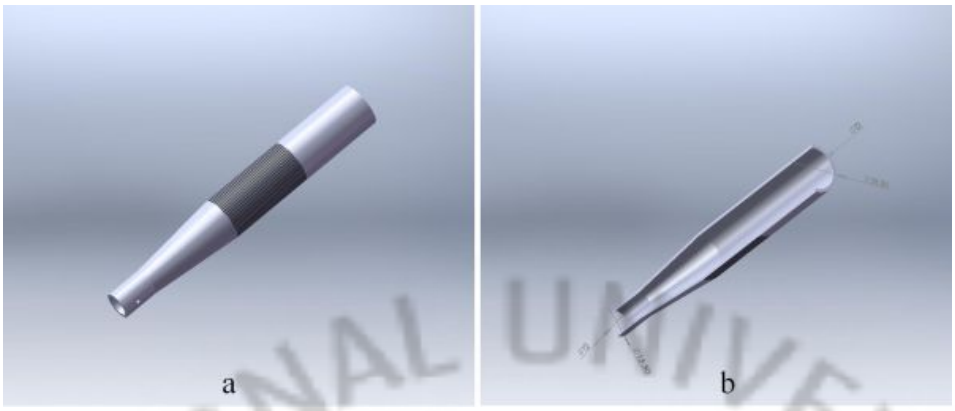

Figure 21: (a) General view and, (b) cross sectional view of the homogenizer

In the experiments was used a standard glass-made optical cable for indoor illumination (Fig. 22) which had a semi-concave optical lens at its end, was used. Properties of the diffuser were investigated at the Korean Institute of Energy Research (KIER) with a goniophotometer (Model: DP-1600) to obtain the luminous intensity distribution (Fig. 23) and an IES file was created for the using in computer simulations.

Figure 22: Optical fiber with lens

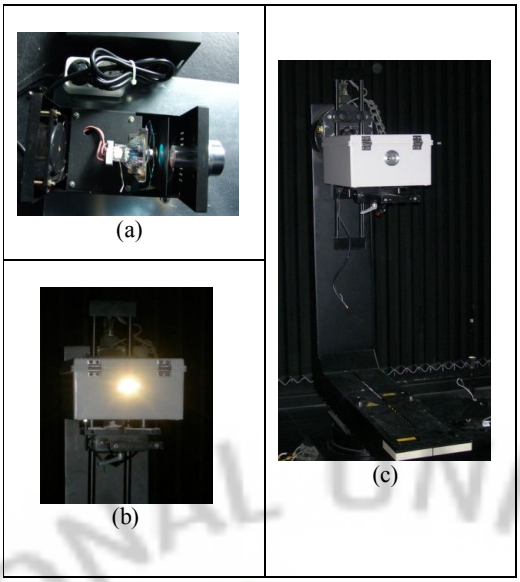

Figure 23: Goniophotometer measurements for luminous intensity distribution: (a) a test kit with a 50W halogen lamp, (b) light emanating from diffuser, (c) test kit mounted on goniophotometer

All abovementioned components were installed to the aluminum and acryl made base which also includes solar tracker components (Fig. 24).

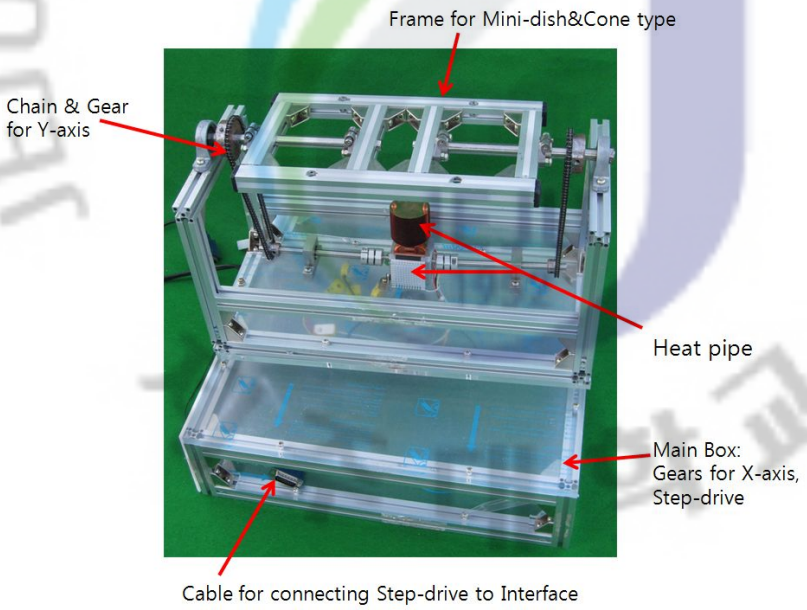

(a)

(b)

Figure 24: (a) Base components and, (b) general view of the full system

2.2 Solar Tracking System

Solar trackers play a central role in concentrating the sun light into an optical fiber where at one end of fiber, a high-density light beam could emerge for indoor illumination, high suns PV applications. Many solar trackers have been developed in the market but they are relatively expensive and high accuracy of trackers may pose long term reliability problems. A key component of the motion controller of trackers is the software, where flexibility, easy-of-use and integration with other I/O ports are parameters for consideration. In this paper, we demonstrate that a cost-effective solution with the off-the-shell software, such as the LabVIEW. It offers solution with excellent accuracy in tracking as well as the output concentration in the fiber reaching up to 200 suns. The tracker system takes advantage of global positioning data (GPS) for the geographical location before applying the simultaneous controls such as the open and closed loop operations. The closed loop feedback control with CdS sensors proves effective in making real time corrections for gear backlashes or under an adverse disturbances arising from strong winds, etc.

A solar tracking system is a device for orienting a day-lighting reflector, solar photovoltaic panel or concentrating solar reflector or lens toward the beam radiation of the sun. The sun's position with respect to the earth varies both with the seasons

and a time of a day as the sun moves around the earth. Such equipment works best when it is pointed directly towards the sun, increasing the effectiveness over the non-tracking systems but it is at a marginally higher cost and system complexity.

The accuracy of the solar trackers depends on the types of application: Concentrators meant for solar cells and day-lighting systems would require higher degree of accuracy, ensuring the concentrated sun rays are directed at the prescribed numerical aperture near the focal point. Typically, concentrator systems are either a single-axis or two-axes devices. Large power plants or high temperature facilities may employ multiple ground-mounted mirrors and an absorber target with or without secondary concentration. One of the key components of a motion controller in a tracker is software where the C-language and Visual Basic are often used, and manufacturers of trackers have supplied their systems with libraries for these algorithms. The problem, however, is that it is difficult for a user to integrate such codes into the one main program. In this study, we have employed a common platform based on a commercially available code, the LabVIEW, which is easily adapted by any user.

2.2.1 Solar Position and Sunrise & Sunset

Generally, there are two methods available for solar tracking: An optical method and the astronomical method to give the position of the sun rays at any time instance in a day. The optical method is called the “closed loop system”, it uses several feedback sensors such as a photo-sensor and a position sensor and a comparator that differentiate the output signals of sensors and thus, continuously adjusting the system towards a brighter spot.

Such a method has a drawback, i.e., it cannot track the sun in a cloudy day without an extensive algorithm.

The astronomical method, on the hand, employs the longitude and latitude data of a location in-situ and it has the advantage of simple programming, high degree accuracy and less error. However, the inherent disadvantage is that it requires the starting position of tracker to be always same from day to day and the operating motors are easily subject to the “backlash” effect due to continuous adjustments from the GPS data. For these reasons, we have combined these methods in this study.

2.2.2 Algorithm for solar tracker

In this Solar tracking algorithm, the solar altitude (θ_e) and azimuth (θ_a) are computed in accordance to the location or site. The tracker device must be positioned horizontally to implement the altitude and azimuth angles along with the hour angle and declination angles with respect to the celestial equator or plane (Fig. 25).

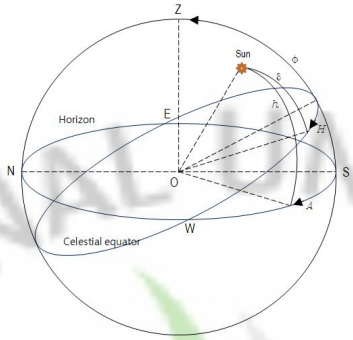

Figure 25: The horizon coordinator and the celestial equator

In this figure, the solar altitude (h) is the angle between a line that points from the site towards the centre of the sun, and the horizon. The solar azimuth (A) is the angle between the line from the observer to the sun projected on the ground and the line from the observer due south.

The declination (δ) is one of the two coordinates of the equatorial coordinate system, the other being either a right ascension or a hour angle. The declination is comparable to latitude, projected onto the celestial sphere, and is measured in degrees north and south of the celestial equator. One of the coordinates is used in the equatorial coordinate system for describing the position of a point on the celestial sphere.

The hour angle (H) of a point is the angle between the half plane determined by the Earth axis and the zenith (half of the meridian plane) and the half plane determined by the Earth axis and the given point. The solar altitude and azimuth are given by Eq. (1) and (2).

$$\sin\theta_e = \sin\delta\sin\phi + \cos\delta\cos\phi\cos H \quad (1)$$

$$\sin\theta_a = -\frac{\cos\delta\sin H}{\cos\theta_e} \quad (2)$$

θ_e : *Solar elevation(altitude)*

θ_a : *Solar azimuth*

δ : *Declination*

ϕ : *Latitude of observer*

H : *Hour angle*

2.2.3 Sunrise and Sunset time

The solar tracking system must be returned to the initial position after the sun disappears below the horizon, otherwise it must be started to track the sun after the sun appears above the horizon.

The sunrise and sunset time are calculated by Eq. (3).

$$T=H+\alpha-(0.06571 \times t)-6.622 \quad (3)$$

where, for sunrise, t = N+((6-lngHour)/24)

For sunset, t=N+((18-lngHour)/24)

T= Sunrise or Sunset time

H= Hour angle

N= day of year

α=Right ascension

lngHour =(longitude)/15

A right ascension (α) is the celestial equivalent of a terrestrial longitude and measures an east-west angle along the equator.

Figure 26 shows the block diagram of LabVIEW for calculating the sunrise and sunset time, which are compared with those of KASI.

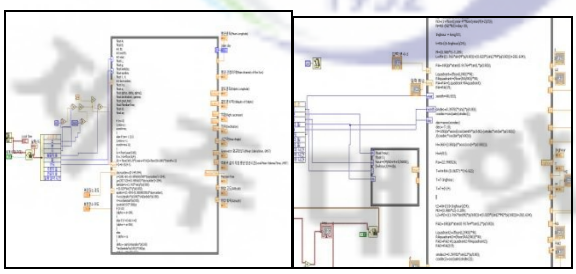

(a) (b)

Figure 26: The algorithm for solar tracking; (a) the altitude and azimuth, (b) the sunrise and sunset time

2.2.4 Major components

The ultimate goal of this study is to develop a high accuracy solar tracking system with an optical and an astronomical method. At first, the solar tracking system begins to work by using the calculated altitude, azimuth, sunrise time and sunset time. The system, then, compensates the malfunction by a feedback device (CdS) when it encounters urgent problems that the backlash of gears occurs owing to a strong wind and non-precision caused by non-exacted initial position

Four CdS sensors were used as the feedback devices. CdS sensor is a sort of variable resister whose internal resistance varies with optical energy. Cds cell generally become close to an insulator and when a light ray is incident on the surface of cell, its internal resistance drops with the incident energy.

When the system becomes perpendicular to the sun, it casts shadow on all sensors, and then the output voltage drops with the resistance increasing.

Unless otherwise, each sensor compares the outputs and makes the system move forward a higher valued sensor.

The principle of working of the solar tracking system developed in this study was showed in Figure 27.

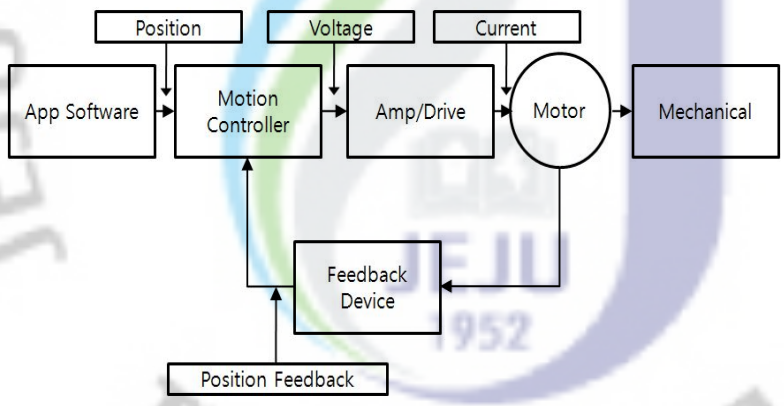

Figure 27: The principle of solar tracking system

The application written by LabVIEW calculates the solar position as well as the sunrise and sunset time and determines the steps of the step motors to transfer the signal to Motion Controller. Motion Controller transfers the signal relevant to the each axis to two step motors that revolve as many as input steps.

If the error signal occurs at the feedback sensor, the application will set up the steps and compensate the position of solar tracker.

Hardware for developing the system includes NI-7352 motion controller, stepper drive, UMI (Universal Motion Interface) and 2-axis stepper motor.

Figure 28 shows the main components of solar tracking system. This system has 2-axis; both X-axis and Y-axis are rotated by stepper motors. A bevel gear with 2:1 of gear ratio was used at X-axis and sprocket gear and chains were used at Y-axis for power delivery. Stepper drive and UMI were installed in a lower part, which power the stepper motors. There is a frame in an upper part at which the mini-dish and the CdS sensors were installed.

The height of the system is 75cm and the width is 40 x 40 cm. The frame was made of aluminium profile.

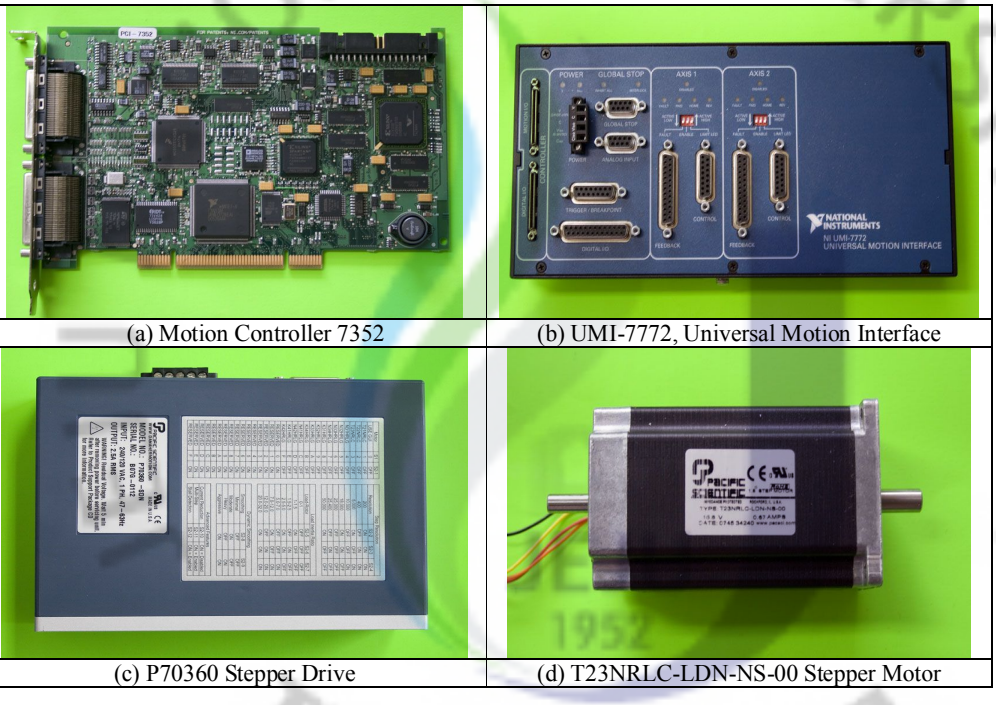

(a) Motion Controller 7352 | (b) UMI-7772, Universal Motion Interface

(c) P70360 Stepper Drive | (d) T23NRLC-LDN-NS-00 Stepper Motor

Figure 28: The main components of solar tracking system

삭제됨:

2.2.5 Application Software

In this study, LabVIEW was used for developing the algorithm and application programme.

LabVIEW (short for Laboratory Virtual Instrumentation Engineering Workbench) is a platform and development environment for a visual programming

language from National Instruments. The graphical language is named "G". Figure 15 shows the control application developed in LabVIEW.

As soon as the application runs, the solar altitude and azimuth angle, sunrise and sunset times are calculated on a real time basis at SubVI in the loop showed in Figure 29 (a). In order to compute the number of step of motors, the solar altitude and azimuth angle are then input into another loop in which the step-angle (0.144) and the gear ratio are multiplied and the final steps are outputted out of loop. The sunrise and sunset times are transmitted to (c) loop and those then are compared with the present time during calculating steps. If the sunrise time corresponds to the present time, the system begins to track the sun from the initial position, otherwise, if the sunset time corresponds, the system halts after returning to the initial position.

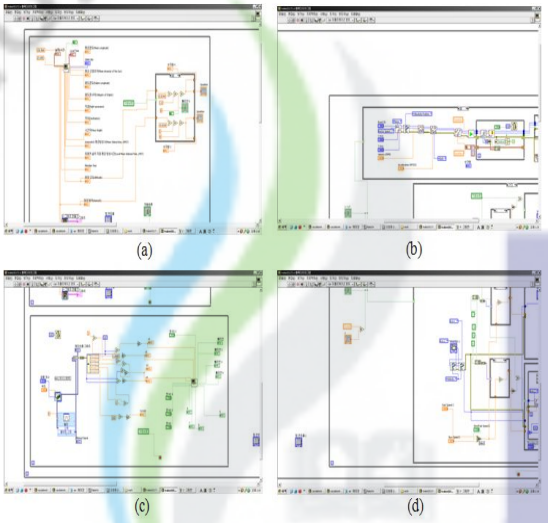

Figure 29: The block diagram for system control

The final steps outputted from (a) loop are transmitted to (b) loop in which the command was transferred to the Motion controller. In (b) loop the real-time values of four CdS sensors are read and compared with each other.

If all signals of sensors are equal, the system continues to work in an open loop. If any signal of sensors differs with others, the direction is decided in the loop and transmitted into (d) loop. In (d) loop, the direction command is continuously transferred to the Motion Controller until all of the outputs of sensors are equal.

Figures 30 and 31 show the results that the solar altitude and azimuth calculated in this study was compared with those of KASI (Korea Astronomy & Space Science Institute).

The experimental conditions are as follows:

• Location : Jeju city, Jeju do, Korea

• Longitude : Long. 126°15′60″ E

• Latitude : 33° 30′ 30″ N. Lat.

• Date : 1st of January, 2009

• Time : 00:01~ 24:00

The maximum error of the solar altitude angle was 0.0371 degree at 4 pm (local time). Otherwise, the minimum error was 0.0006degree at 10 am (local time). The maximum error of the solar azimuth angle was 0.0823 degree at about 1 pm (local time), otherwise the minimum error was 0.0012 degree at about 5 pm (local time). It was found that the both maximum errors were occurred at dawn but this has not effect on the result as there is no sun.

The sunrise and sunset time were calculated for the month of January, 2009, which were compared with those of KASI. It was found that the average errors were less than 1 second. Figure 8 shows the still shots of the solar tracking system where the concentrated beam emerged from the other end of the fibre. The concentrated beam could be used either for space illumination or for irradiation onto the multi-junction cells for electricity production at high efficiency. The emergence of the concentrated beams at the end of fibre is a testimony of the accuracy achieved by the solar tracker.

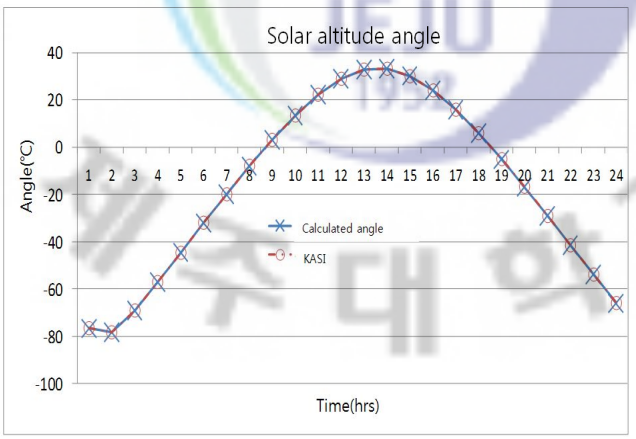

Figure 30: Solar altitude

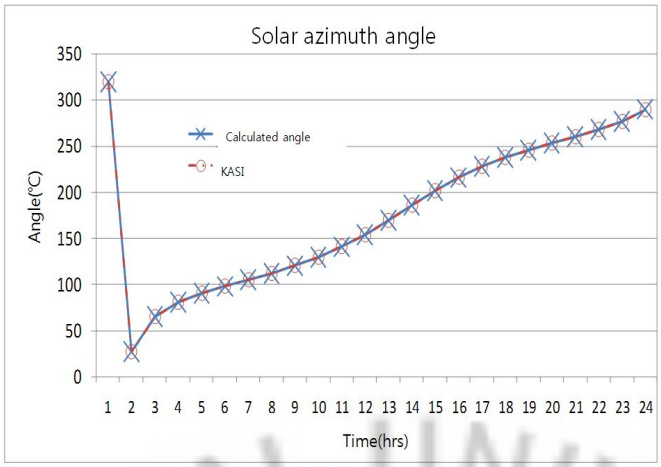

Figure 31: Solar azimuth

The solar tracking system is found to be accurate and cost-effective and it can be used in many fields such as data-processing, concentrated PV, the photocatalyst generation of hydrogen, and contributing to the harnessing of the solar energy.

2.3 The concept of total daylighting system

The total daylighting system consists of one master module (unit) with a solar tracker which controls other slave modules (Fig. 32).

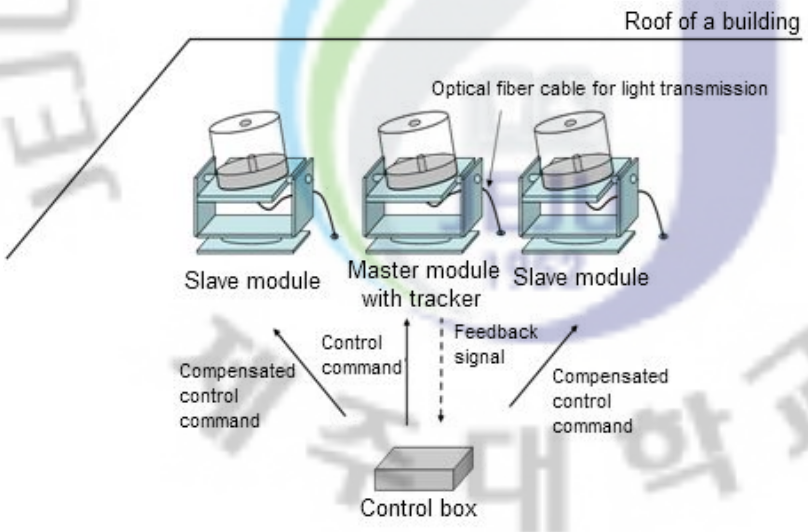

Figure 32: A fiber optic mini-dish solar concentrator daylighting system installed on the roof of a building [30]

A control algorithm of the daylighting system is depicted in Figure 33. An internal clock mechanism, sun sensors and a microprocessor allows precisely align system's units directly against the sun.

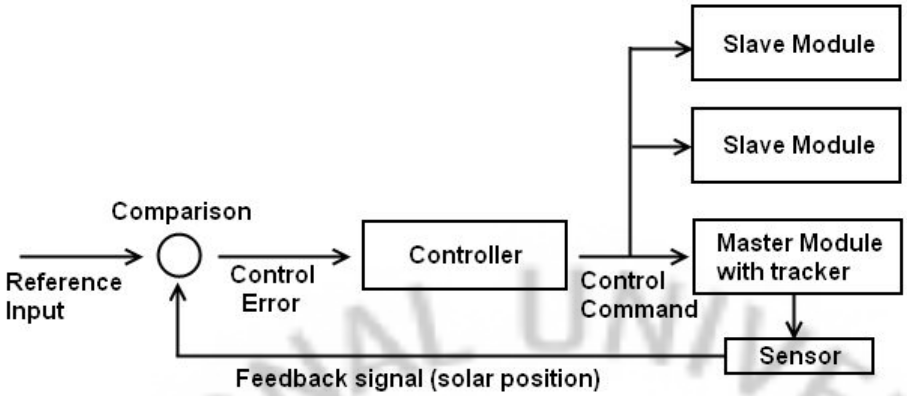

Figure 33: Control algorithm of the daylighting system

III. EXPERIMENTAL PROCESS

3.1 Photometric measurements

In order to assess the daylighting system's efficiency, there was carried out two photometric measurements of the typical classrooms as shown in Figures 34 and 35 with south- and north-oriented windows in Jeju city, Korea (Latitude: 33.3 N, Longitude: 126.3 E).

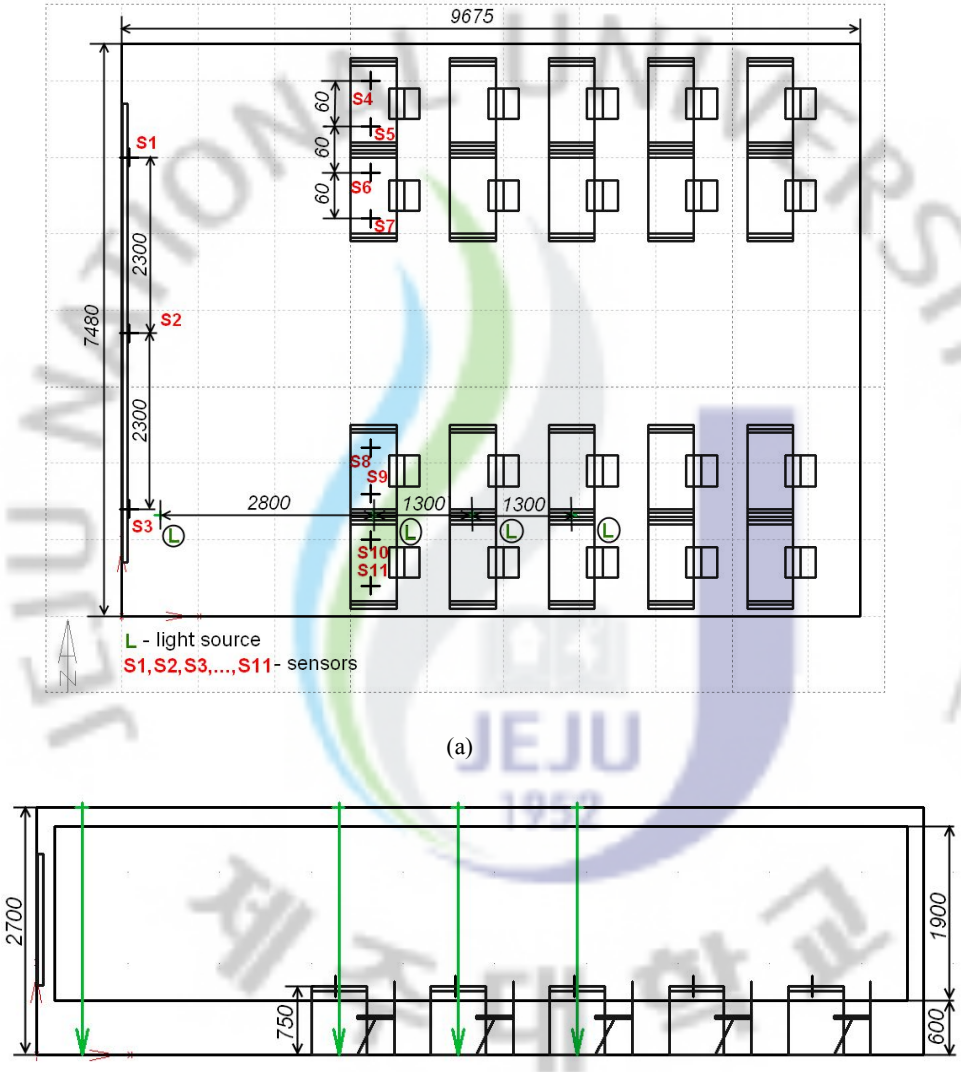

(a)

(b)

Figure 34: (a) Overall dimensions and (b) sensors' location

(a)

(b)

Figure 35: Hemispherical pictures of classroom with (a) north-oriented and (b) south-oriented windows

At the same time classrooms were modeled by using ECOTECT and exported to RADIANCE for the daylighting simulation. Results from measurements and simulations were analyzed comprehensively, then after validation of strong reliability between them, we modeled both classrooms with installed abovementioned daylighting systems according to ergonomic lighting conditions in classrooms.

3.2 Measurement instruments

3.2.1 Photometric sensor LP 471 PHOT

Photometric sensor (probe) LP 471 PHOT was used for illuminance measurements (Fig. 36). Its measurement range is 0.01 lux – 200 x 10^3 lux.

Figure 36: Photometric sensor (probe) LP 471 PHOT

This kind sensor was used also for measuring the outside diffuse illuminance (Fig. 37):

Figure 37: LP 471 PHOT sensor with its shadowing ring

3.2.2 Luminance meter LS-100

The Luminance Meter LS-100 (Konica Minolta) is a compact, lightweight meter (Fig. 38) for measuring the luminance of light sources or reflective surfaces. The TTL (through-the-lens) viewing system enables accurate targeting of the subject.

Figure 38: Luminance Meter LS-100

Main Specifications:

Type	SLR spot luminance meter for measuring light-source and surface brightness
Acceptance angle	1°
Optical system	85mm f/2.8 lens; SLR viewing system; flare factor less than 1.5%
Angle of view	9°
Focusing distance	1014mm (40 in.) to infinity
Minimum measuring area	Φ14.4mm
Relative Spectral Response	Within 8% (fl´) of the CIE spectral luminous efficiency V (λ)
Luminance units	cd/m^2 or fL (switchable)
Measuring range	FAST: 0.001 to 299,900cd/m^2 (0.001 to 87,530fL) SLOW: 0.001 to 49,990cd/m^2 (0.001 to 14,590fL)
Accuracy	0.001 to 0.999cd/m^2 (or fL): ±2% ±2 digits of displayed value 1.000cd/m^2 (or fL) or greater: ±2% ±1 digit of displayed value
	(Illuminant A measured at ambient temperature of 20 to 30°C/68 to 86°F)
Color correction factor	Set by numerical input; range: 0.001 to 9.999
Dimensions	79×208×150mm (3-1/8×8-3/16×5-7/8 in.)
Weight	850g (30 oz.) without battery

3.2.3 Thermal Imaging InfraRed camera FLIR i40

The daylighting system affects also to the cell's internal temperature. Therefore for thermal analysis we used the thermal imaging infrared camera FLIR i40 (Fig. 39).

Figure 39: Thermal Imaging InfraRed camera FLIR i40

Main Specifications:

Temperature range	-4°F to 662°F (-20°C to 350°C)
Temperature accuracy	±2°C or ±2% of reading
Image Storage	>1000 Images (1GB micro SD memory card)
Emissivity	0.1 to 1.0 (adjustable); Emissivity Table
Field of view/min focus distance	25° X 25°/0.10m (3.9")
Thermal sensitivity (N.E.T.D)	<0.1°C at 25°C
Detector Type	Focal plane array (FPA) uncooled microbolometer; 14,400 pixels (120 X 120)
Spectral range	7.5 to 13µm
Display	3.5" color LCD
Visible Light Camera Resolution	0.6 Megapixels
Image Modes	Thermal, Visual, Fusion
Image Controls	Palettes (Iron, Rainbow, and Black/White), level, span, auto adjust (continuous/manual)
Dimensions	9.3x3.2x6.9" (235x81x175mm)
Weight	<1.32lbs (600g), including battery

3.2.4 Pyranometer LP PYRA 02

Pyranometer LP PYRA 02, which fully complies with ISO 9060 standards, is well suited for the measurement of incoming global solar radiation (0.3µm ÷ 3µm spectral range). Its shadow ring is designed to shield the instrument sensor from direct radiation; by that, an exact measurement of the diffuse sky radiation will be possible (Fig. 40).

Figure 40: Pyranometer LP PYRA 02

Main Specifications:

Typical sensitivity	10 µV/(W/m2)
Impedance	33 Ω ÷ 45 Ω
Measuring range	0 ÷ 2000 W/m2
Viewing field	2π sr
Spectral field	305 nm ÷ 2800 nm W/m^2 (50%)
Operating temperature	-40 °C ÷ 80 °C
Response time	< 28 sec < 30sec
Dimensions	9.3x3.2x6.9" (235x81x175mm)
Weight	0.9 kg

3.2.5 UV-Vis Spectrophotometer SCINCO S-3100

The S-3100 System is a multi-channel spectrophotometer (Fig. 41) with a 1 inch 1024 channel photodiode array giving optimum wavelength resolution. One of features of a PDA is an integrating photo-detector which integrates charge depending on the light intensity. The advantage of the integrating function is named Felgette`s S/N advantage or Multi-channel advantage.

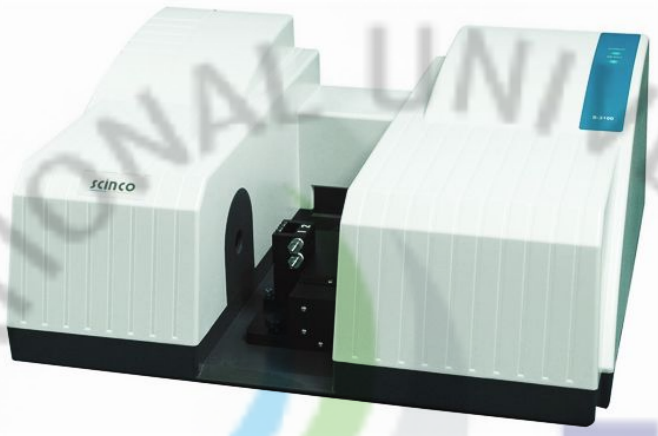

Figure 41: UV-Vis Spectrophotometer SCINCO S-3100

Main Specifications:

Wavelength Range	190 ~ 1100 nm
Detector	1024 Channels PDA
Wavelength Resolution	0.95 nm
Wavelength Accuracy	0.5 nm
Wavelength Reproducibility	< 0.02 nm
Baseline Flatness	< 0.0005 AU
Integration Time	0.02 ~ 6 sec

3.3 Simulation

3.3.1 RADIANCE

RADIANCE is a sophisticated lighting visualization system (Fig.42). Originally started as a research project at the Lawrence Berkeley Laboratories, it has evolved into an extremely powerful package that is capable of producing physically correct results and images that are indistinguishable from real photographs.

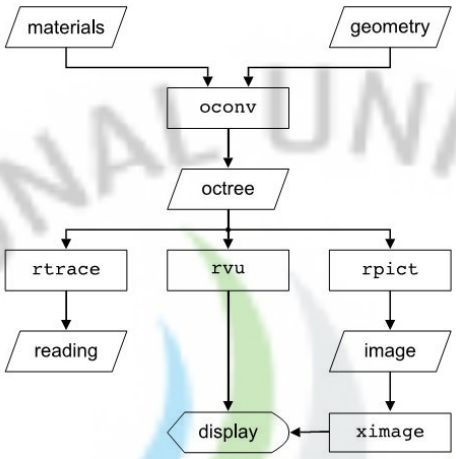

Figure 42: The main components of the RADIANCE rendering system

Its versatility makes RADIANCE the ideal choice not only for 'serious' researchers but also for architects, lighting designers and other professionals. Although a challenge to learn, Radiance, especially in a UNIX environment, is capable of producing results that no other visualization package can achieve.

The major portion of the RADIANCE package, and the part that is of chief interest to users, is the lighting simulation engine that calculates light levels and renders images. The input required for this simulation is a description of the 3-dimensional surface geometry, materials, and light sources in a scene. Rendering an image requires additional specification for the view point, direction, and angles desired.

Once a scene's geometry has been described, it is compiled into an "octree" that acts as an efficient data structure for the ray tracing process (ie. determining which surface a ray intersects). Without an octree or similar sorting method, ray tracing is not practical.

The lighting simulation engine of RADIANCE uses a hybrid approach of Monte Carlo and deterministic ray tracing to achieve a reasonably accurate result in a reasonable time. The method employed starts at a measurement point (usually a viewpoint) and traces rays of light backwards to the sources (i.e. emitters). The calculation can be divided into three main parts: the direct component, the specular indirect component, and the diffuse indirect component.

The direct component consists of the light arriving at a surface directly from light sources or via one or more perfectly specular transfers from other surfaces. A list of emitters is used and sorted based on potential contribution to minimize the number of rays required for visibility testing. Monte Carlo sampling is coupled with adaptive subdivision of the large sources for accurate penumbra calculation. Specular transfers from large planar surfaces are handled efficiently through the use of "virtual" light sources, which guide the direct calculation to the original sources.

The specular indirect component consists of light arriving at a surface from other surfaces and being reflected off or transmitted through in a directional manner. Perfectly specular transfers are handled by simply redirecting the ray in the appropriate reflected or transmitted direction. Rough specular transfers are modeled with Monte Carlo sampling of the reflected and/or transmitted direction.

The diffuse indirect component consists of light arriving at a surface and being reflected or transmitted with no directional preference. The nature of this component requires that hundreds of directions be examined in order to make a reasonable Monte Carlo estimate. Fortunately, the diffuse indirect component changes slowly over surfaces, thus a few carefully calculated values at properly spaced intervals may be interpolated at the points in between. This is the basic assumption of the "radiosity" method, which is similar in principle to the diffuse indirect calculation of RADIANCE, but places additional restrictions on the input (ie. simple geometry and diffuse surfaces). The indirect irradiance caching scheme of RADIANCE also makes use of gradient information available during each Monte Carlo evaluation to further improve the interpolation used.

In addition to the basic simulation method described, a secondary light source calculation may be performed for windows, skylights and other illumination "portholes". The distribution of such a source is computed in a preprocess, greatly improving the efficiency and accuracy of the final rendering.

Radiance employs backward ray-tracing algorithms. This means that the light 'rays' are traced back from the point of measurement or view to the light source. There are a number of other ray-tracers on the market because the basic principle is relatively simple to implement on computers. However, where Radiance stands out is its ability to handle diffuse inter-rejections between objects. Very efficient algorithms together with caching are applied for this. Other packages usually try to equate for indirect contributions by denying the 'ambient' light that has no real source and somehow is everywhere. Examples for other ray-tracers include POV or 3DStudio Max.

Because the calculations are started from the view point, an entirely new calculation has to be done for each individual view. Walk-throughs and videos are therefore extremely resource-hungry requiring fast computers and a lot of time.

There is another conceptually different approach to compute light distributions. This method is called radiosity. Radiosity-based algorithms start off with the energy that is radiated from the light source. Assuming diffuse reflectance properties of the objects, the incoming energy is then modified by the material's reflective properties and bounced back into the room. This is done until the contribution of the reflected light towards the average illuminance in the scene becomes insignificant.

The energy distribution of the entire scene is calculated and stored. This means that once all the calculations are done, new viewpoints can be created in no time at all. This makes the radiosity solutions ideal for the creation of virtual worlds such as VRML. Scenes created this way can usually be told because of their lack of reflective and transparent surfaces, although newer software implements get-arounds to these problems. A typical example of a simulation package that uses radiosity is VIZ (ex Lightscape) by AutoDesk.

3.3.2 ECOTECT

The original ECOTECT software was written as a demonstration of some of the ideas presented in PhD thesis by Dr. Andrew Marsh at the School of Architecture and Fine Arts at The University of Western Australia. The fundamental theme of this thesis was that building performance concerns are best addressed by architects at the most conceptual stages of design, not at the very end of the process where nothing but few cosmetic changes are possible. A great deal of time and money can be saved getting it right from the start.

As ECOTECT deals with many different aspects of building performance, it needs a wide range of data to describe the building. To reduce the burden on the designer, ECOTECT uses a unique system of progressive data input. Initially only simple geometric details are needed. As the design model is refined and more accurate or detailed feedback is required, the user makes more choices and enters more data as it becomes important. This means that you can be analyzing the sun penetration, shading options and available light after only a few mouse clicks.

Performance information is critical at the earliest stages if you are to avoid abortive work on inappropriate design solutions, hence yielding significant operational cost savings for both you and your client. However, designing in this way means moving beyond traditional CAD systems to a tool that actually knows that you're designing a building and not a gearbox. Obviously some background knowledge is required to fully utilize the wide range of analysis options available in ECOTECT.

The most significant feature of ECOTECT is its interactive approach to analysis. Change the type of carpet on the floor and compare changes in the room's acoustic response, its reverberation time, light levels and internal temperatures. Add a new window and immediately see its thermal effect, weighing that up against changes in daylight factor, incident solar radiation and overall building cost. Spray sound particles around an enclosure and watch the wave fronts reflect and slowly decay in 3D. ECOTECT is also the only application of its kind to include comfort, greenhouse gas emissions and embodied energy analysis alongside capital and running costs for direct comparison.

Another major part of ECOTECT was the development of its innovative 3D interface. A traditional geometric CAD system is actually not that appropriate for early design development, being far too onerous and specific in its input requirements - forcing a designer to think mathematically at a time when they are only really thinking intuitively. Thus, a flexible and intuitive relational 3D construction system has been designed that exploits a surprisingly simple set of inherent relationships between building elements to greatly simplify the creation of even the most complex geometry, and to vastly increase its ongoing editability.

ECOTECT allows to do the following:

- Display and animate complex shadows and reflections,

- Generate interactive sun-path diagrams for instant overshadowing analysis,
- Calculate the incident solar radiation on any surface and its percentage shading,
- Work out daylight factors and artificial lighting levels either spatially or at any point,
- Calculate monthly heat loads and hourly temperature graphs for any zone,
- Generate full schedules of material costs and environmental impact,
- Trace the paths of acoustic particles and rays within any enclosures of any shape,
- Spray sound particles around an enclosure and watch the rate of decay,
- Quickly calculate statistical and raytraced reverberation times in any space,
- Export to VRML for interactive visualisation and presentation to clients,
- Export to the RADIANCE Lighting Program for physically accurate lighting analysis,
- Read and write a wide range of CAD and analysis file formats.

Figures 43 and 44 depict the schoolroom modeled in ECOTECT and RADIANCE.

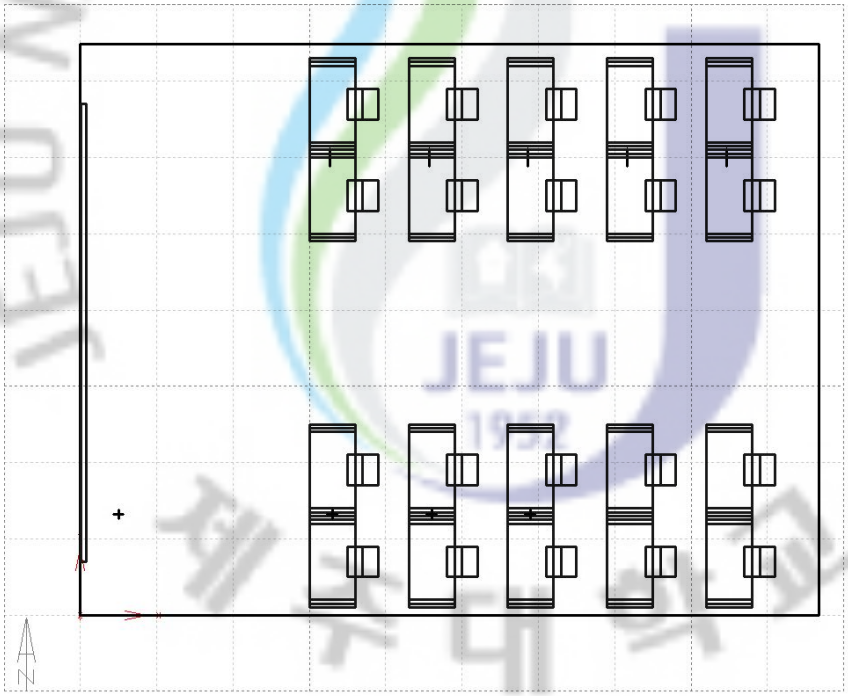

(a)

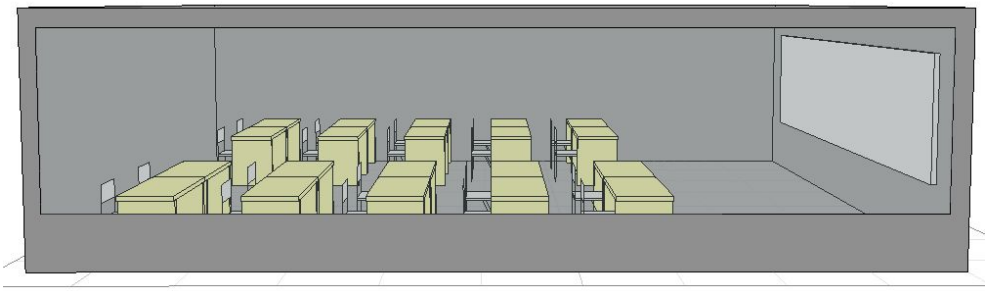

(b)

Figure 43: (a) Plan view, (b) general view of classroom model in ECOTECT

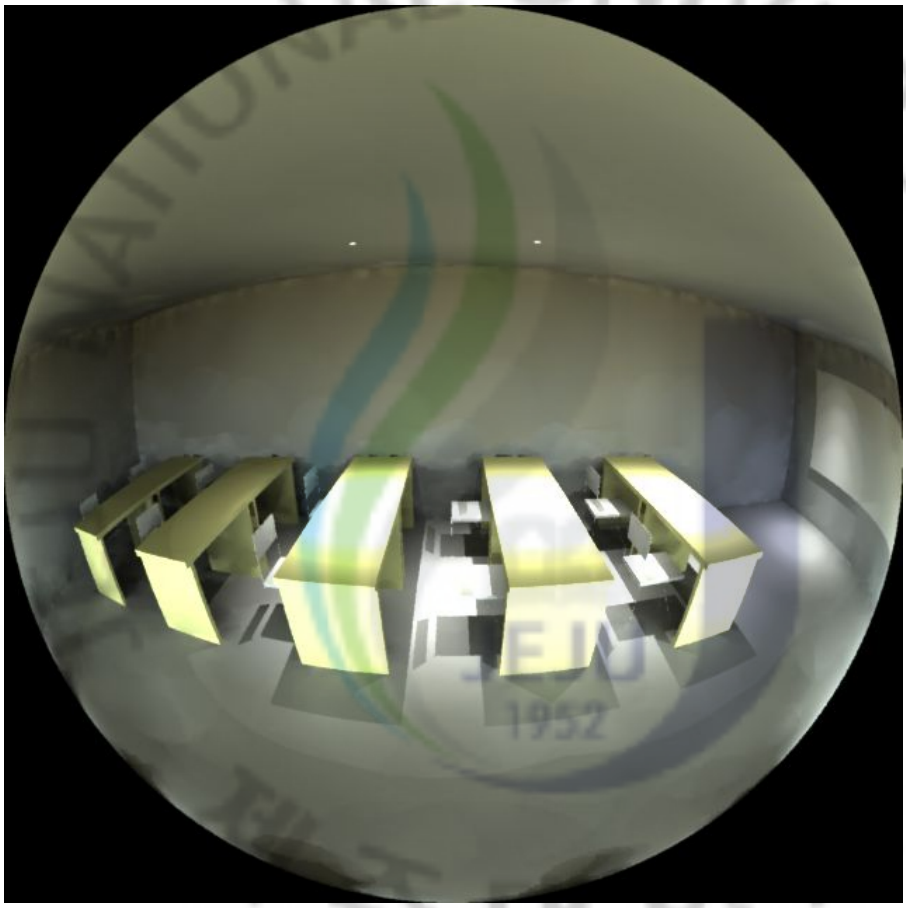

Figure 44: Internal view of classroom model generated by RADIANCE

IV. RESULTS AND DISCUSSION

Reliability of the simulation results was proven in previous researches and in our case we made a measurement and simulation analysis of sensor values.

Table 6: Measurement and simulation comparison of sensor values

Sensor	101	102	103	106	107	108	109	110
MEASUREMENT	1059.5	587.9	381.9	901.4	717.2	355.2	302.2	373.9
RADIANCE	1058.4	586.1	381.9	1009.1	766.5	324.5	278.3	250.8

Figure 45: Sensors' location in the schoolroom model generated by RADIANCE

Luminance values were measured each hour with luminance meter (LS-100). The height of measured points was 175 cm (Fig. 46).

Table 7: Luminance values (cd/m^2) in the north-oriented classroom in December 22, 2009 (sunny day)

	1	2	3	4	5	6	7 (outside)
10:00	230	192	149	116	102	242	4200
11:00	272	204	148	128	104	256	4360
12:00	282	221	164	148	115	278	4540
13:00	298	231	174	152	120	283	4582
14:00	303	241	174	152	121	271	4401
15:00	302	217	141	121	100	206	3169
16:00	178	129	89	78	61	136	2038
17:00	56	36	24	20	15	28	355

Table 8: Luminance values (cd/m^2) in the north-oriented classroom in December 23, 2009 (cloudy day)

	1	2	3	4	5	6	7 (outside)
10:00	369	64	13	32	10	86	282
11:00	569	101	21	46	15	176	642
12:00	1257	203	43	101	36	352	1455
13:00	935	200	38	89	35	336	1083
14:00	719	172	34	61	29	307	927
15:00	414	99	20	41	17	154	406
16:00	295	63	15	29	13	131	387
17:00	29	7	1.2	2.3	1	11	57

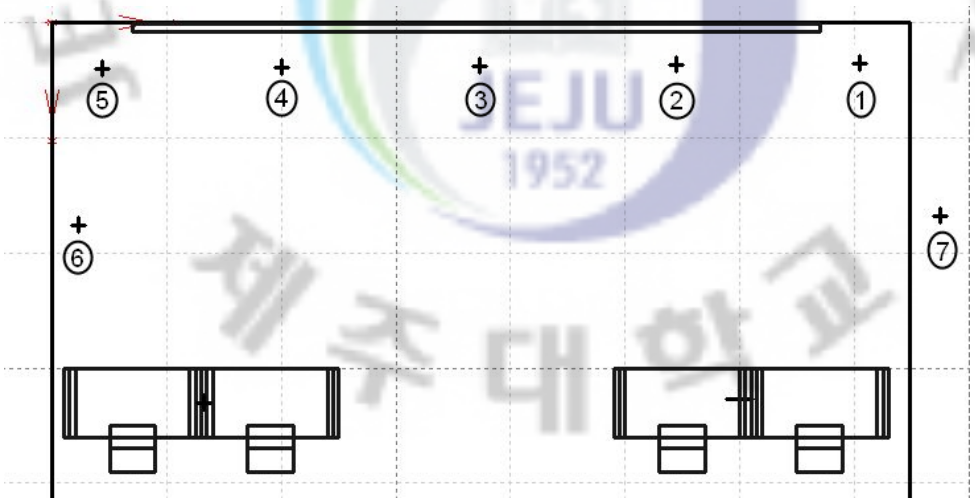

Figure 46: Location of measured points in the schoolroom

Figure 47 shows the luminance ratio (contrast) maps of sky luminance produced by RADIANCE. The sky images are taken by a digital camera using fisheye lens. For consistency, the pictures are taken at a point throughout the observation. The luminance maps reflect sky conditions, which constantly change as time elapses. As shown in figure, the region near the sun is presented by the contours of the highest luminance value indicating the presence of the sun in its vicinity.

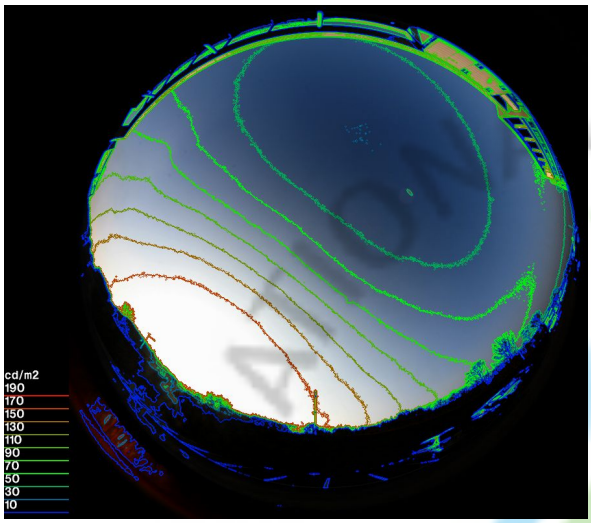

10:00 a.m.

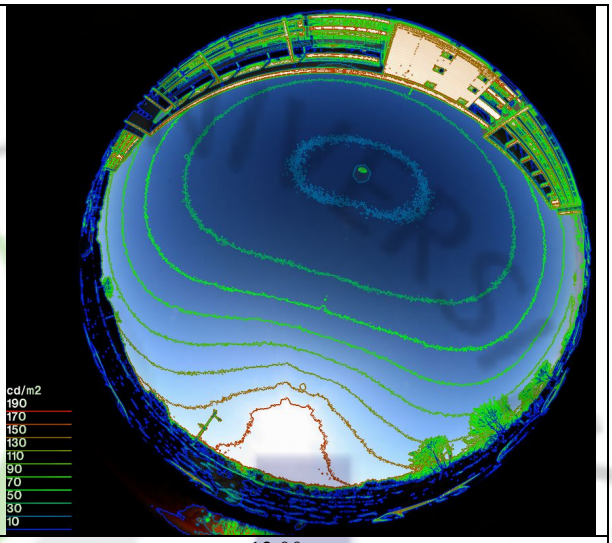

12:00 p.m.

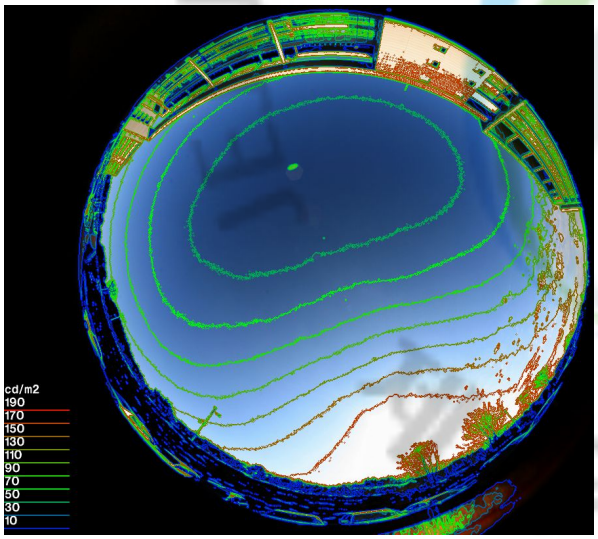

2:00 p.m.

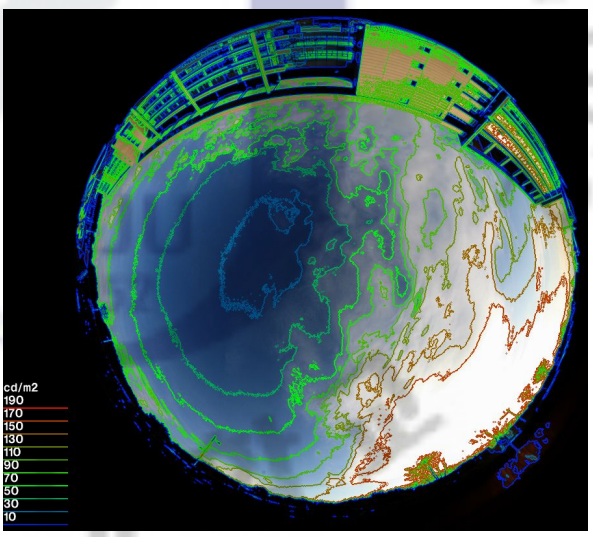

4:00 p.m.

Figure 47: Luminance ratio (contrast) maps of sky luminance in December 22, 2009

Figure 48 shows the iso-contour lines generated by superimposing the results of RADIANCE photometric analysis on the original picture. They provide the spatial distribution of the illuminance and luminance values for the classroom at different hours of the day (without daylighting systems): 10:00 am, 12:00 pm, 2:00 pm and 4:00 pm.

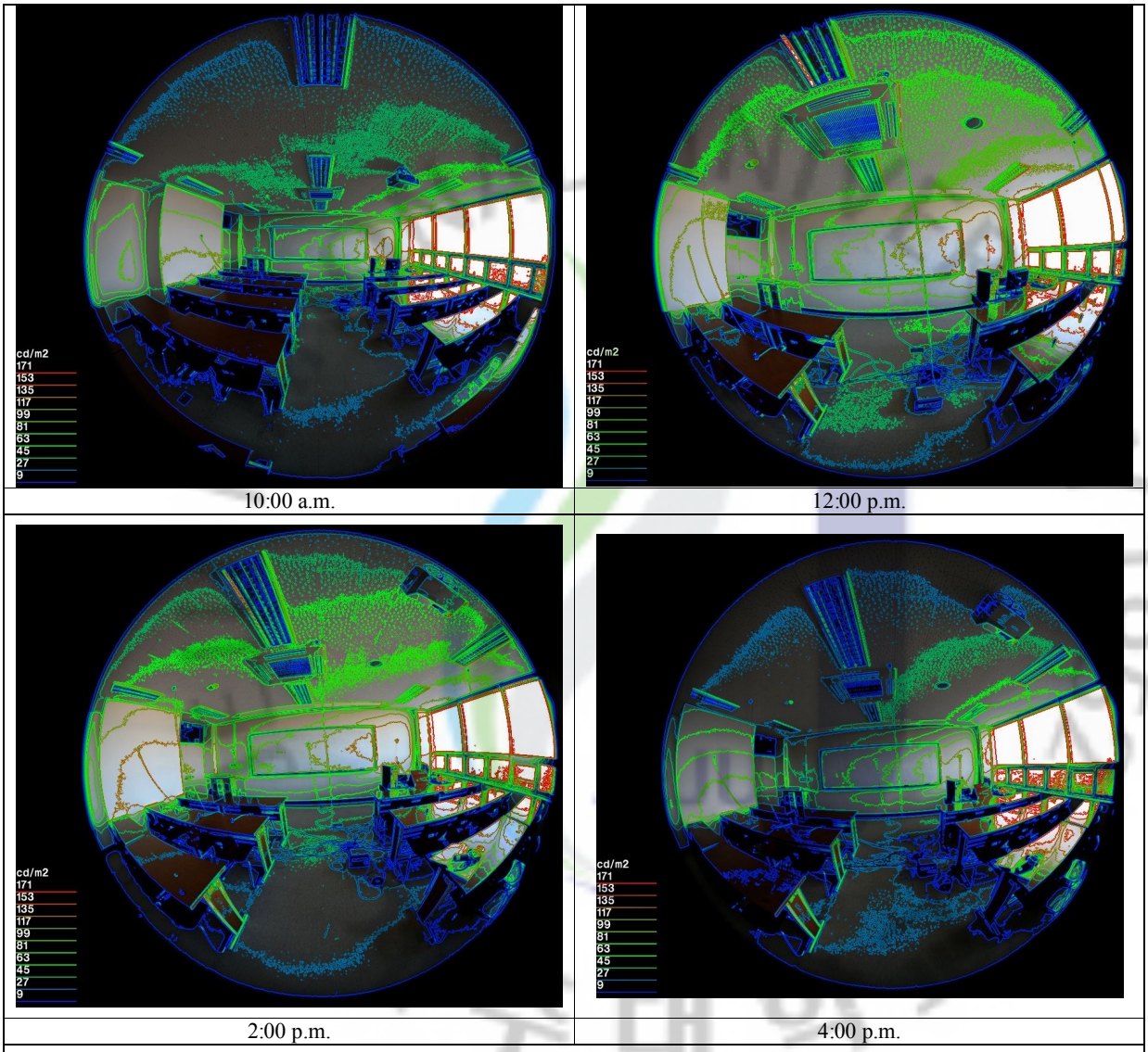

10:00 a.m. | 12:00 p.m.

2:00 p.m. | 4:00 p.m.

Figure 48: Luminance distribution in classrooms

4.1 Classroom with north-oriented windows

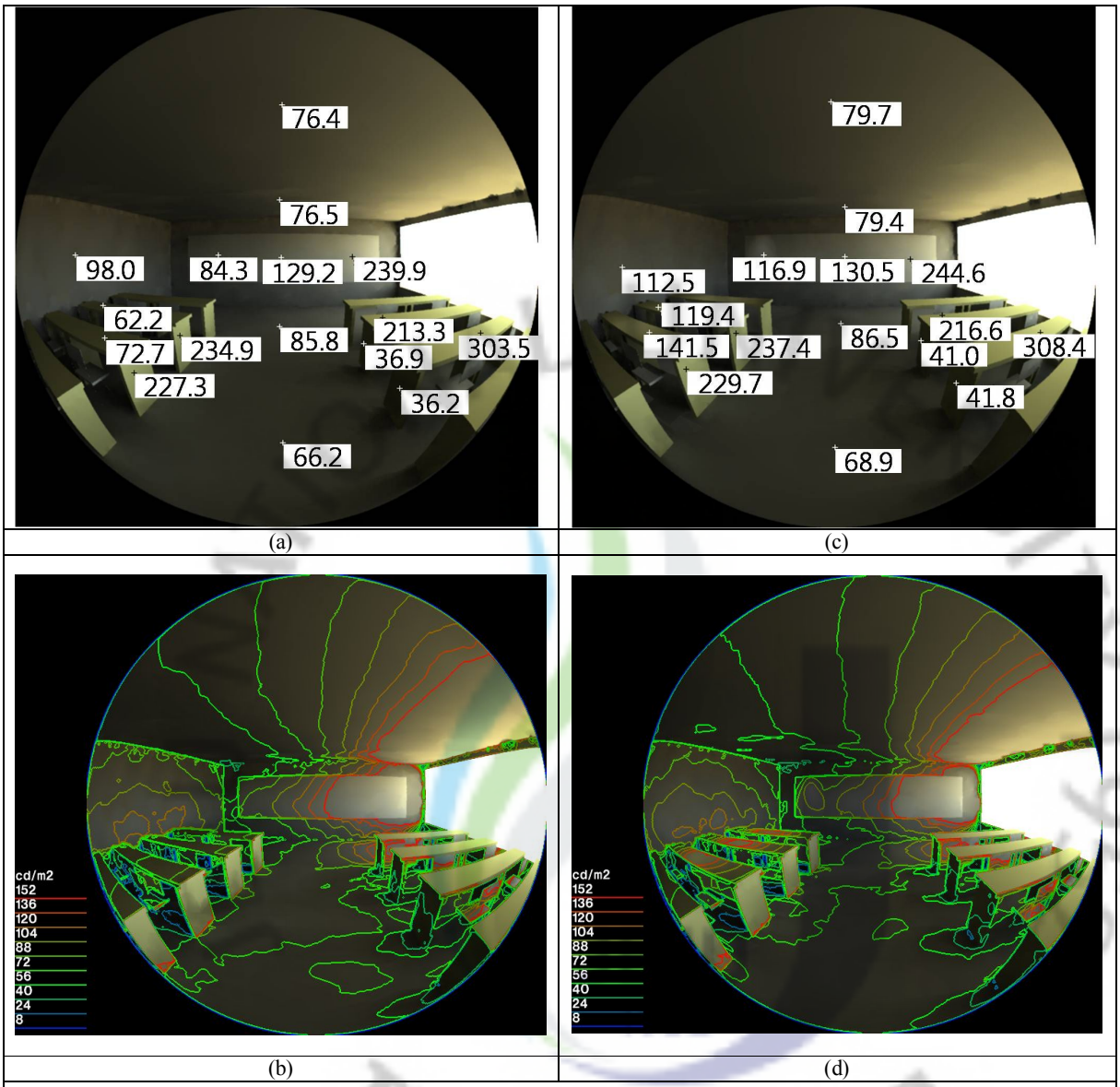

Figure 49: Luminance distribution without [(a),(b)] and with [(c), (d)] at 10:00 am

Luminance values in the north-oriented classroom at 10:00 am changed slightly on the south-side wall from 98.0 cd/m^2 to 112.5 cd/m^2 with the daylighting system and on the table under the diffuser – from 72.7 cd/m^2 to 141.5 cd/m^2.

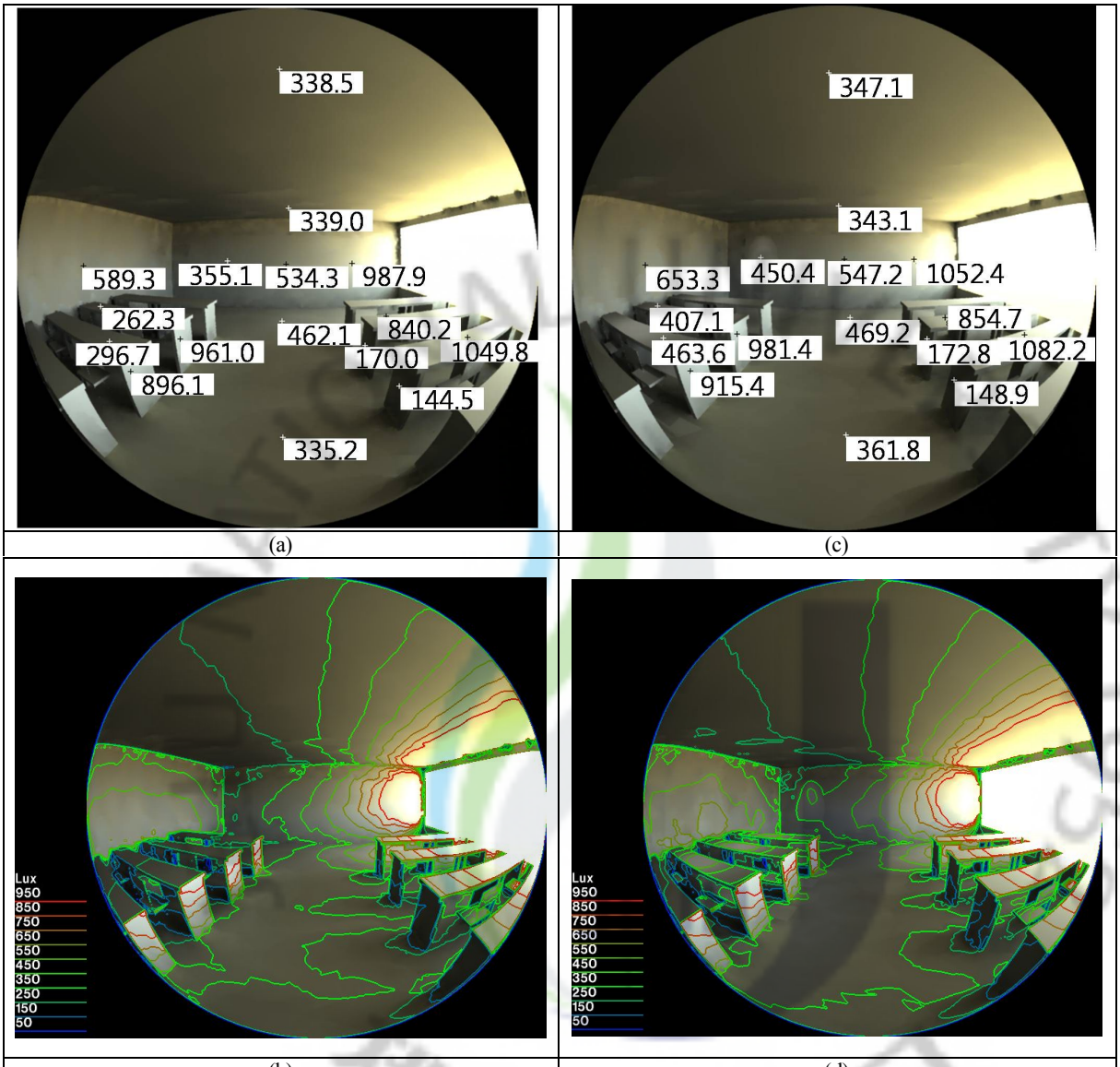

Figure 50: Illuminance distribution without [(a),(b)] and with [(c), (d)] at 10:00 am

Illuminance distribution in the north-oriented classroom at 10:00 am was in the similar situation: on the south-side wall from 589.3 lux to 653.3 lux with the daylighting system and on the table under the diffuser – from 296.7 lux to 463.6 lux.

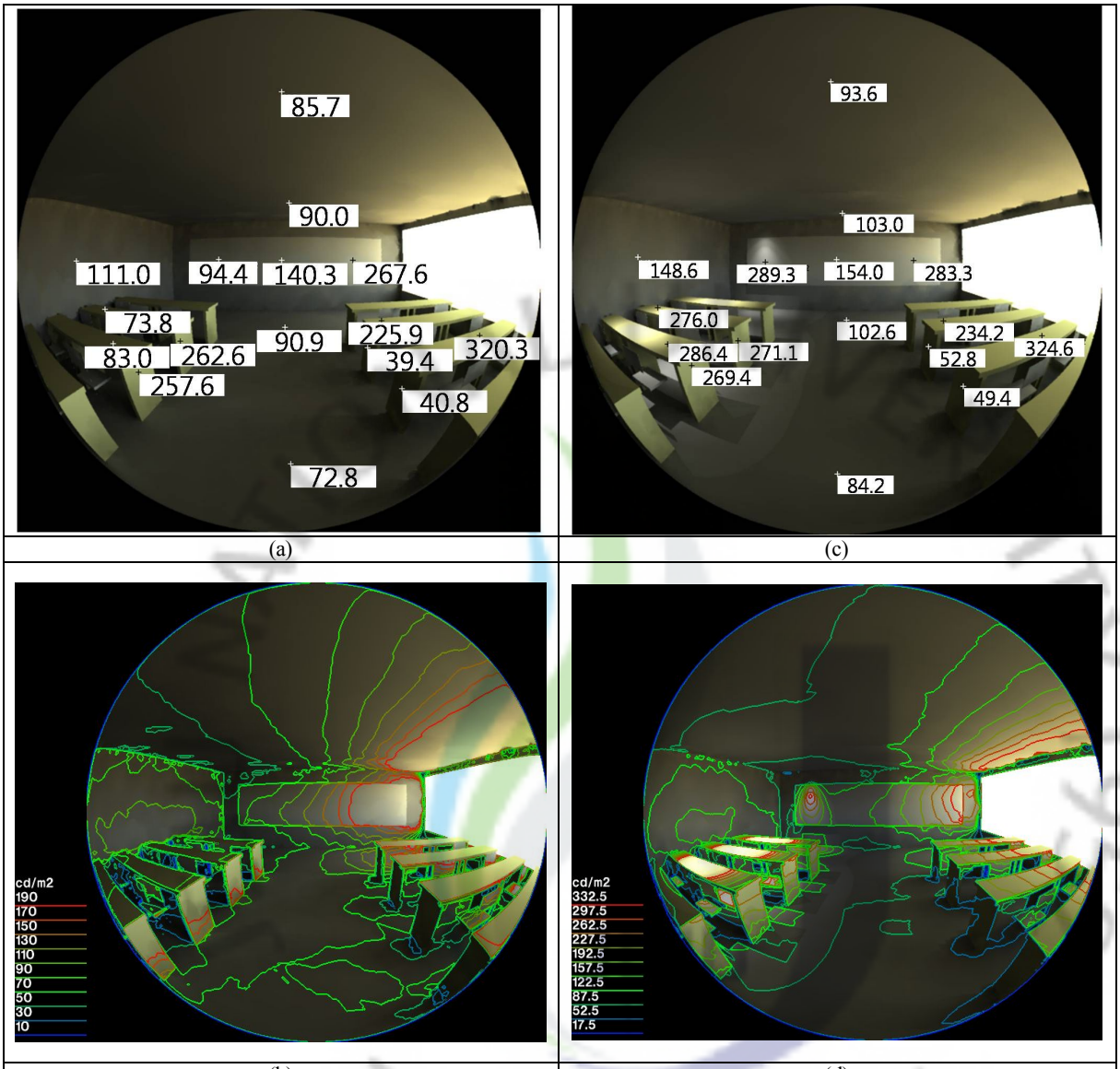

(a) (c)

(b) (d)

Figure 51: Luminance distribution without [(a),(b)] and with [(c), (d)] at 12:00 pm

Luminance distribution in the north-oriented classroom at noon had highest values: on the south-side wall from 111.0 cd/m^2 to 148.6 cd/m2 with the daylighting system and on the table under the diffuser – from 83 cd/m^2 to 286.4 cd/m^2.

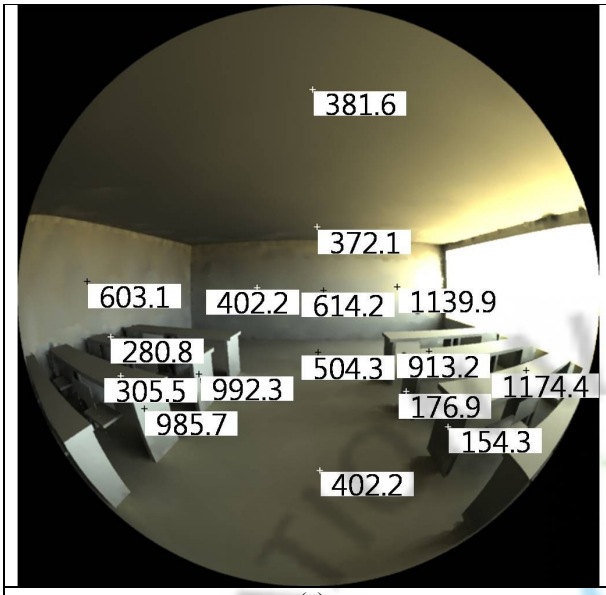

(a)

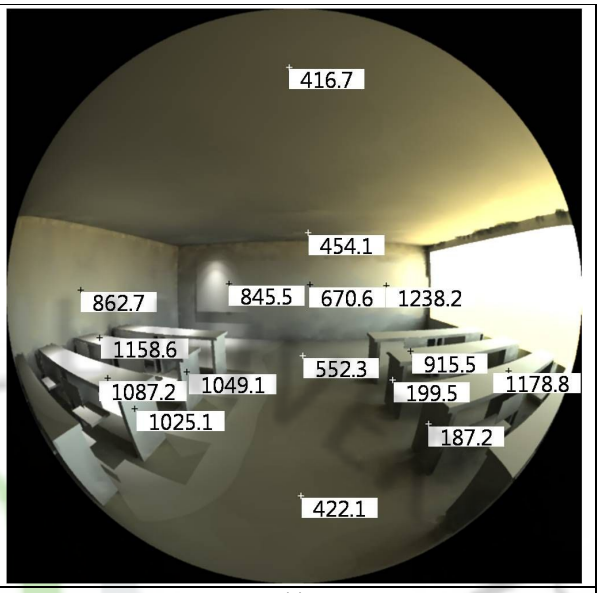

(c)

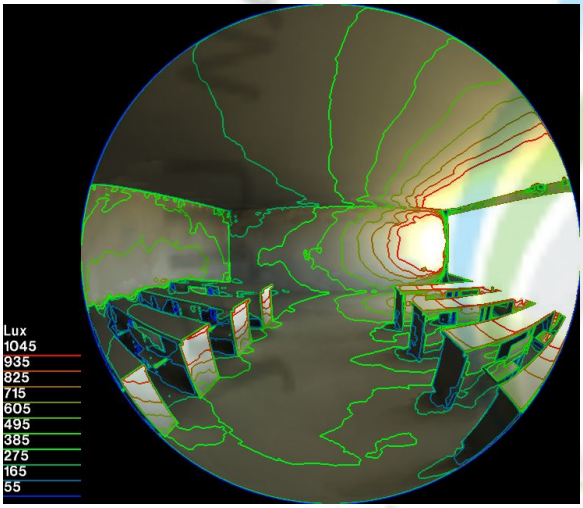

(b)

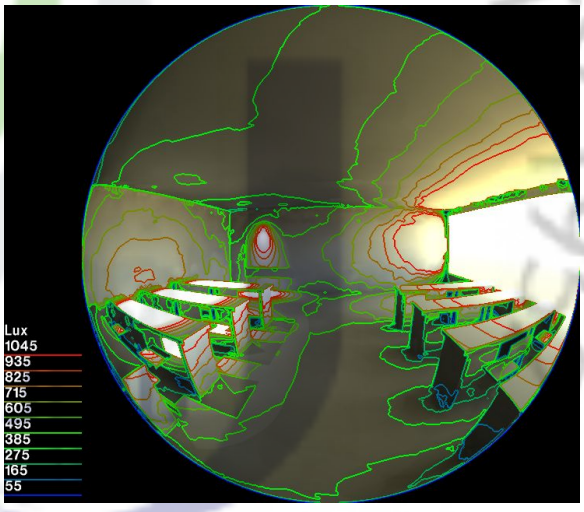

(d)

Figure 52: Illuminance distribution without [(a),(b)] and with [(c), (d)] at 12:00 pm

Illuminance distribution in the north-oriented classroom at noon changed as: on the south-side wall from 603.1 lux to 862.7 lux with the daylighting system and on the table under the diffuser – from 305.5 lux to 1087.2 lux.

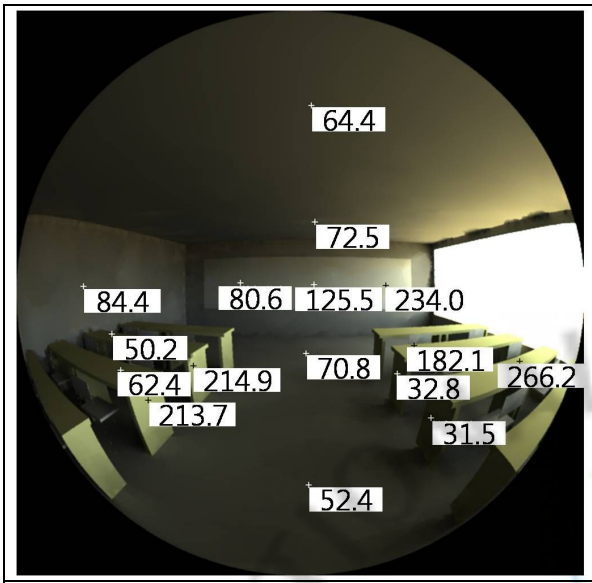

(a)

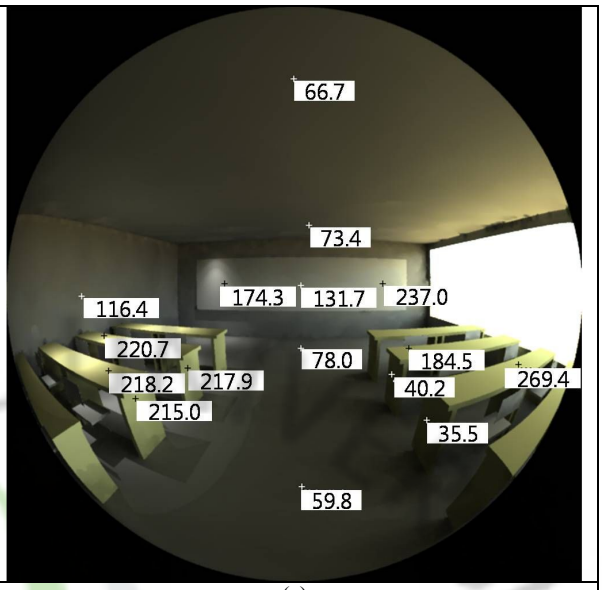

(c)

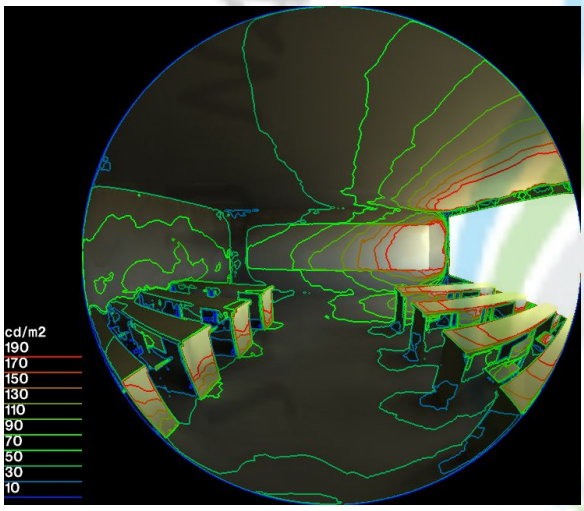

(b)

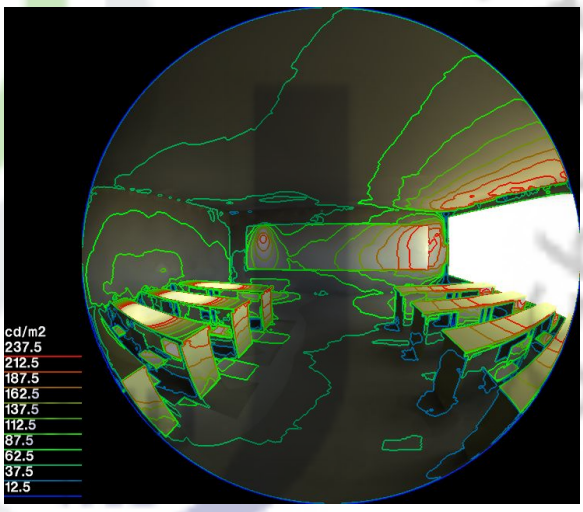

(d)

Figure 53: Luminance distribution without [(a),(b)] and with [(c), (d)] at 2:00 pm

Luminance values in the north-oriented classroom at 2:00 pm were 84.4 cd/m^2 and 116.4 cd/m^2 on the south-side wall and on the table under the diffuser – 62.4 cd/m^2 and 218.2 cd/m^2.

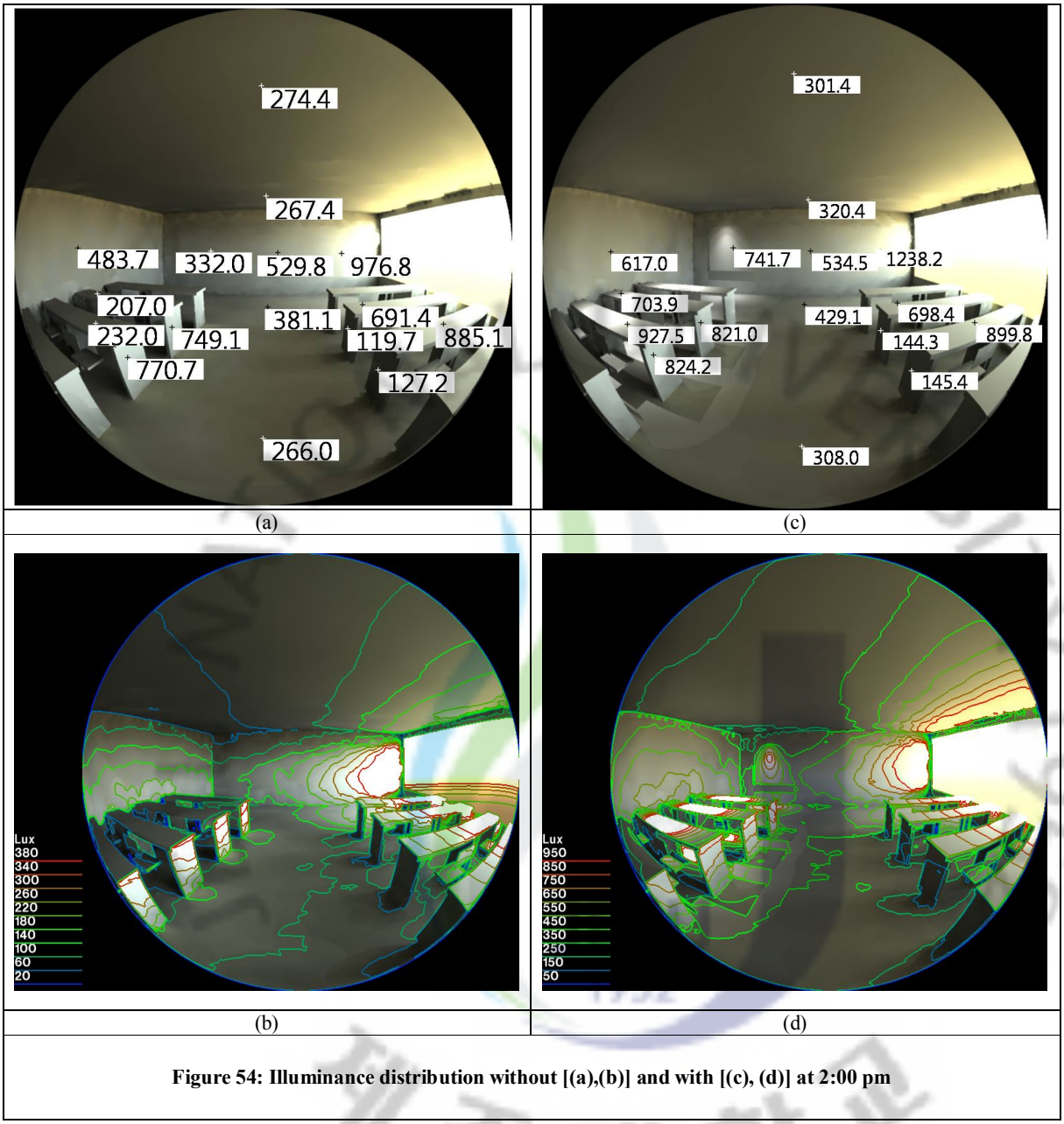

(a) (c)

(b) (d)

Figure 54: Illuminance distribution without [(a),(b)] and with [(c), (d)] at 2:00 pm

Illuminance distribution in the north-oriented classroom at 2:00 pm showed following values: on the south-side wall from 603.1 lux to 862.7 lux with the daylighting system and on the table under the diffuser – from 305.5 lux to 1087.2 lux.

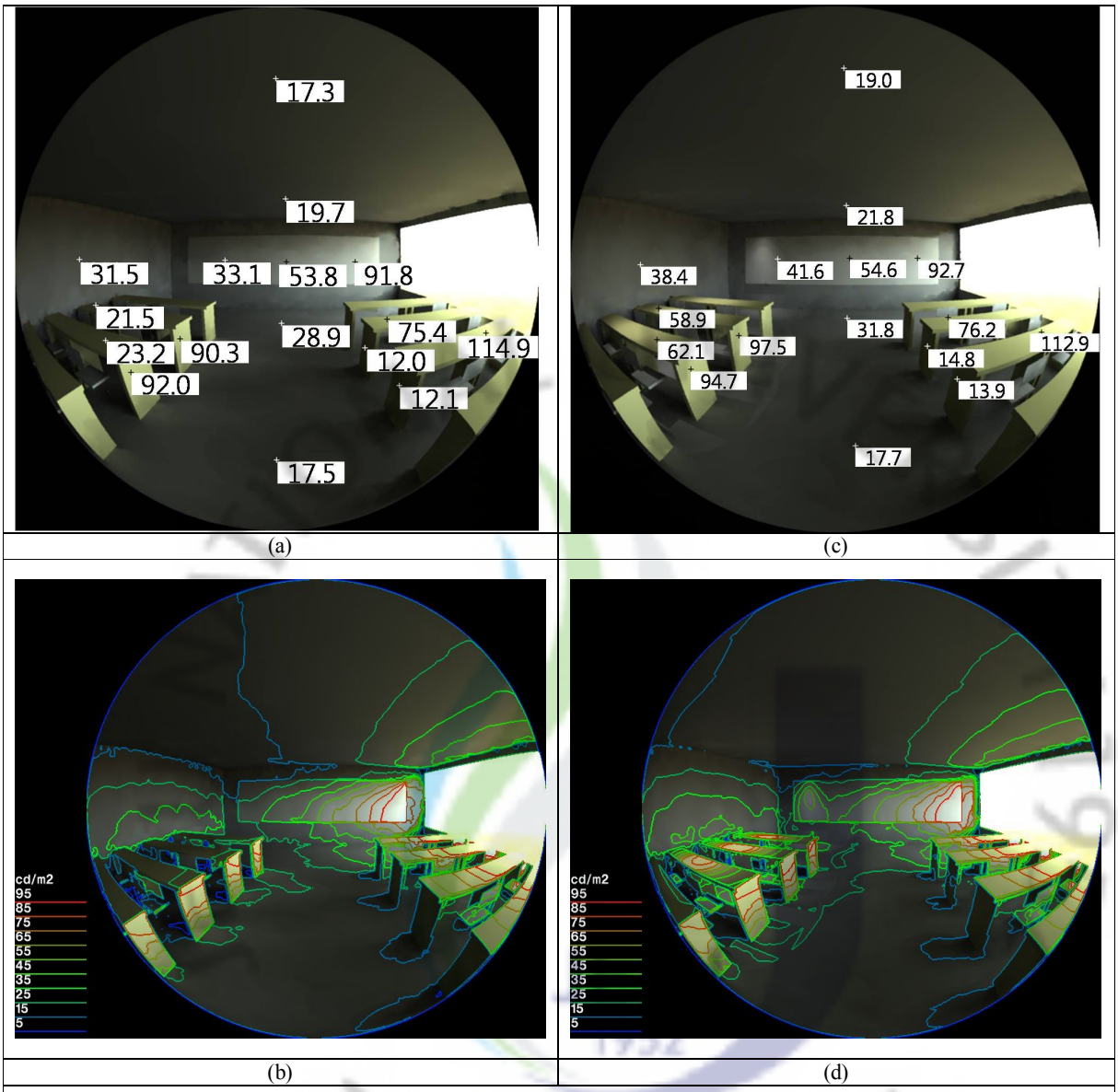

Figure 55: Luminance distribution without [(a),(b)] and with [(c), (d)] at 4:00 pm

Luminance distribution change at 4:00 pm in the north-oriented classroom was smaller: on the south-side wall from 31.5 cd/m^2 to 38.4 cd/m^2 with the daylighting system and on the table under the diffuser – from 23.2 cd/m^2 to 62.1 cd/m^2.

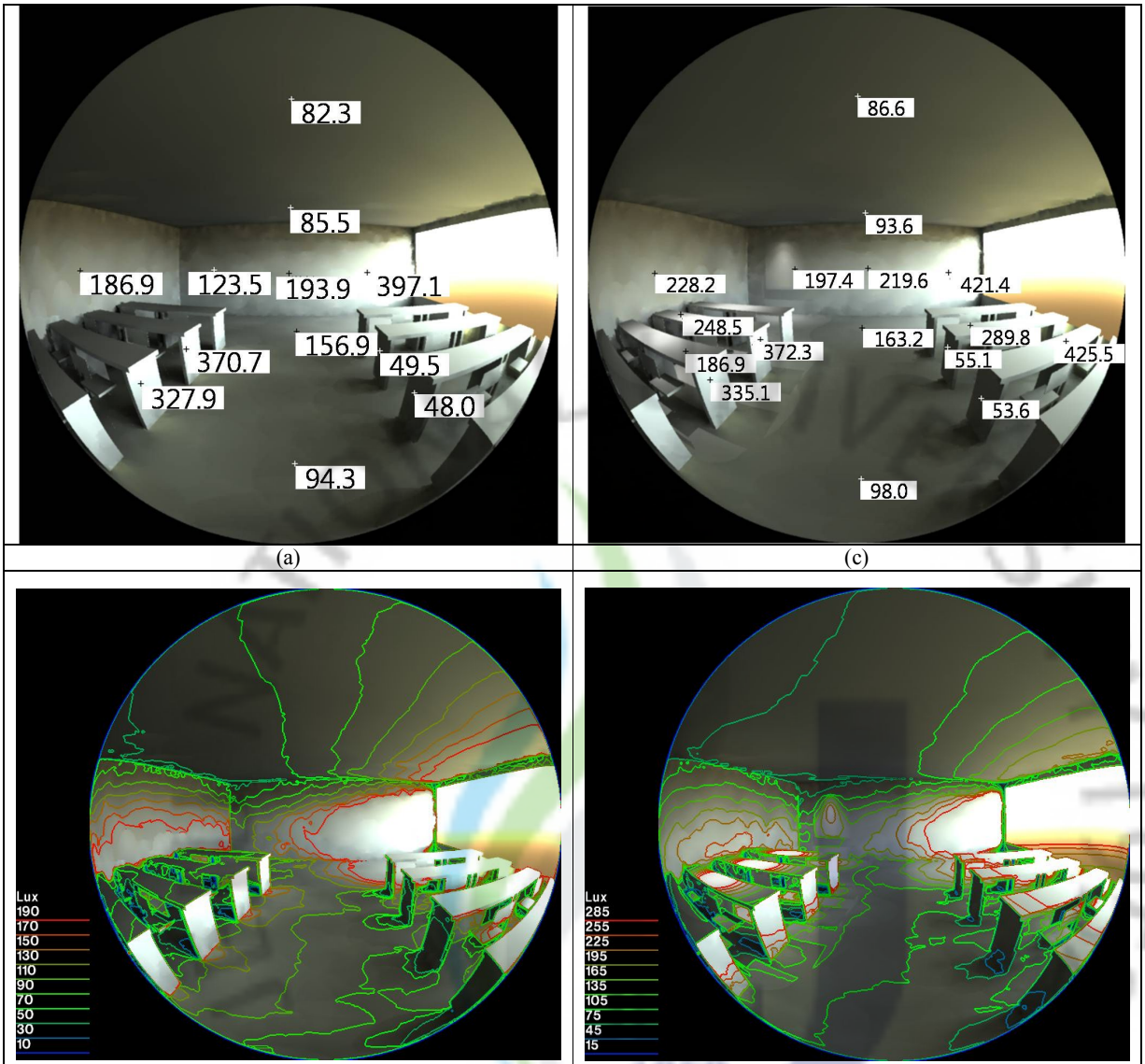

(a) (c)

(b) (d)

Figure 56: Illuminance distribution without [(a),(b)] and with [(c), (d)] at 4:00 pm

Illuminance distribution in the north-oriented classroom at 4:00 pm fluctuated: on the south-side wall from 186.9 lux to 228.2 lux with the daylighting system and on the left corner of blackboard – from 123.5 lux to 197.4 lux.

4.2 Classroom with south-oriented windows

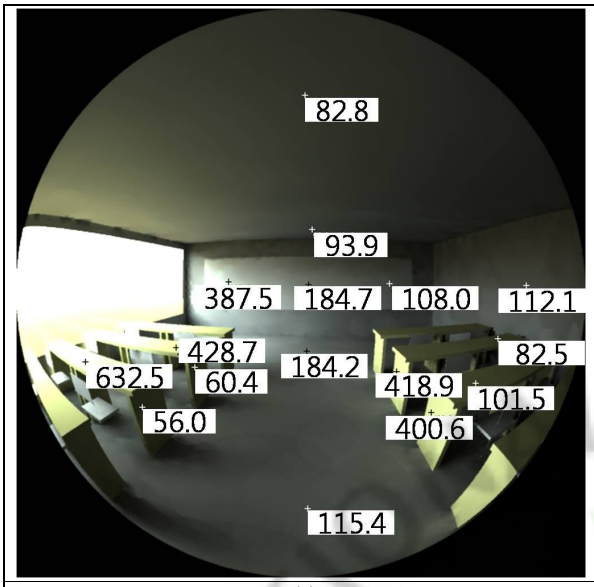

(a)

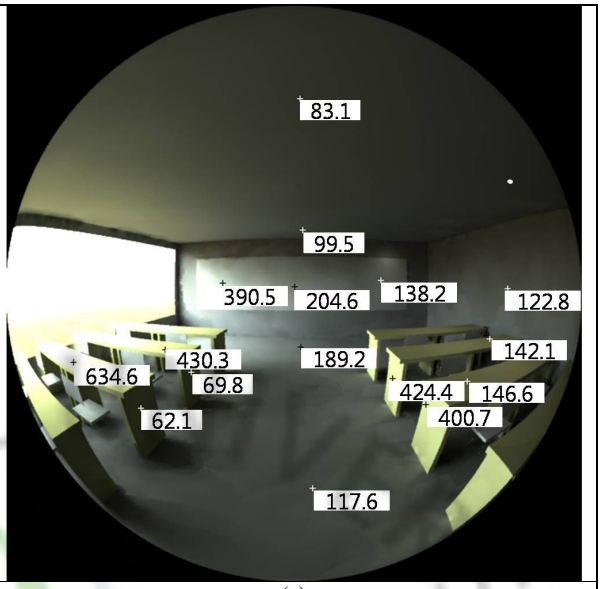

(c)

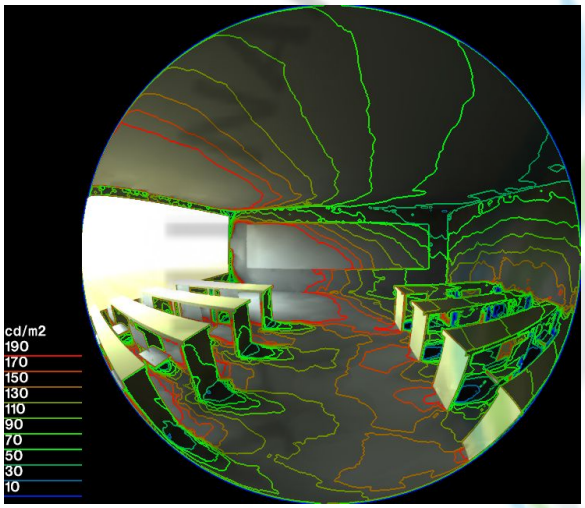

(b)

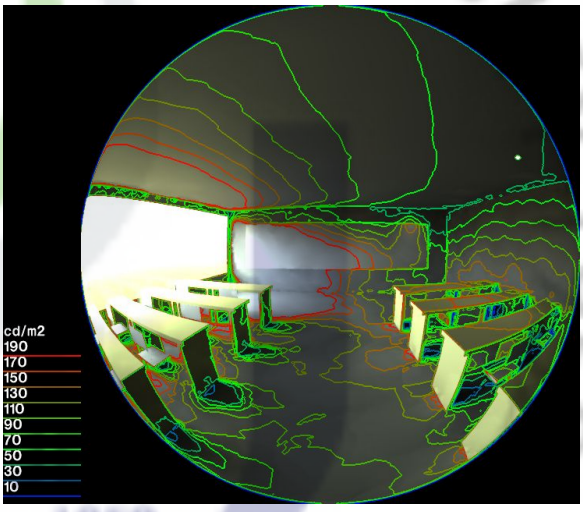

(d)

Figure 57: Luminance distribution without [(a),(b)] and with [(c), (d)] at 10:00 am

Luminance values in the south-oriented classroom at 10:00 am fluctuated on the north-side wall from 112.1 cd/m^2 to 122.8 cd/m^2 with the daylighting system and on the table under the diffuser – from 101.5 cd/m^2 to 146.6 cd/m^2.

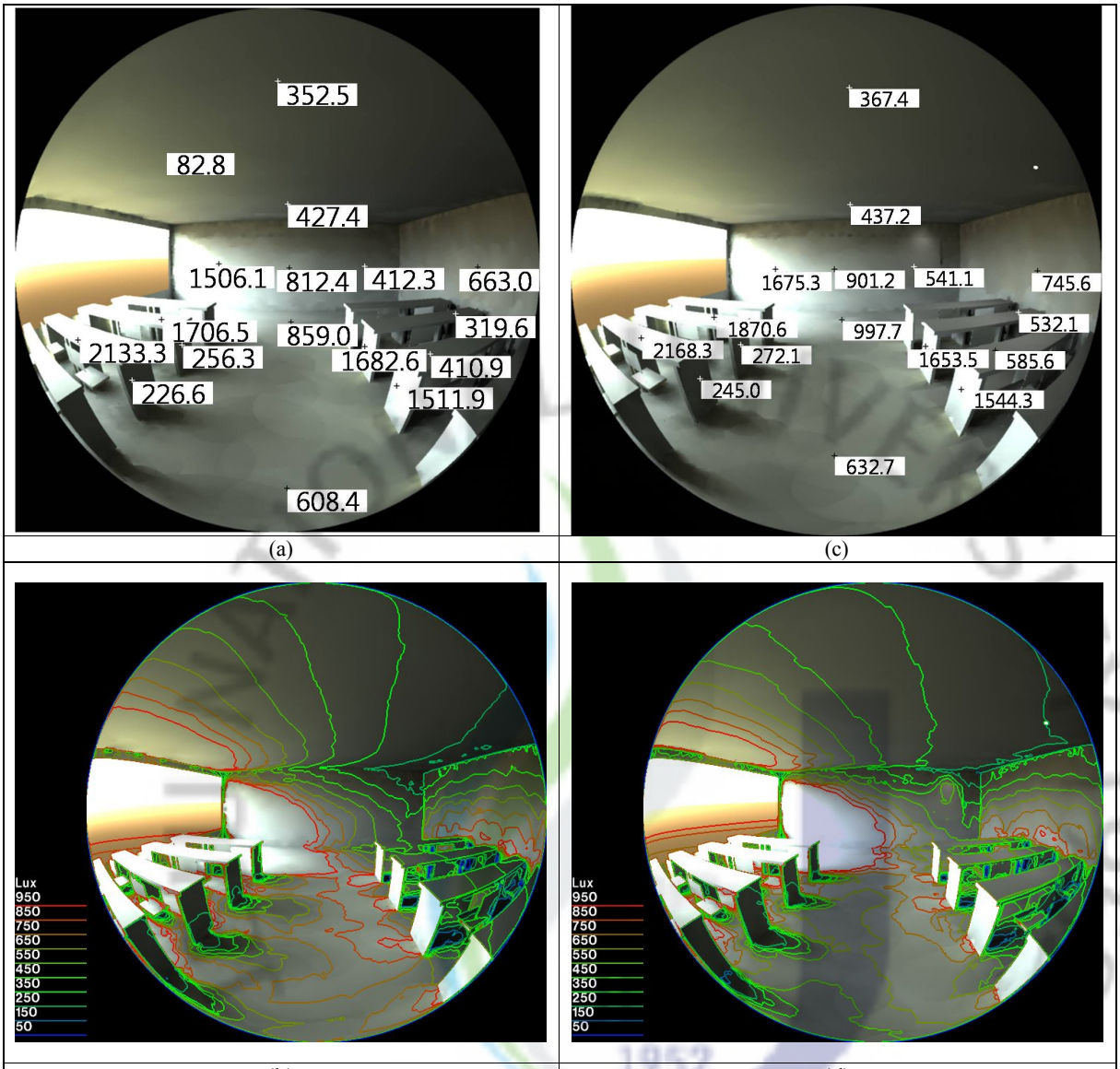

Figure 58: Illuminance distribution without [(a),(b)] and with [(c), (d)] at 10:00 am

Illuminance distribution in the south-oriented classroom at 10:00 am changed as: on the north-side wall from 663.0 lux to 745.6 lux with the daylighting system and on the table under the diffuser – from 410.9 lux to 585.6 lux.

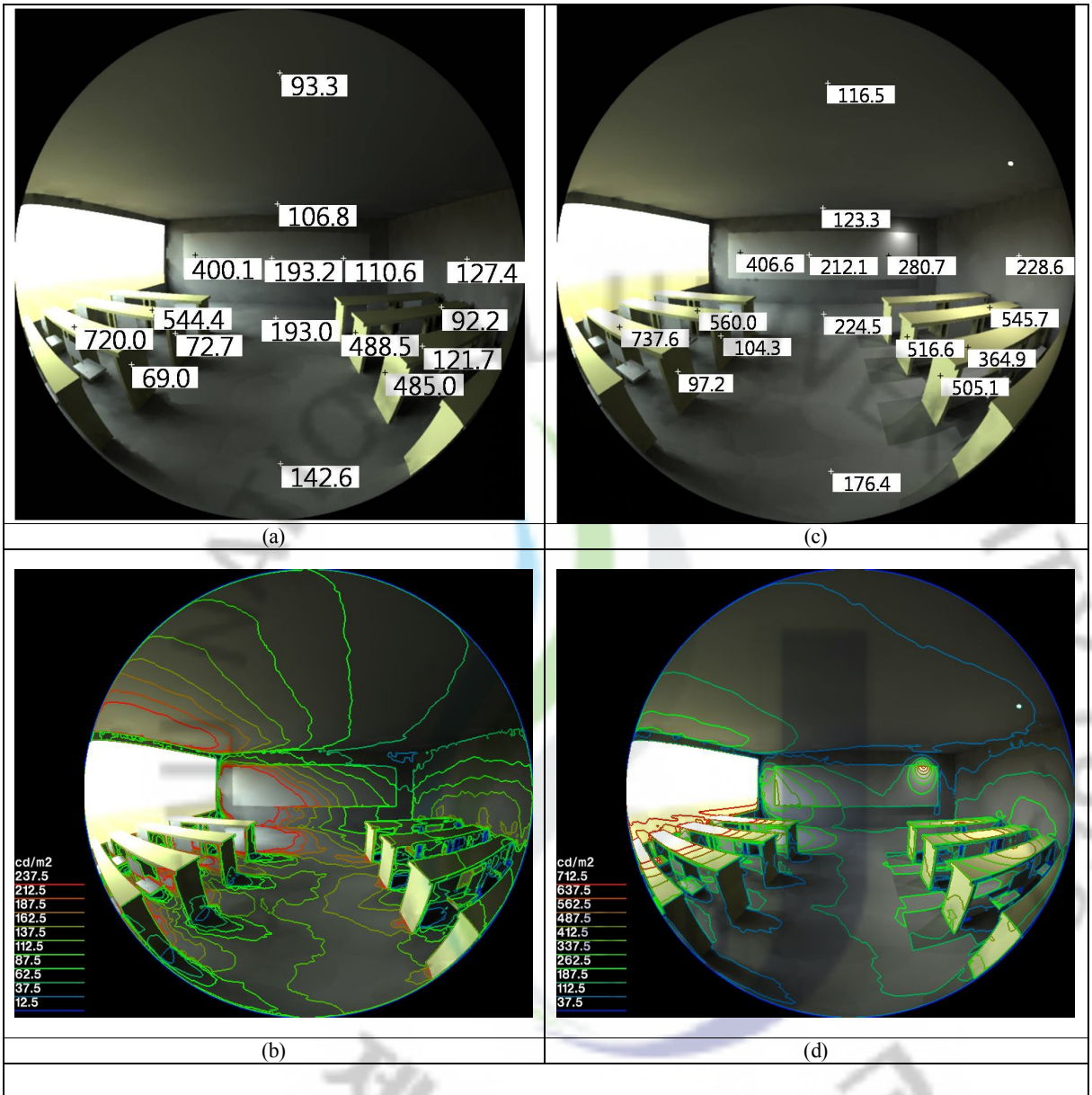

(a) (c)

(b) (d)

Figure 59: Luminance distribution without [(a),(b)] and with [(c), (d)] at 12:00 pm

Luminance distribution in the south-oriented classroom at noon had highest values too: on the north-side wall from 127.4 cd/m^2 to 228.6 cd/m2 with the daylighting system and on the table under the diffuser – from 121.7 cd/m^2 to 364.9 cd/m^2.

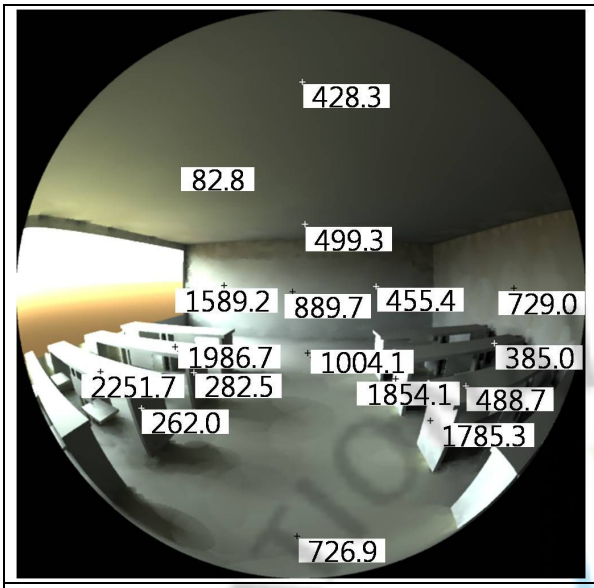

(a)

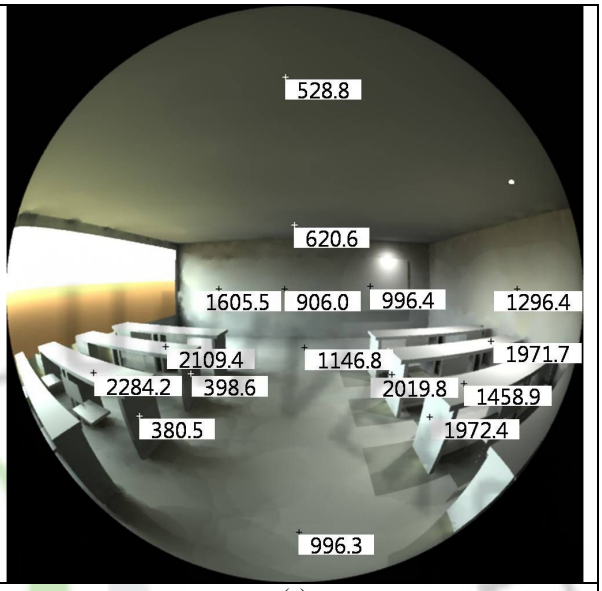

(c)

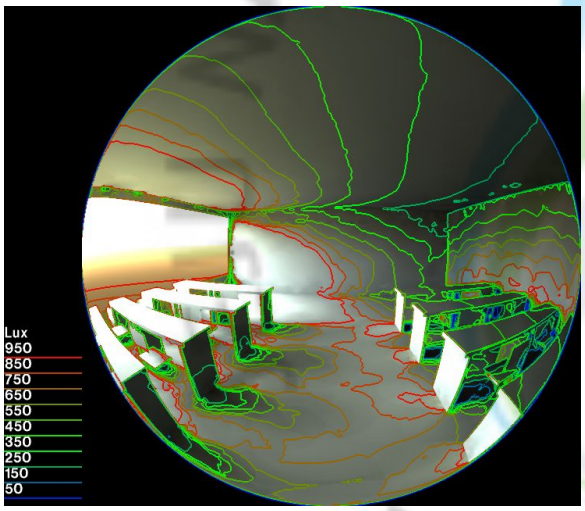

(b)

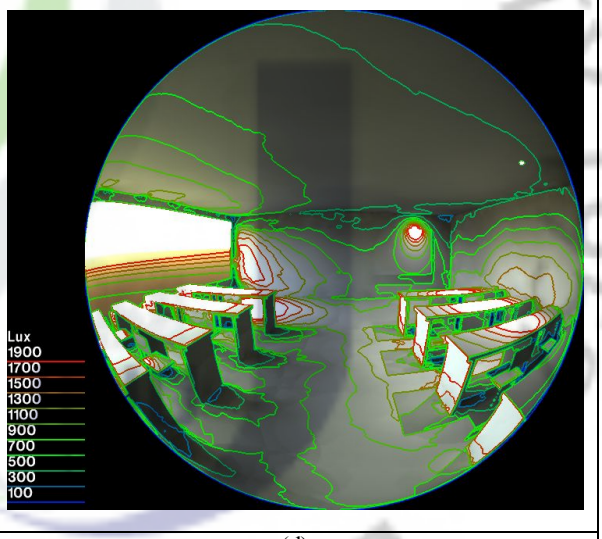

(d)

Figure 60: Illuminance distribution without [(a),(b)] and with [(c), (d)] at 12:00 pm

Illuminance distribution in the south-oriented classroom at noon changed as: on the north-side wall from 729.0 lux to 1296.4 lux with the daylighting system and on the table under the diffuser – from 488.7 lux to 1458.9 lux.

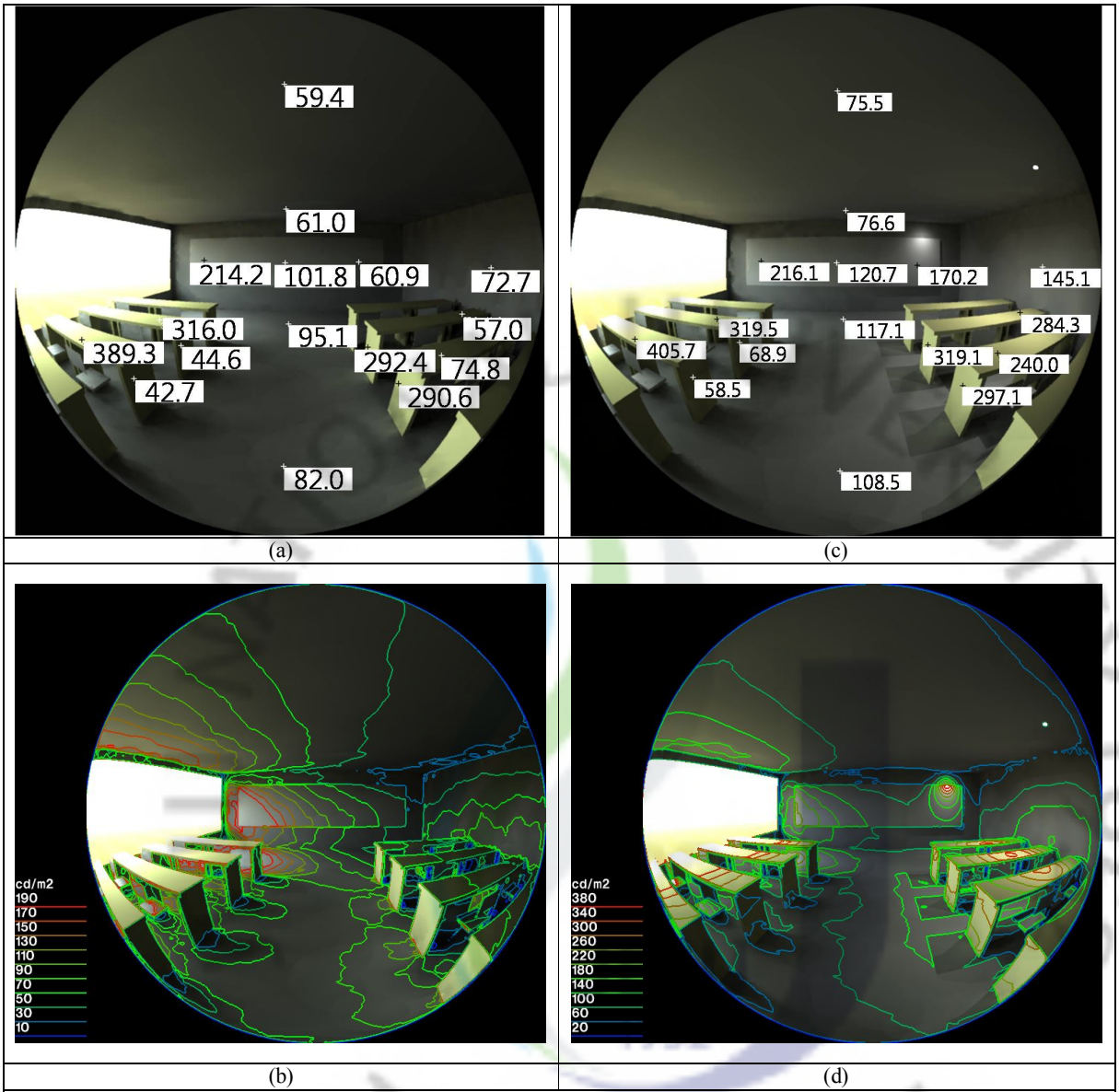

Figure 61: Luminance distribution without [(a),(b)] and with [(c), (d)] at 2:00 pm

Luminance values in the south-oriented classroom at 2:00 pm were 72.7 cd/m^2 and 145.1 cd/m^2 with the daylighting system on the north-side wall and on the table under the diffuser – 74.8 cd/m^2 and 240 cd/m^2.

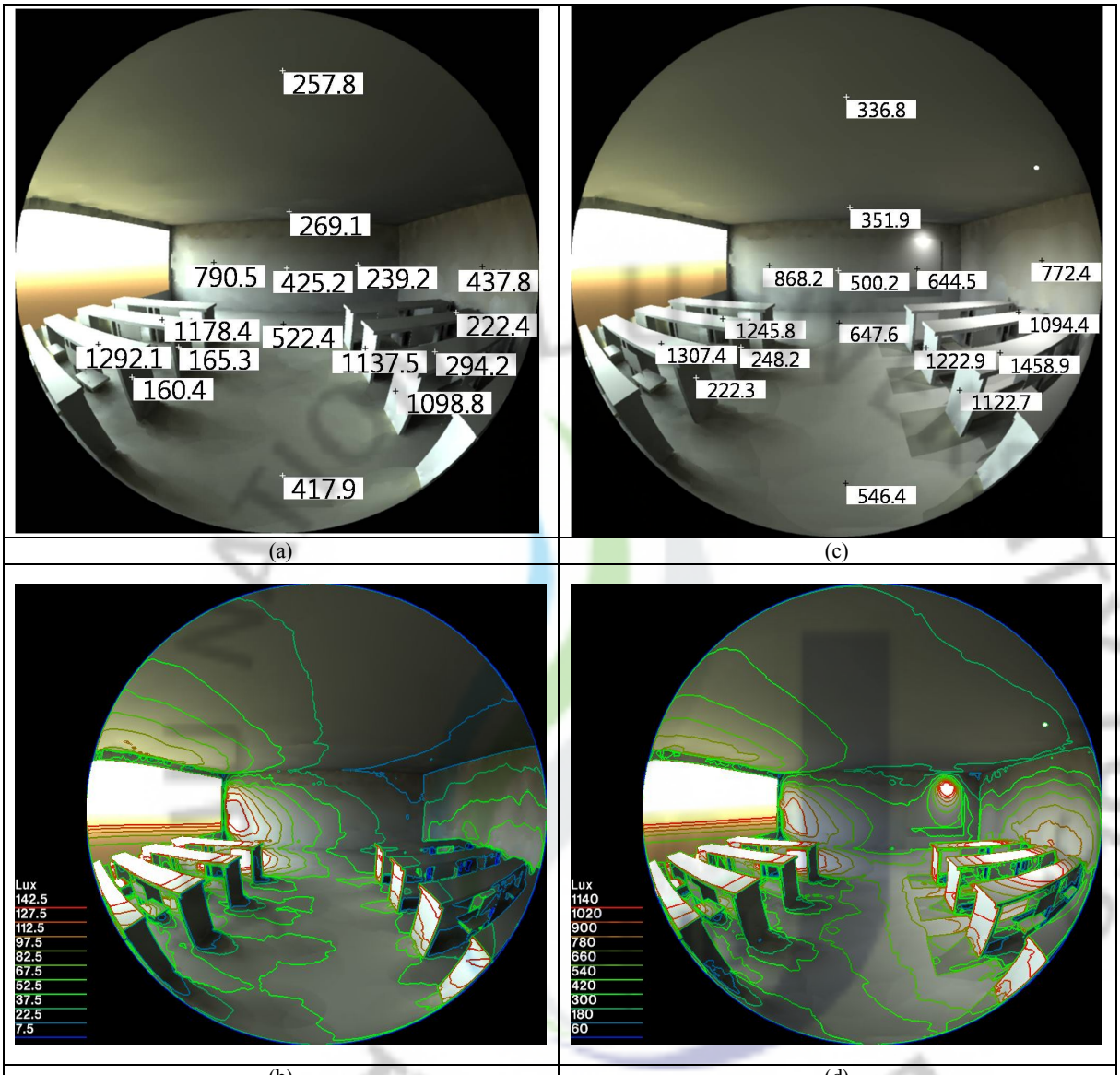

(a) (c)

(b) (d)

Figure 62: Illuminance distribution without [(a),(b)] and with [(c), (d)] at 2:00 pm

Illuminance distribution in the south-oriented classroom at 2:00 pm varied as: on the north-side wall from 437.8 lux to 772.4 lux with the daylighting system and on the table under the diffuser – from 294.2 lux to 1458.9 lux.

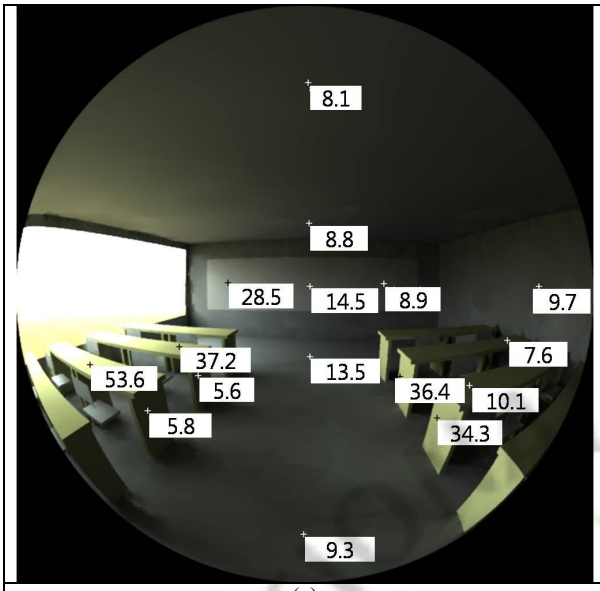

(a)

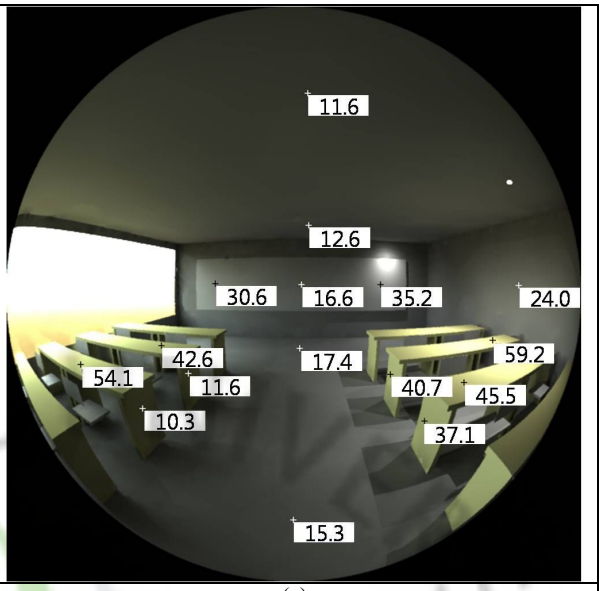

(c)

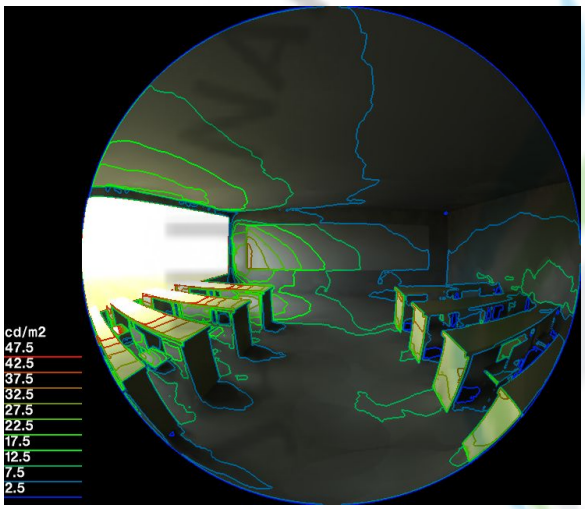

(b)

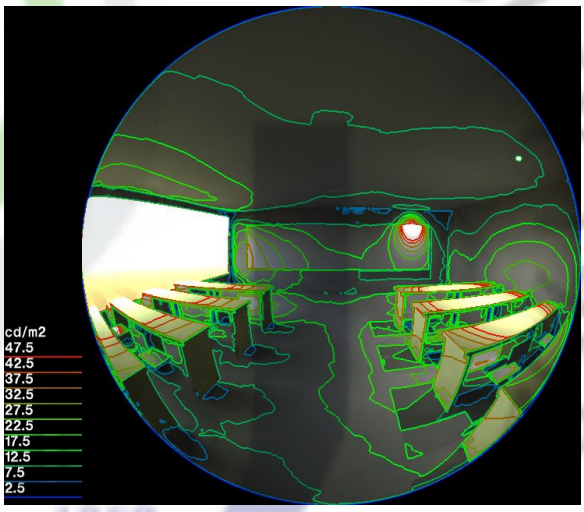

(d)

Figure 63: Luminance distribution without [(a),(b)] and with [(c), (d)] at 4:00 pm

Luminance distribution at 4:00 pm in the south-oriented classroom changed as: on the north-side wall from 9.7 cd/m^2 to 24.0 cd/m^2 with the daylighting system and on the table under the diffuser – from 10.1 cd/m^2 to 45.5 cd/m^2 respectively.

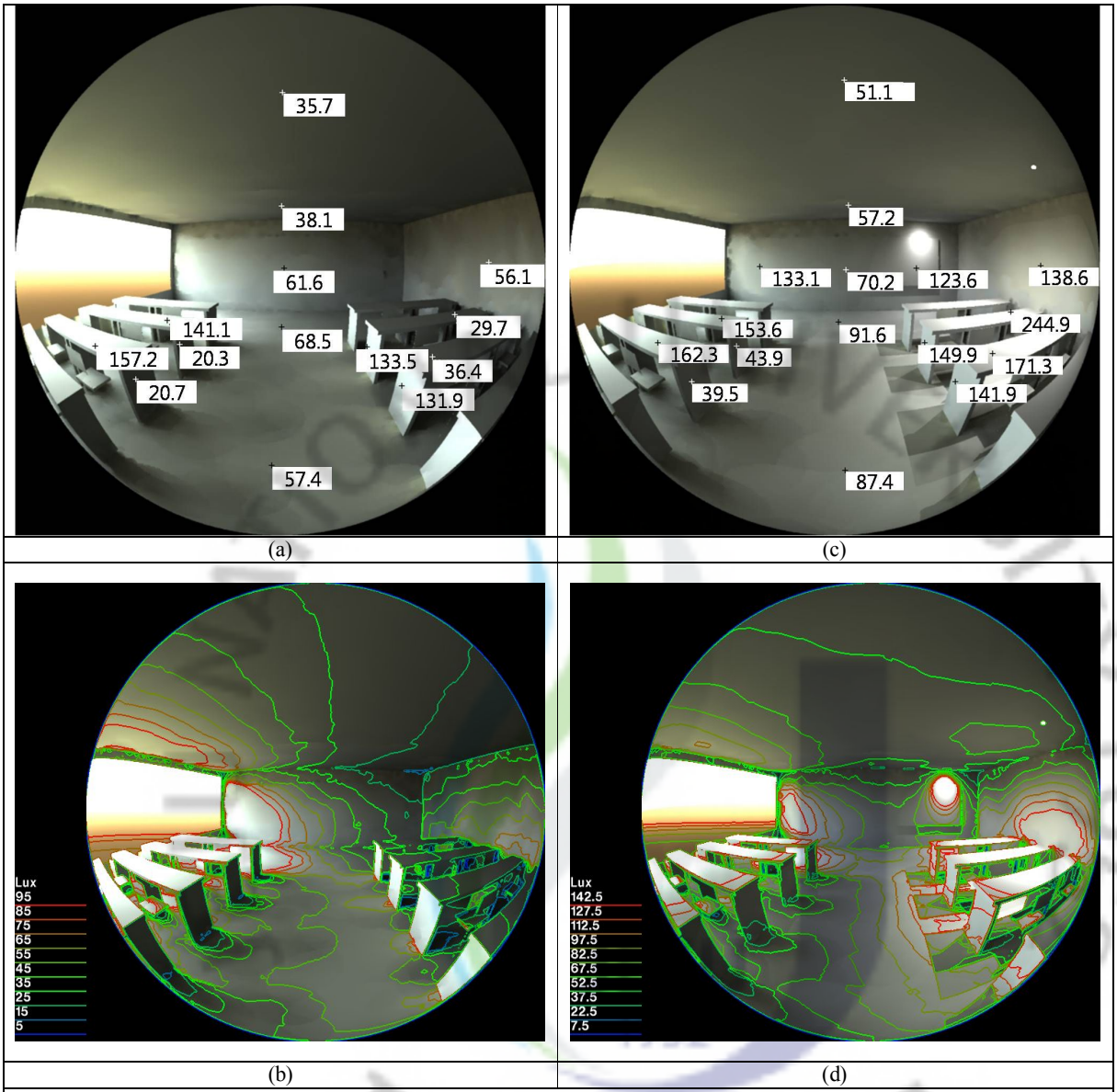

(a) (c)

(b) (d)

Figure 64: Illuminance distribution without [(a),(b)] and with [(c), (d)] at 4:00 pm

Illuminance distribution in the south-oriented classroom at 4:00 pm fluctuated: on the north-side wall from 56.1 lux to 138.6 lux with the daylighting system and on the table under the diffuser – from 36.4 lux to 171.3 lux.

4.3 Test cells

Two identical test cells were built in Jeju city, Korea (Latitude: 33.3 N, Longitude: 126.3 E) with a size of 3 m x 1.5 m x 1.5 m (1:0.5) as shown in Fig.65. Each test cell has south-oriented windows with window blinds. One of the cells has a solar tracker in order to analyze daylighting system's performance by comparing both measurement results.

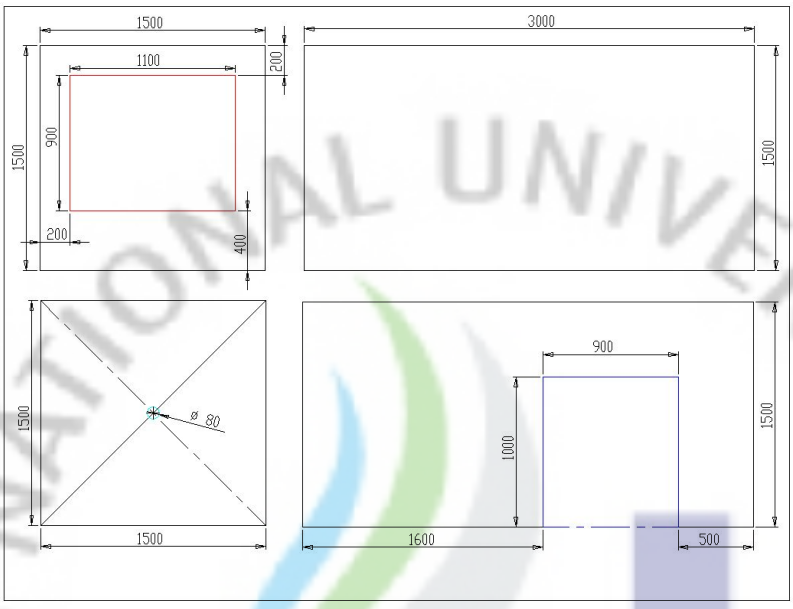

(a)

(b)

Figure 65: (a) Overall dimensions and, (b) general view of test cells

In the test cells sensors were installed as shown in the Fig. 66:

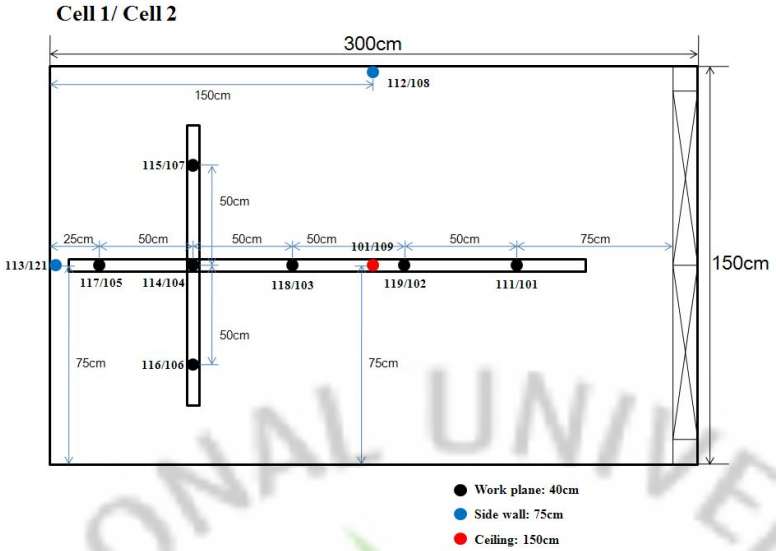

Figure 66: Sensors' location in test cells (cell 1/cell 2 respectively)

According to experiments (due to weather conditions) optimal results were received in October 6, 2009 at 1 p.m. Figure 67 shows the difference of luminance values in test cells.

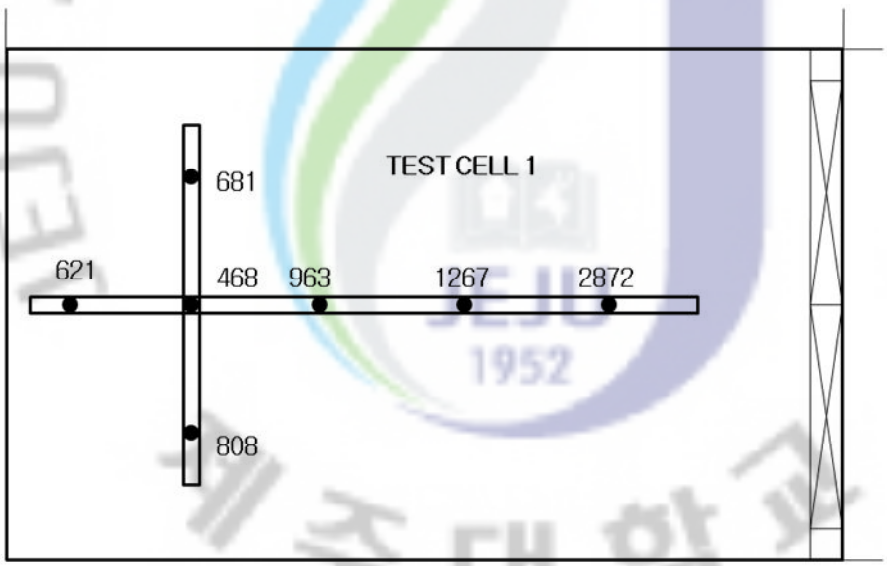

(a)

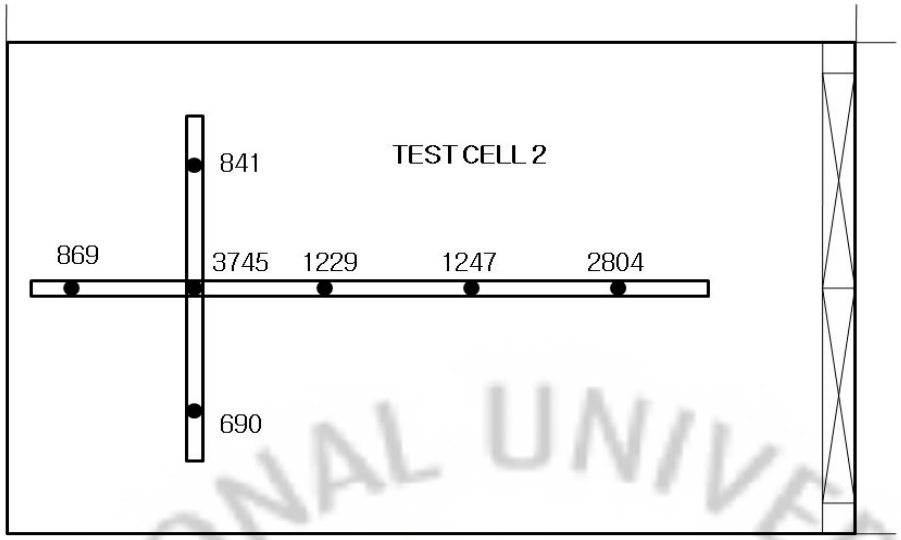

(b)

Figure 67: Illuminance values in test cells without (a) and with (b) daylighting system in October 6, 2009 at 1 pm

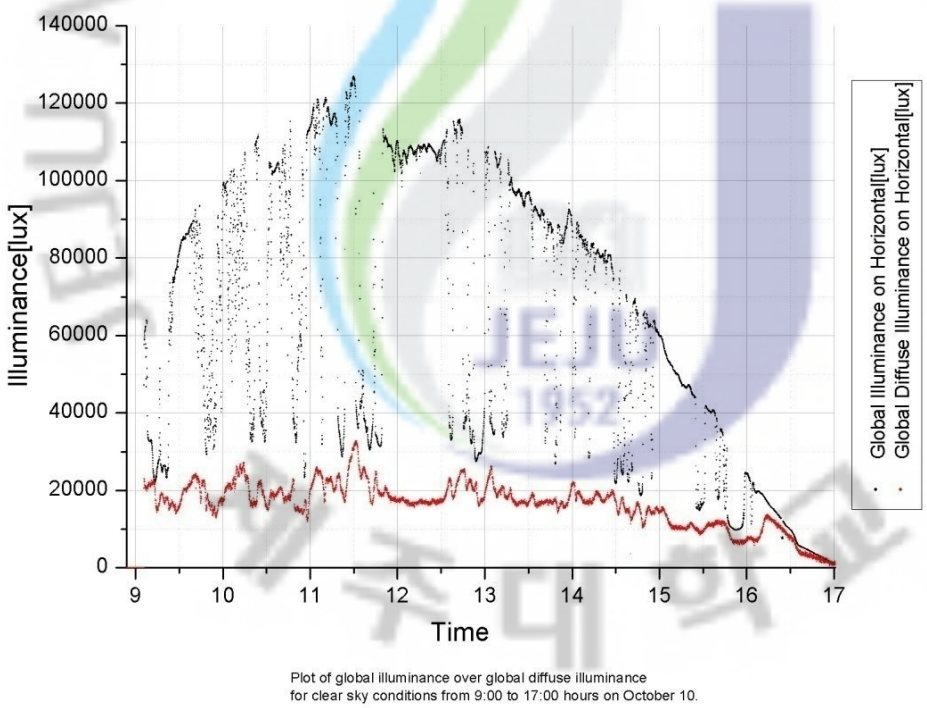

Figure 68: Global total and diffuse illuminances at different times on a clear day

Figure 68 shows the global total and diffuse illuminances at different times on a clear day, which clearly demonstrates the dominance of the beam component of solar radiation. Differences between the global and diffuse illuminance are relatively large, which mounts to its maximum ratio of 6 at 11:30 a.m. Figure 69 shows the correlation between the global illuminance and irradiance. Majority of the data points are clustered around the right half of the regression curve indicating higher values.

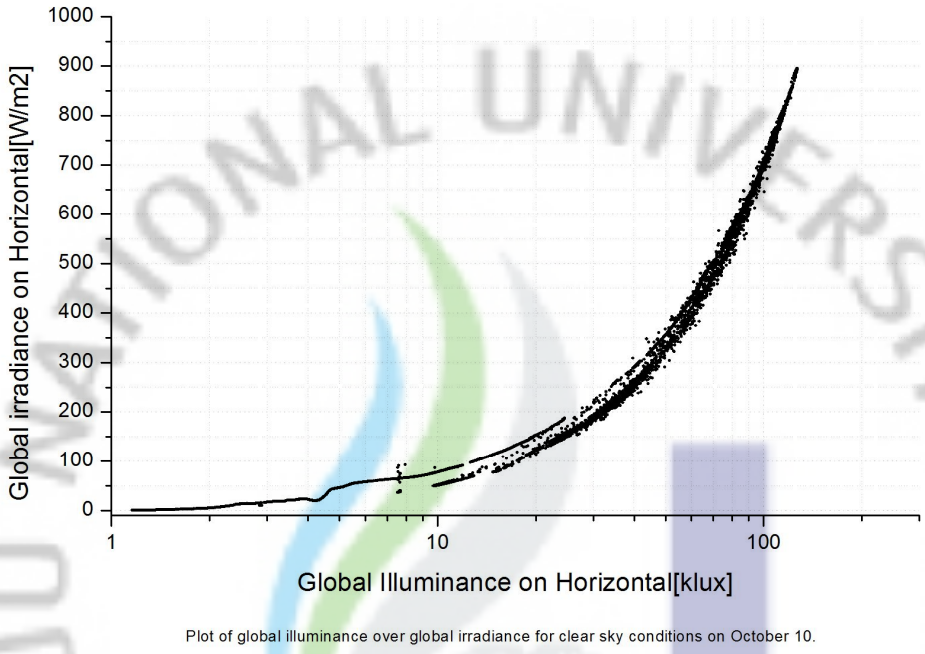

Figure 69: Correlation between the global illuminance and irradiance

Figure 70 depicts a contour map of illuminance for the test cell applying a 3.2cm convex lens to diffuse sunlight for indoor illumination. Measurements are made using nine photo sensors 40cm above the floor with an interval of 50cm. Windows were completely shaded to block any light from entering the test cell. As shown, the light emanating from the diffuser is mostly concentrated near the center because of the optical features of the convex lens used in the present investigation.

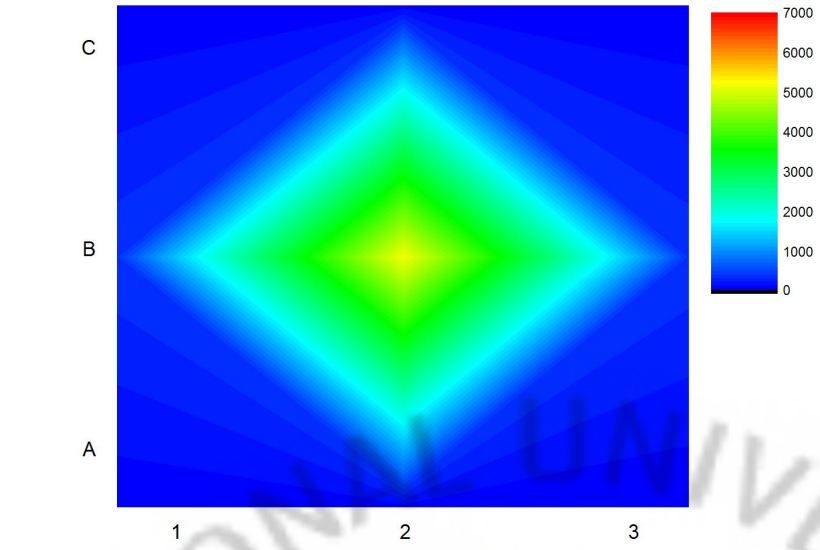

(a)

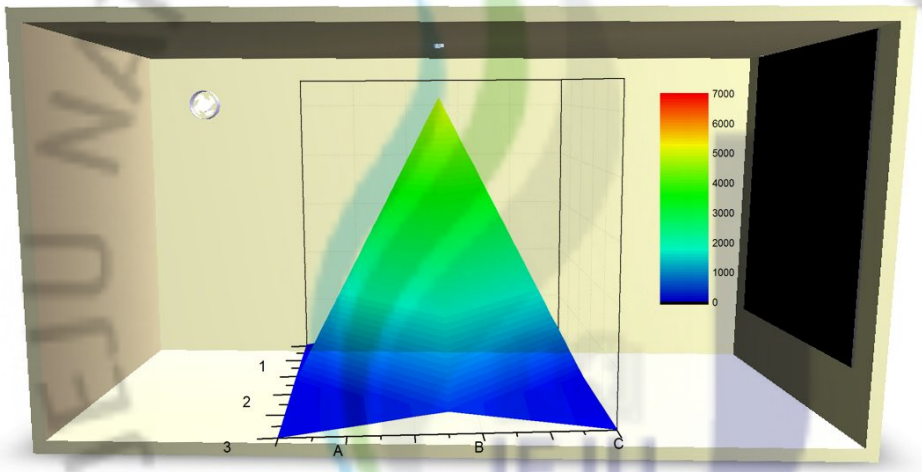

(b)

Figure 70: Iso-illuminance contour map for the test cell with the solar daylighting system in September 26, 2009 at 1:00 pm: (a) 2D, (b) 3D

In the Figure 70 is depicted iso-illuminance contour map on the workplane for the test cell with the solar daylighting system in September 26, 2009 at 1:00 pm. The maximum illuminance value was observed under the diffuser with around 5300 lux.

During experiments thermal conditions were also observed. Internal temperatures were measured with a standard K-type thermocouple sensors and thermal imaging infrared camera FLIR i40 (Fig. 71). The temperature difference between cells was about 3-4 ˚C.

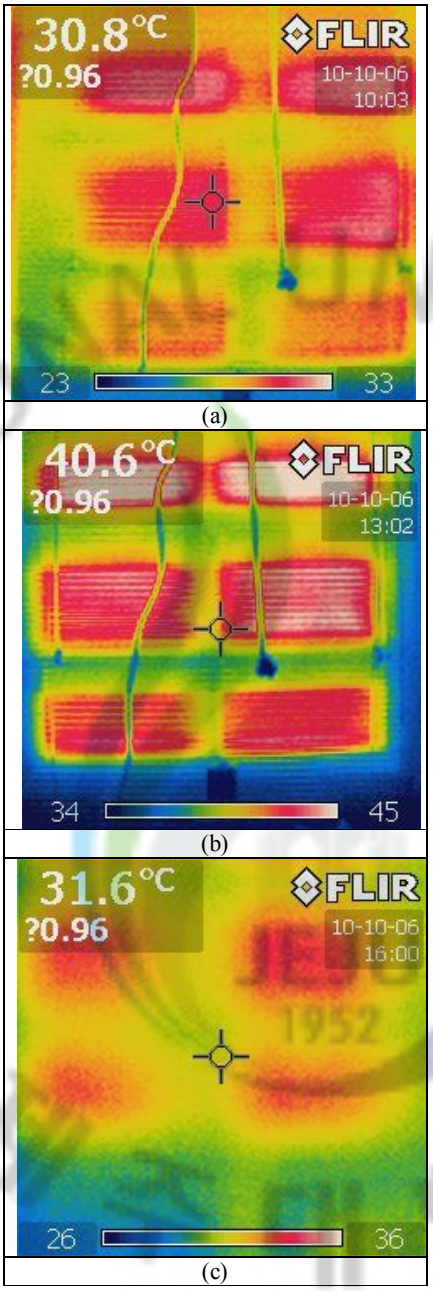

Figure 71: Infrared pictures showing the distribution of internal temperatures in test cell with solar daylighting systems at different hours of the day: 10:03 am, 1:02 pm and 4:00 pm

4.4 Computer-based thermal and daylighting performance analysis of the standard schoolroom

The configuration of the schoolroom model, as depicted in the Figure 72, consists of two parts (zones): a schoolroom with 7.5m (length) x 9m (width) x 3.3m (height) and hallway with 2.7m x 9m x 3.3m. The schoolroom has large south facing windows whereas the hallway locates relatively small windows on the north side of the wall. The walls, ceiling and floor of the schoolroom are made of concrete and heavily insulated.

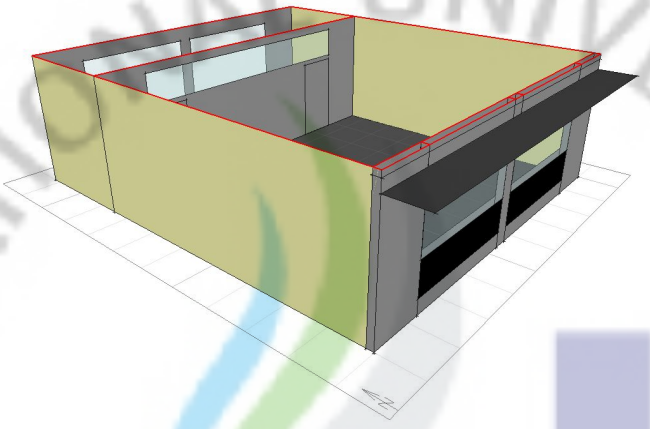

(a)

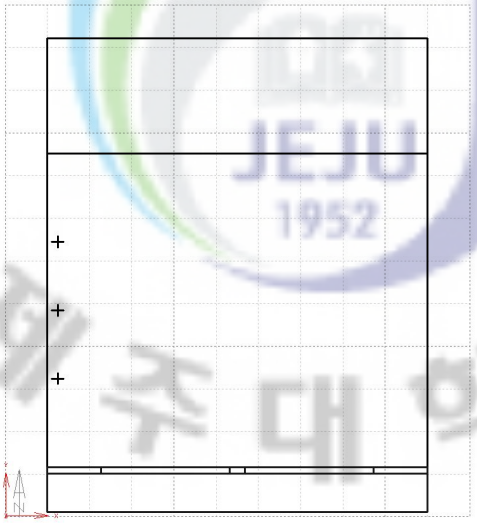

(b)

Figure 72: Schematic (a) and plan (b) views of the schoolroom model

The south-facing area of the schoolroom is comprised of two sections as shown in the Figure 73. The upper half consists of two layers of operable windows for direct gains, while the lower half is characterized by a non-operable glazing followed by a black iron plate for quick absorption and emission of solar energy. The black iron plate is covered with 3 mm single glass layer for protection from environment impacts. As the sun's rays pass through the outer glazing and hit the surface of black plate, this immediately raises its temperature and in turn heats the air trapped within glazing and the iron plate.

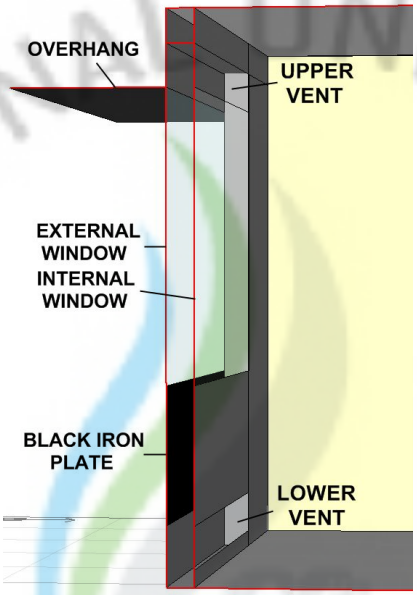

Figure 73: Schematic view of the schoolroom south-facing area

Thermosyphoning could be induced by opening the upper and lower vents which allows continuous flow of hot air into the schoolroom during heating periods. In summer, overhang prevents the indoor temperature from overheating and cross-ventilation is induced by opening the windows in the opposite (north) side of the schoolroom.

Weather conditions were taken from the weather database of the U.S. Department of Energy for Seoul, Korea. The interzonal air flow between the schoolroom and hallway is assumed to be 0.35 air changes per hour. This accounts for the occasional opening of the door during intermissions. Most of the heat flow

between the zones is through the partition wall that separates the schoolroom and hallway. Each schoolroom is occupied with 50 students. Classes are held from 9 a.m. to 5 p.m.

To measure the effect of solar lighting for the schoolroom, photometric analysis was carried out (Tab. 9). Nine photo sensors were placed on the western wall (where a chalkboard is situated) horizontally and vertically at a regular interval of 45 cm. The illuminance values shown in Table 9 are those recorded at 12:30 p.m. under an overcast sky condition in Seoul (37.5° N and 126.9° E). Simulations were also carried out for daylighting using RADIANCE whose accuracy has long been established by many previous studies.

Table 9: Illuminance value compared at different locations between the measured and simulation (lux)

Sensor	Simulation	Measured
1	421.6	421
2	470.9	414
3	468.0	434
4	323.5	343
5	350.0	350
6	360.3	359
7	254.6	254
8	274.1	265
9	271.8	271

From this table, we could see two agrees quite well despite measurement uncertainties and other unknown factors that could have influenced otherwise.

Thermal analysis also was analysed by ECOTECT and its results were compared with previous simulation results of SUNCODE (Tab. 10). In general, ECOTECT values fluctuated from 6.0 °C to 9.6 °C and SUNCODE values showed a range of 5.9 - 8.2 °C. The highest values were observed at 1 p.m. in both cases.

Table 10: Temperature comparison between SUNCODE and ECOTECT (°C)

Hour	ECOTECT	SUNCODE	Temp. Diff.	Hour	ECOTECT	SUNCODE	Temp. Diff.
00	6.2	6.3	0.1	12	9.4	8.0	1.4
01	6.2	6.4	0.2	13	9.6	8.2	1.4
02	6.2	6.3	0.1	14	9.4	8.0	1.4
03	6.2	6.2	0.0	15	9.2	8.0	1.2
04	6.2	6.1	0.1	16	9.2	8.1	1.1
05	6.2	6.1	0.1	17	9.0	7.8	1.2
06	6.2	6.0	0.2	18	6.2	7.5	1.3
07	6.3	5.9	0.4	19	6.1	7.1	1.0
08	6.4	5.9	0.5	20	6.1	7.0	0.9
09	9.3	6.4	2.9	21	6.0	6.8	0.8
10	9.4	6.5	2.9	22	6.0	6.5	0.5
11	9.4	7.2	2.2	23	6.0	6.3	0.3

Temperatures varied proportionate to the intensity of solar radiation, which changes throughout the day. A maximum temperature difference of 2.9 °C was observed in two cases which deem relatively reasonable considering the complexity of the schoolroom model in the present analysis.

V. CONCLUSIONS

A new daylighting system with solar tracker was analyzed for its performance in indoor illumination. In order to analyze the system's performance for daylighting, a series of several measurements and simulations were performed. First, photometric measurements were carried out for two classrooms with north- and south-oriented windows. After validating the simulated results by comparing them with those of measurements, both the ECOTECT and RADIANCE models were extended to simulate the performance of the daylighting system considered in the present analysis for a number of cases applicable to existing buildings. As a result, illuminance and luminance values boosted up to 862.7 lux and 148.6 cd/m^2 at the center of opposite wall in the north-oriented classroom, 1296.4 lux and 228.6 cd/m^2 at the center of opposite wall in the south-oriented classroom from their lowest original values (i.e., the cases without daylighting systems) of 603.1 lux and 111.0 cd/m^2, 729 lux and 127.4 cd/m^2 respectively. Following the analysis on classrooms, a study has been done with regard to two identical test cells for a comparative examination of its performance. One of them was equipped with the solar daylighting system. The illuminance value under the diffuser on the workplane (40 cm) in the test cell with the daylighting system was 3745 lux whereas in the test cell without the daylighting system sensors showed 468 lux. Finally, a typical passive schoolroom model was investigated for its indoor thermal and daylighting performance. For thermal analysis, ECOTECT was brought in whose results were compared with those of SUNCODE. Meanwhile, its indoor daylighting performance was examined using RADIANCE and then compared with some measured values. It is felt that the procedures taken for thermal and lighting analyses in the present case could be further extended for other types of solar buildings (systems) to elicit the most feasible design in reality for maximum efficiency in utilizing the sun's energy.

REFERENCES

[1] Met Office Hadley Centre and Climatic Research Unit the University of East Anglia. www.metoffice.gov.uk.

[2] Intergovernmental Panel on Climate Change Data Distribution Center: http://www.ipcc-data.org/

[3] Pritchard D.C. (1999). “Lighting”, Addison Wesley Longman Ltd.

[4] Tregenza, P. and Loe, D. (1998). “The design of lighting”. London: E & FN Spon. ISBN: 0-419-20440-7.

[5] US Department of Energy's Federal Energy Management Program: http://www1.eere.energy.gov/femp

[6] Nicklas, M. H. and Bailey, G. B. "Analysis of the Performance of Students in Daylit Schools." Raleigh: Innovative Design. Online: www.deptplanetearth.com/pdfdocs/studentdaylit.pdf.

[7] Heschong Mahone Group (1999). Daylighting in Schools. An investigation into the relationship between daylight and human performance. Detailed Report. Fair Oaks , CA.

[8] U.S. Department of Energy. 2002 Annual Report. Online: http://management.energy.gov/documents/report2002.pdf

[9] http://www.himawari-net.co.jp/

[10] Federal Energy Management Program (2007). "Hybrid Solar Lighting Illuminates Energy Savings for Government Facilities". DOE/EE-0315. Online: http://www1.eere.energy.gov/femp/pdfs/tf_hybridsolar.pdf

[11] http://www.parans.com

[12] http://www.solar-track.com/

[13] M. Wilson, A. Jacobs, J. Solomon, W. Pohl, A. Zimmermann, A. Tsangrassoulis, M. Fontoynont. Sunlight, Fibres and Liquid Optics: The UFO Project, EPIC, Lyon, 2002. Online: http://www.learn.londonmet.ac.uk/packages/helioptics/papers/ufo_epic2002.pdf

[14] http://www.monodraught.com/suncatcher/index.php

[15] http://www.whilkor.com

[16] Tabet, Kheira. & Shelley, Gary. "An investigation on the effect of access to windows on visual comfort, motivation and productivity. 3rd European Conference on Architecture, Florence, Italy. (17-21 May):157-160.

[17] S.H. Lim, N.H. Lee, and B.K. Lim, 1991. A performance study on Direct Gain Passive Solar School Buildings. Journal of Solar Energy Society of Korea, Vol. 11. No. 3. pp.37-43. Korea.

[18] Norbert Lechner, 2000. Heating, Cooling, Lighting: Design Methods for Architects (2nd edition).

[19] H. Han, A comparative study on the thermal performance of passive solar schoolroom, MS Thesis, Chungnam Nat'l University, Korea, 1991.

[20] G. Makaka, E.L.Meyer, M. McPherson, 2008. Thermal behaviour and ventilation efficiency of a low-cost passive solar energy efficient house. Renewable Energy, Vol. 33. Issue 9. pp. 1959-1973.

[21] D.B. Crawley, J.W. Hand, M. Kummert, B.T. Griffith, 2008. Contrasting the capabilities of building energy performance simulation programs. Building and Environment, Volume 43. Issue 4. pp. 661-673.

[22] C. Reinhart, A. Fitz, 2006. Findings from a survey on the current use of daylight simulations in building design. Energy and Buildings. Volume 38. Issue 7. pp. 824-835.

[23] KIER, A Report on the Analysis and Planing of Energy & Resource Technologies, 2005

[24] Olgyay, V. W. Architectural Lighting, McGraw-HilEgan, M. D. andl, NY, 2002

[25] Augustesen, C., Brandi U., Dietrich, U., Friederici, A., Geissmar-Brandi, C., Kristensen, P. T., Madsen, M., Storch, A., Wand, B., Lighting Design, Birkhäuser, 2006

[26] Rea, M. S., The IESNA Lighting Handbook Ninth Edition, IESNA Publications Department, 2000

[27] POHL, W. and ANSELM, C., "Review of Existing Heliostats", European Commission DG XII (2000)

[28] Han, H. and Kim, J. T., Design and Preliminary Performance Test of a Daylighting Device with Mini-dishes, Proceedings of SET2006, Vicenza, Italy, 2006, pp. 225~228

[29] Han, H., Dutton, S., Riffat, S., Kim, J. T., Performance Prediction of Fiber Optic Concentrators for Natural Lighting, Proceedings of SET2007, Santiago, Chile, 2007, pp. 68~72

[30] Han, H. and Kim, J. T., Application of high-density daylight for indoor illumination, Energy-the International Journal (in press).

[31] http://www.sunlight-direct.com/

[32] Feuermann, D. and Gordon, J. M., High-concentration Photovoltaic Designs Based on Miniature Parabolic Dishes, Pergamon, 2000

[33] Hecht, J., Understanding Fiber Optics, Pearson Education, Inc., Upper Saddle River, New Jersey 07458, 2006

[34] Andersen, M., Validation of the performance of a new bidirectional video-goniophotometer, LESO-PB, EPFL, Lausanne, Switzerland

[35] Muñoz-Martínez, V. F., Serón-Barba, J., Molina-Mesa, R., Gómez-de-Gabriel, J. M., Fernández-Lozano, J., García-Cerezo, A., Double reflection goniophotometer, BIPM and IOP Publishing Ltd., 2006

[36] Schlegel, G. O., Burkholder, F. W., Klein, S. A., Beckman, W. A., Wood, B. D., Muhs, J. D., Analysis of a full spectrum hybrid lighting system, Elsevier Ltd., 2003

[37] Tsangrassoulis, A., Doulos, L., Santamouris, M., Fontoynont, M., Maamari, F., Wilson, M., Jacobs, A., Solomon, J., Zimmerman, A., Pohl, W., Mihalakakou, G., On the energy efficiency of a prototype hybrid daylighting system, Elsevier Ltd., 2004

[38] Rosemann, A., Kaase, H., Lightpipe applications for daylighting systems, Elsevier Ltd., 2004

[39] A Report of IEA SHC Task 21, 2000. Daylight in Buildings

[40] Duffie, A. D. and Beckmann, W. A., Solar Engineering of Thermal Processes, John Wiley & Sons, 1980

[41] Szokolay, S. V., Introduction to Architectural Science – The Basis of Sustainable Design, Architectural Press, 2005

[42] Nabil A. and Mardaljevic, J., Useful daylight illuminances: A replacement for daylight factors, Energy and Buildings, Vol. 38, 2006.

[43] Weather database of the U.S. Department of Energy: http://apps1.eere.energy.gov/

[44] ECOTECT tutorials: http://www.squ1.com/archive/ecotect/tutorials/tutorials.htm

[45] http://usa.autodesk.com/adsk/servlet/pc/index?id=12602821&siteID=123112

[46] Jacobs, A. RADIANCE Cookbook. 2008

[47] G. Ward Larson, R. Shakespeare. Rendering with Radiance: the art and science of lighting visualisation. Morgan Kaufmann Publishers, San Francisco, 1997.

[48] Radiance community web site: http://www.radiance-online.org.

[49] Official Radiance web site: http://radsite.lbl.gov/radiance.